Linear-scaling methods in *ab initio* quantum-mechanical calculations

A dissertation submitted for the degree of

Doctor of Philosophy

at the University of Cambridge

Peter David Haynes

Christ's College, Cambridge

July 1998

Preface

This dissertation describes work done between October 1995 and June 1998 in the Theory of Condensed Matter group at the Cavendish Laboratory, Cambridge, under the supervision of Dr. M. C. Payne.

Except where stated otherwise, this dissertation is the result of my own work and contains nothing which is the outcome of work done in collaboration. This dissertation has not been submitted in whole or in part for any degree or diploma at this or any other university.

Peter Haynes
Cambridge, July 1998

O Lord, our Lord,
    how majestic is your name in all the earth!

You have set your glory
    above the heavens.
From the lips of children and infants
    you have ordained praise
because of your enemies,
    to silence the foe and the avenger.

When I consider your heavens,
    the work of your fingers,
the moon and the stars,
    which you have set in place,
what is man that you are mindful of him,
    the son of man that you care for him?
You made him a little lower than the heavenly beings
    and crowned him with glory and honour.

You made him ruler over the works of your hands;
    you put everything under his feet:
all flocks and herds,
    and the beasts of the field,
the birds of the air,
    and the fish of the sea,
    all that swim the paths of the seas.

O Lord, our Lord,
    how majestic is your name in all the earth!

Psalm 8

Acknowledgements

The research described in this dissertation was supported financially by an EPSRC studentship, and it is a great pleasure to be able to thank some of the people who have helped me in various ways, and whose support has been invaluable over the past three years.

My supervisor, Mike Payne, has been a faithful source of wisdom and encouragement throughout, as well as a generous supplier of wine. I am also grateful to Richard Needs and Roger Haydock for stimulating discussions which have helped to broaden my knowledge and understanding of condensed matter physics.

I am indebted to Nicola Marzari for his hospitality and also for pointing out several **k**-points, not least the concept of the roto-occupations (the f_{ij}). I also benefitted from discussions with Eric Sandré concerning computational minimisation schemes.

Thanks are due to those who have had the dubious pleasure of sharing offices with me: Murray Jarvis, Duncan Kerr, Yong Mao and Matt Segall have all made life at the Cavendish much more interesting than it would have been on my own.

Ian *Bung Bung* White has been a continual source of entertainment and diversion, whose initiative in proposing frequent experimental investigations into the aerodynamics of spinning disks and ellipsoids made the days pass much more quickly.

There is insufficient space to thank all my friends at Christ's College and St. Andrew the Great individually, but I value those times spent together which have contributed to making Cambridge a great place to live as well as to work.

Finally, I thank my family for their love and support, without which I would never have got here in the first place.

Contents

1 Introduction **1**
1.1 Quantum mechanics . . . 1
1.2 Computer simulations . . . 2
1.3 Dissertation outline . . . 3

2 Many-body Quantum Mechanics **5**
2.1 Principles of quantum mechanics . . . 5
2.1.1 Wave-functions and operators . . . 5
2.1.2 Expectation values . . . 7
2.1.3 Stationary states . . . 8
2.2 The Born-Oppenheimer approximation . . . 9
2.3 Identical particles . . . 12
2.3.1 Symmetries . . . 12
2.3.2 Spin and statistics . . . 13
2.4 Variational principles . . . 16

3 Quantum Mechanics of the Electron Gas **19**
3.1 Density-functional theory . . . 20
3.1.1 The Hohenberg-Kohn theorems . . . 20
3.1.2 The constrained search formulation . . . 22
3.1.3 Exchange and correlation . . . 23
3.1.4 The Kohn-Sham equations . . . 24
3.1.5 The local density approximation . . . 26
3.2 Periodic systems . . . 27
3.2.1 Bloch's theorem . . . 28
3.2.2 Brillouin zone sampling . . . 30
3.3 The pseudopotential approximation . . . 32
3.3.1 Operator approach . . . 33
3.3.2 Scattering approach . . . 34

3.3.3 Norm conservation . . . 35
3.3.4 Kleinman-Bylander representation . . . 37

4 Density-Matrix Formulation 39
4.1 The density-matrix . . . 40
4.2 Partial occupation of the Kohn-Sham orbitals . . . 42
4.3 Density-matrix DFT . . . 44
4.4 Constraints on the density-matrix . . . 45
4.4.1 Trace . . . 45
4.4.2 Idempotency . . . 45
4.4.3 Penalty functional . . . 46
4.4.4 Purifying transformation . . . 47
4.4.5 Idempotency-preserving variations . . . 48
4.5 Requirements for linear-scaling methods . . . 51
4.5.1 Separability . . . 51
4.5.2 Spatial localisation . . . 52
4.6 Non-orthogonal orbitals . . . 53

5 Localised basis-set 57
5.1 Introduction . . . 57
5.2 Origin of the basis functions . . . 58
5.3 Fourier transform of the basis functions . . . 60
5.4 Overlap matrix elements . . . 61
5.5 Kinetic energy matrix elements . . . 64
5.6 Non-local pseudopotential . . . 66
5.6.1 Green's function method . . . 66
5.6.2 Kleinman-Bylander form . . . 71
5.7 Computational implementation . . . 72

6 Penalty Functionals 75
6.1 Kohn's method . . . 75
6.1.1 Variational principle . . . 75
6.1.2 Implementation problems . . . 78
6.2 Corrected penalty functional method . . . 80
6.2.1 Derivation of the correction . . . 80
6.2.2 Further examples of penalty functionals . . . 86
6.2.3 Minimisation efficiency . . . 87

7 Computational implementation **91**
7.1 Total energy and Hamiltonian . . . 91
7.1.1 Kinetic energy . . . 92
7.1.2 Hartree energy and potential . . . 92
7.1.3 Exchange-correlation energy and potential . . . 93
7.1.4 Local pseudopotential . . . 94
7.1.5 Non-local pseudopotential . . . 95
7.2 Energy gradients . . . 95
7.2.1 Density-kernel derivatives . . . 95
7.2.2 Support function derivatives . . . 96
7.3 Penalty functional and electron number . . . 97
7.4 Physical interpretation . . . 98
7.5 Occupation number preconditioning . . . 100
7.6 Tensor properties of the gradients . . . 103
7.7 Practical details . . . 104
7.7.1 Expansion coefficient derivatives . . . 104
7.7.2 Normalisation constraint . . . 104
7.7.3 General outline of the scheme . . . 107

8 Relating linear-scaling and plane-wave methods **109**
8.1 Wave-functions from density-matrices . . . 109
8.2 Density-matrices from Kohn-Sham orbitals . . . 110
8.2.1 Projecting plane-wave eigenstates onto support functions . . . 110
8.2.2 Obtaining auxiliary matrices . . . 112
8.2.3 Optimising the support functions . . . 112
8.3 Density-matrix initialisation . . . 113

9 Results and discussion **115**
9.1 Bulk crystalline silicon . . . 115
9.1.1 Convergence with density-matrix cut-off . . . 115
9.1.2 Electronic density . . . 117
9.1.3 Predictions of physical properties . . . 117
9.2 Scaling . . . 120
9.2.1 System-size scaling . . . 121
9.2.2 Scaling with density-matrix cut-off . . . 121

10 Conclusions **125**

10.1 Summary . . . 125

10.2 Further work . . . 126

A Bessel function identities **129**

B Conjugate gradients **131**

Bibliography **137**

List of Figures

2.1 Indistinguishable particles in quantum mechanics. 12

3.1 Supercell approximation. 28
3.2 Pseudopotential approximation. 33

4.1 Purifying transformation. 48

5.1 Test of analytic kinetic energy matrix elements. 66
5.2 Green's function method for non-local pseudopotential. 70
5.3 Kleinman-Bylander method for non-local pseudopotential. 71

6.1 Kohn's penalty functional. 77
6.2 Schematic illustration of Kohn's variational principle. 78
6.3 Failure of quadratic interpolation for Kohn's penalty functional. 79
6.4 Convergence properties of Kohn's penalty functional. 80
6.5 One possible choice of analytic penalty functional. 81
6.6 Schematic illustration of the analytic penalty functional. 82
6.7 Variation of the occupation number errors with α. 83
6.8 Total energy, total functional and corrected energy versus α. 85
6.9 Two further examples of analytic penalty functionals. 87

7.1 Rate of convergence for different numbers of inner cycles. 107
7.2 Performance of the conjugate gradients algorithm. 108

9.1 Convergence of total energy with respect to support region radius. 116
9.2 Convergence of total energy with respect to density-kernel cut-off. 116
9.3 Electronic density in the (110) plane. 118
9.4 Diamond structure of silicon, highlighting a $\{110\}$ plane. 118
9.5 CASTEP electronic density. 119
9.6 Electronic density difference. 119
9.7 Energy-volume curve for silicon. 121

9.8 Variation of computational effort with system-size. 122

B.1 Steepest descents method. 132
B.2 Conjugate gradients method. 135

List of Tables

9.1 Parameters used to calculate energy-volume curve. 120
9.2 Comparison of calculated and experimental data for silicon. 120
9.3 Comparison of common crystal structures. 124

Chapter 1

Introduction

1.1 Quantum mechanics

Newton's *Principia Mathematica* was the climax of a revolution in man's perception of the Universe, resulting in the acceptance of mathematical physics as a reliable and powerful tool for describing nature. The same laws which accurately predicted the motion of planets around the sun also accounted for the trajectories of terrestrial projectiles, including that legendary windfall apple. So remarkable was the enormous range of scales over which the laws were observed to work, that many believed that they applied universally. Two centuries later, however, a second revolution took place in which classical Newtonian mechanics was found to be inadequate for explaining phenomena on the atomic scale, and a new theory was required. This theory was quantum mechanics.

Despite the philosophical questions of interpretation [1] which arise from the new theory, few question the astounding accuracy with which quantum mechanics describes the world around us. The favourite example cited is that of relativistic quantum field theory's prediction of the gyromagnetic ratio of the electron [2], which agrees with experiment [3] to better than one part in a million. Today there is little doubt that quantum theory applied to electrons and atomic nuclei provides the foundation for all of low-energy physics, chemistry and biology, and that if we wish to describe complex processes occurring in real materials precisely, we should attempt to solve the equations of quantum mechanics.

Unfortunately, the equations are too complicated to be solved analytically for all but the simplest (and hence most trivial) of systems. The only hope of bringing the power of quantum mechanics to bear on real phenomena of genuine interest to contemporary scientists, and of relevance to our society in general, is to solve the equations numerically by modelling the processes of interest computationally.

1.2 Computer simulations

Many aspects of computational modelling make it a worthy partner of experimental science. The chemist studying a particular reaction can reach into the computer simulation, alter bond lengths or angles, and then observe the effect of such changes on the process taking place. The geophysicist interested in phase transitions occurring deep inside the earth can model pressures and temperatures which could never be reached in a laboratory. All of this can be achieved with a single piece of apparatus – the computer itself.

Quantum-mechanical calculations stand out because they are by design *ab initio* i.e. from first-principles, calculations. They do not depend upon any external parameters except the atomic numbers of the constituent atoms to be modelled and cannot therefore be biased by preconceptions about the final result. Such calculations are reliable and can be used with confidence to predict the behaviour of nature.

Nevertheless, the same complexity which precludes exact analytical solution also results in the highly unfavourable scaling of computational effort and resources required. The computational demands of exact calculations grow exponentially with the size of the system being studied, so that they are too costly to be of significant practical use. Despite the relentless progress of computer technology, this scaling makes this approach inviable for some time yet.

Well-controlled approximations can be employed to enable the equations to be solved much more efficiently without sacrificing the predictive power or parameter-free nature of quantum-mechanical calculations. Much progress has been made in recent years in developing methods which exhibit polynomial rather than exponential scaling. One such method, that of density-functional theory, coupled with a simple description of the quantum-mechanical effects of exchange and correlation and the pseudopotential approximation, has proved to be remarkably successful and is currently applied worldwide by scientists in a wide range of disciplines. Even this method, however, requires a computational effort which scales with the cube of the system-size i.e. is $\mathcal{O}(N^3)$, and so is limited in the scale of simulation which can be realistically attempted.

The aim of the work described in this dissertation is to develop new schemes for performing density-functional calculations which lose none of the accuracy of current approaches, but which require an effort which scales only *linearly* with system-size i.e. $\mathcal{O}(N)$. A ten-fold increase in computing power then results in a ten-fold increase in accessible system-size. Therefore these methods are sought after not only because they increase the range of applicability of quantum-mechanical calculations now, but also because they will take full advantage of future improvements in computing resources.

1.3 Dissertation outline

In chapter 2 we outline some of the founding principles of quantum mechanics, highlighting the origin of the complexity of the problem of quantum-mechanical many-body systems, describing how the electronic and nuclear degrees of freedom can be separated and demonstrating the power of variational methods for solving the quantum-mechanical equations.

In chapter 3 we turn to a description of the problem of the inhomogeneous "gas" of interacting electrons moving in a static potential due to the nuclei. Density-functional theory allows us to tackle the many-body problem and obtain all of the ground-state properties of the electronic system. We outline in particular the local density approximation for exchange and correlation, the treatment of periodic systems and the pseudopotential approximation. The latter allows the calculation to be simplified by eliminating the chemically inert core electrons from the simulation.

In chapter 4 we generalise DFT to include partial occupation of single-particle states. From this the density-matrix formulation of density-functional theory can be derived, and we show how this can be used to obtain a foundation for linear-scaling methods. We discuss the various requirements this makes on the form of the density-matrix, and also the constraints which must be applied to obtain physically meaningful solutions, focusing in particular on the difficult idempotency condition. We also consider some of the issues which arise when the density-matrix is expressed in terms of a set of non-orthogonal functions.

In chapter 5 we address one of the issues raised by preliminary investigations: how to describe the density-matrix in real-space and still deal accurately with quantities naturally treated in reciprocal-space, particularly the kinetic energy. We propose a new set of localised basis functions, for which analytic results for the overlap, kinetic energy and non-local pseudopotential matrix elements can be obtained, thus satisfying the demand to concentrate on a real-space description while still evaluating these quantities accurately.

In chapter 6 we discuss the use of penalty functionals to impose the idempotency constraint. We begin by reviewing Kohn's proposal for the use of a penalty functional to exactly impose the idempotency constraint, and show how this is incompatible with computational minimisation schemes. We then present an original method which uses a penalty functional to approximately impose the idempotency constraint, but which still allows the use of efficient minimisation algorithms. Because the density-matrix obtained by this method is only approximately idempotent, the total energy calculated from it differs from the true ground-state energy. We therefore show how it is possible to derive a correction to the total energy from the penalty functional, which gives very accurate estimates of the true ground-state energy from only approximately idempotent density-matrices.

In chapter 7 we outline how the scheme of chapter 6 can be implemented computationally, focusing first on the calculation of the energy and its derivatives. We then examine these derivatives to show that the two types of variation which are made are equivalent to solving the Kohn-Sham equations and making the Hamiltonian and density-matrix commute. We describe how the gradients may be improved by preconditioning, and also how they should be corrected to take account of their tensor properties. Finally we discuss the imposition of the normalisation constraint, and give a general outline of the scheme as currently implemented.

In chapter 8 we describe methods for relating the different quantities used in traditional and linear-scaling calculations and show how the results obtained from one method can be used in the other. We concentrate on the application of such methods to obtain good initial density-matrices for linear-scaling calculations which can speed up the convergence to the ground-state solution.

In chapter 9 we present results for the scheme outlined in chapters 6 and 7 when applied to bulk crystalline silicon. We show how the energy converges as the range of the density-matrix is increased, and compare predicted physical properties with those calculated using traditional methods and with experiment. We also consider the scaling of the method with respect to system-size and the density-matrix range.

Finally in chapter 10 we summarise the results obtained so far and outline the direction for future work in this field.

Chapter 2

Many-body Quantum Mechanics

In this chapter we introduce some of the principles of many-body quantum mechanics, applied to systems consisting of atomic nuclei and electrons. First we outline the general principles of quantum mechanics, the properties of wave-functions and operators, which will later be used to reformulate the problem in terms of the density-matrix. We present the Born-Oppenheimer approximation used to separate the motion of the nuclei from that of the electrons, so that the problem is reduced to that of solving the equations of motion for an electron gas in a static potential. The consequences of the indistinguishability of identical particles are then discussed, as well as results of the relativistic theory of quantum mechanics which need to be included by hand in our non-relativistic treatment. Finally the powerful variational principle is introduced which is often used in solving the equations of quantum mechanics.

2.1 Principles of quantum mechanics

2.1.1 Wave-functions and operators

The theory of quantum mechanics is built upon the fundamental concepts of *wave-functions* and *operators*. The wave-function is a single-valued square-integrable function of the system parameters and time which provides a complete description of the system. Linear Hermitian operators act on the wave-function and correspond to the physical *observables*, those dynamical variables which can be measured, e.g. position, momentum and energy.

For systems of atomic nuclei[1] and electrons, which are the subject of this dissertation, the system parameters might be taken to be a set of position variables of the constituent particles (the notation adopted in this and the following chapters is to refer to electronic

[1] At the atomic energy scales which are of interest in this work, the nuclei are extremely well-described as massive point charges and their internal structure is safely neglected.

variables using a latin index and nuclear variables with a greek index) i.e. $\{\{\mathbf{r}_i\},\{\mathbf{r}_\alpha\}\}$, their momenta $\{\{\mathbf{p}_i\},\{\mathbf{p}_\alpha\}\}$ or even a mixture of the two e.g. $\{\{\mathbf{r}_i\},\{\mathbf{p}_\alpha\}\}$. In contrast to a Newtonian system which is completely described by the positions *and* momenta of its constituents, the quantum-mechanical wave-function is a function of only one of these parameters per particle[2]. The wave-function for the system is thus typically denoted by $\Psi\left(\{\mathbf{r}_i\},\{\mathbf{r}_\alpha\},t\right)$.

A notation due to Dirac [4] is often employed, which reflects the fact that this wave-function is simply one of many representations of a single *state-vector* in a Hilbert space, which is written as $|\Psi\rangle$, known as a *ket*. There also exists a *dual space* containing a set of *bra* vectors, denoted $\langle\Psi|$, defined by their scalar products and in one-to-one correspondence with the kets. The scalar product is written as a *braket* and is anti-linear in the first argument and linear in the second: thus $\langle\Psi|\Phi\rangle = (\langle\Phi|\Psi\rangle)^*$. It is worth noting here that state-vectors which differ only by a multiplicative non-zero complex constant describe the same state: we can thus restrict our interest to the set of *normalised* vectors defined such that the scalar product of the vector with its own conjugate equals unity:

$$\langle\Psi|\Psi\rangle = \int \prod_j \mathrm{d}\mathbf{r}_j \prod_\beta \mathrm{d}\mathbf{r}_\beta \;\Psi^*\left(\{\mathbf{r}_i\},\{\mathbf{r}_\alpha\},t\right)\Psi\left(\{\mathbf{r}_i\},\{\mathbf{r}_\alpha\},t\right) = 1. \tag{2.1}$$

The operator corresponding to some observable O is often written $\hat{O}$, and in general when this operator acts on some state-vector $|\Psi\rangle$, a different (not necessarily normalised) state-vector $|\Phi\rangle$ results:

$$\hat{O}|\Psi\rangle = |\Phi\rangle. \tag{2.2}$$

However, for each operator there exists a set of normalised *eigenstates*, say $\{|\chi_n\rangle\}$, which remain unchanged by the action of the operator i.e.

$$\hat{O}|\chi_n\rangle = \lambda_n|\chi_n\rangle, \tag{2.3}$$

in which the constant λ_n (always real for Hermitian operators) is the *eigenvalue*.

The postulates of quantum mechanics [5] state that for a system in state $|\Psi\rangle$:

- the outcome of a measurement of a dynamical variable is always one of the eigenvalues λ_n of the corresponding operator,
- immediately following a measurement, the state-vector collapses to the eigenstate $|\chi_n\rangle$ corresponding to the measured eigenvalue[3],

[2] We are neglecting spin in this discussion.

[3] For the case of eigenvalue degeneracy, the state-vector collapses to a vector lying in the subspace spanned by all of the eigenvectors corresponding to the measured eigenvalue.

- the probability of such a measurement[4] is

$$P(\lambda_n) = |\langle \chi_n | \Psi \rangle|^2 . \tag{2.4}$$

2.1.2 Expectation values

Much of the power of the theory comes from the fact that the quantum-mechanical states can be linearly superposed since this leads to no ambiguity in the action of linear operators[5]. We now consider the quantity $\langle \Psi | \hat{O} | \Psi \rangle$. From Sturm-Liouville theory, the eigenstates of the operator $\hat{O}$ form a *complete set*, which means that any valid state-vector can be expressed as a linear superposition of those eigenstates with appropriate complex coefficients $\{c_n\}$:

$$|\Psi\rangle = \sum_n c_n |\chi_n\rangle. \tag{2.5}$$

These coefficients are easily obtained for Hermitian operators because the eigenstates are *orthogonal* (or can always be chosen to be orthogonal in the case of degenerate eigenvalues) which means that the scalar product of two different eigenstates vanishes:

$$\langle \chi_n | \chi_m \rangle = \delta_{nm}. \tag{2.6}$$

Either taking scalar products of both sides of equation 2.5 with the eigenstates $\{\langle \chi_m |\}$, or by using the following concise expression of completeness;

$$\sum_n |\chi_n\rangle\langle\chi_n| = 1, \tag{2.7}$$

the expansion coefficients $\{c_n\}$ can be determined:

$$\begin{aligned} c_n &= \langle \chi_n | \Psi \rangle, && (2.8) \\ |\Psi\rangle &= \sum_n |\chi_n\rangle\langle\chi_n|\Psi\rangle. && (2.9) \end{aligned}$$

Now this result is applied to the quantity $\langle \Psi | \hat{O} | \Psi \rangle$:

$$\begin{aligned} \langle \Psi | \hat{O} | \Psi \rangle &= \sum_m \left(\langle \chi_m | \Psi \rangle\right)^* \langle \chi_m | \hat{O} \sum_n |\chi_n\rangle\langle\chi_n|\Psi\rangle \\ &= \sum_n \lambda_n \, |\langle \chi_n | \Psi \rangle|^2 && (2.10) \end{aligned}$$

[4]Again, for the degenerate case, the probabilities must be summed for all eigenvectors corresponding to the measured eigenvalue.

[5]For a linear operator $\hat{O}$, $\hat{O}(\alpha|A\rangle + \beta|B\rangle) = \alpha\hat{O}|A\rangle + \beta\hat{O}|B\rangle$.

in which we have used the fact that $\hat{O}$ is linear, that the $\{|\chi_n\rangle\}$ are eigenstates of $\hat{O}$ (2.3) and the orthonormality relation (2.6).

Since the only possible outcomes of a measurement of the observable O corresponding to operator $\hat{O}$ are the eigenvalues $\{\lambda_n\}$, with corresponding probabilities $|\langle\chi_n|\Psi\rangle|^2$ (2.4), the quantity $\langle\Psi|\hat{O}|\Psi\rangle$ is to be interpreted as the *expectation value* of O for a system in state $|\Psi\rangle$. The normalisation condition $\langle\Psi|\Psi\rangle = 1$ corresponds to the condition that the probabilities sum to unity.

2.1.3 Stationary states

The final postulate of quantum mechanics states that between measurements, the state-vector evolves in time according to the time-dependent Schrödinger equation[6]:

$$\hat{H}|\Psi\rangle = \mathrm{i}\frac{\partial}{\partial t}|\Psi\rangle. \tag{2.11}$$

This treatment is non-relativistic: for heavy atoms there are significant relativistic effects but these can be incorporated *a posteriori* in the construction of the pseudopotentials (see 3.3). The operator $\hat{H}$ is known as the Hamiltonian and is the energy operator, which for systems of atomic nuclei and electrons takes the form

$$\hat{H} = -\frac{1}{2}\sum_i \nabla_i^2 - \sum_\alpha \frac{1}{2m_\alpha}\nabla_\alpha^2 - \sum_i\sum_\alpha \frac{Z_\alpha}{|\mathbf{r}_i - \mathbf{r}_\alpha|} + \frac{1}{2}\sum_i\sum_{j\neq i}\frac{1}{|\mathbf{r}_i - \mathbf{r}_j|} + \frac{1}{2}\sum_\alpha\sum_{\beta\neq\alpha}\frac{Z_\alpha Z_\beta}{|\mathbf{r}_\alpha - \mathbf{r}_\beta|} \tag{2.12}$$

in which the nuclear masses m_α and atomic numbers Z_α appear. The first two terms on the right-hand side represent the kinetic energies of the electrons and nuclei respectively. The subsequent terms describe the electron-nuclear, electron-electron and inter-nuclear Coulomb interaction energies respectively.

Finally we note that if we solve the time-independent Schrödinger equation, the eigenvalue equation for the Hamiltonian, then the time-dependence of the wave-function takes a particularly simple form. The following separation of variables is made:

$$\Psi\left(\{\mathbf{r}_i\},\{\mathbf{r}_\alpha\},t\right) = \tilde{\Psi}\left(\{\mathbf{r}_i\},\{\mathbf{r}_\alpha\}\right)\Theta(t) \tag{2.13}$$

which is successful and leads to the following equations, where E is the separation constant:

$$\begin{aligned} \hat{H}\tilde{\Psi}\left(\{\mathbf{r}_i\},\{\mathbf{r}_\alpha\}\right) &= E\tilde{\Psi}\left(\{\mathbf{r}_i\},\{\mathbf{r}_\alpha\}\right), && (2.14)\\ \mathrm{i}\frac{\mathrm{d}}{\mathrm{d}t}\Theta(t) &= E\Theta(t). && (2.15) \end{aligned}$$

[6] Atomic units are used throughout (unless otherwise stated): $\hbar = m_\mathrm{e} = e = 4\pi\varepsilon_0 = 1$.

The ordinary differential equation 2.15 is straightforwardly solved, so that eigenfunctions of the Hamiltonian with energy E take the form:

$$\Psi\left(\{\mathbf{r}_i\},\{\mathbf{r}_\alpha\},t\right)=\tilde{\Psi}\left(\{\mathbf{r}_i\},\{\mathbf{r}_\alpha\}\right)\exp\left(-\mathrm{i}Et\right). \tag{2.16}$$

States which are eigenfunctions of the Hamiltonian are also known as *stationary states* because the expectation values of time-independent operators for these states are also independent of time:

$$\begin{aligned}\langle\Psi|\hat{O}|\Psi\rangle &= \int\prod_j \mathrm{d}\mathbf{r}_j \prod_\beta \mathrm{d}\mathbf{r}_\beta\ \Psi^*\left(\{\mathbf{r}_i\},\{\mathbf{r}_\alpha\}\right)\hat{O}\Psi\left(\{\mathbf{r}_i\},\{\mathbf{r}_\alpha\}\right)\\ &= \int\prod_j \mathrm{d}\mathbf{r}_j \prod_\beta \mathrm{d}\mathbf{r}_\beta\ \tilde{\Psi}^*\left(\{\mathbf{r}_i\},\{\mathbf{r}_\alpha\}\right)\exp\left(\mathrm{i}Et\right)\hat{O}\tilde{\Psi}\left(\{\mathbf{r}_i\},\{\mathbf{r}_\alpha\}\right)\exp\left(-\mathrm{i}Et\right)\\ &= \langle\tilde{\Psi}|\hat{O}|\tilde{\Psi}\rangle. \end{aligned} \tag{2.17}$$

From now on we shall be dealing with eigenstates of the Hamiltonian, and so will suppress the exponential time-dependence of the state and deal directly with the time-independent state $|\tilde{\Psi}\rangle$ instead.

2.2 The Born-Oppenheimer approximation

The forces on both electrons and nuclei due to their electric charge are of the same order of magnitude, and so the changes which occur in their momenta as a result of these forces must also be the same. One might, therefore, assume that the actual momenta of the electrons and nuclei were of similar magnitude. In this case, since the nuclei are so much more massive than the electrons, they must accordingly have much smaller velocities. Thus it is plausible that on the typical time-scale of the nuclear motion, the electrons will very rapidly relax to the instantaneous ground-state configuration, so that in solving the time-independent Schrödinger equation resulting from the Hamiltonian in equation 2.12, we can assume that the nuclei are stationary and solve for the electronic ground-state first, and then calculate the energy of the system in that configuration and solve for the nuclear motion. This separation of electronic and nuclear motion is known as the Born-Oppenheimer approximation [6].

Following Ziman [7], we assume the following form of an eigenfunction for the Hamiltonian (2.12):

$$\tilde{\Psi}\left(\{\mathbf{r}_i\},\{\mathbf{r}_\alpha\}\right)=\Psi\left(\{\mathbf{r}_i\};\{\mathbf{r}_\alpha\}\right)\Phi\left(\{\mathbf{r}_\alpha\}\right) \tag{2.18}$$

and require that $\Psi\left(\{\mathbf{r}_i\};\{\mathbf{r}_\alpha\}\right)$ (which is a *wave*-function only of the $\{\mathbf{r}_i\}$ with the $\{\mathbf{r}_\alpha\}$

as parameters) satisfies the time-independent Schrödinger equation for the electrons in a static array of nuclei:

$$\left[-\frac{1}{2}\sum_i \nabla_i^2 - \sum_i \sum_\alpha \frac{Z_\alpha}{|\mathbf{r}_i - \mathbf{r}_\alpha|} + \frac{1}{2}\sum_i \sum_{j\neq i} \frac{1}{|\mathbf{r}_i - \mathbf{r}_j|}\right] \Psi\left(\{\mathbf{r}_i\};\{\mathbf{r}_\alpha\}\right) = \mathcal{E}_\mathrm{e}\left(\{\mathbf{r}_\alpha\}\right)\Psi\left(\{\mathbf{r}_i\};\{\mathbf{r}_\alpha\}\right) \tag{2.19}$$

in which the dependence of the eigenvalues $\mathcal{E}_\mathrm{e}$ on the nuclear positions is acknowledged. Applying the full Hamiltonian (2.12) to the whole wave-function:

$$\begin{aligned}\hat{H}\tilde{\Psi}\left(\{\mathbf{r}_i\},\{\mathbf{r}_\alpha\}\right) &= \left[-\sum_\beta \frac{1}{2m_\beta}\nabla_\beta^2 + \mathcal{E}_\mathrm{e}\left(\{\mathbf{r}_\alpha\}\right) + \frac{1}{2}\sum_\beta\sum_{\gamma\neq\beta}\frac{Z_\beta Z_\gamma}{|\mathbf{r}_\beta - \mathbf{r}_\gamma|}\right]\tilde{\Psi}\left(\{\mathbf{r}_i\},\{\mathbf{r}_\alpha\}\right) \\ &= \Psi\left(\{\mathbf{r}_i\};\{\mathbf{r}_\alpha\}\right)\left[-\sum_\beta \frac{1}{2m_\beta}\nabla_\beta^2 + \mathcal{E}_\mathrm{e}\left(\{\mathbf{r}_\alpha\}\right) + \frac{1}{2}\sum_\beta\sum_{\gamma\neq\beta}\frac{Z_\beta Z_\gamma}{|\mathbf{r}_\beta - \mathbf{r}_\gamma|}\right]\Phi\left(\{\mathbf{r}_\alpha\}\right) \\ &\quad -\sum_\beta \frac{1}{2m_\beta}\Big[2\nabla_\beta\Phi\left(\{\mathbf{r}_\alpha\}\right)\cdot\nabla_\beta\Psi\left(\{\mathbf{r}_i\};\{\mathbf{r}_\alpha\}\right) + \Phi\left(\{\mathbf{r}_\alpha\}\right)\nabla_\beta^2\Psi\left(\{\mathbf{r}_i\};\{\mathbf{r}_\alpha\}\right)\Big]\end{aligned} \tag{2.20}$$

The energy $\mathcal{E}_\mathrm{e}\left(\{\mathbf{r}_\alpha\}\right)$ is called the *adiabatic* contribution of the electrons to the energy of the system. The remaining non-adiabatic terms contribute very little to the energy, which can be demonstrated using time-independent perturbation theory [8]. The first order correction arising from the first non-adiabatic term in the last line of equation 2.20 is of the form:

$$\begin{aligned}& -\int\prod_j \mathrm{d}\mathbf{r}_j \prod_\beta \mathrm{d}\mathbf{r}_\beta \Psi^*\left(\{\mathbf{r}_i\};\{\mathbf{r}_\alpha\}\right)\Phi^*\left(\{\mathbf{r}_\alpha\}\right)\sum_\gamma\frac{1}{m_\gamma}\Big[\nabla_\gamma\Phi\left(\{\mathbf{r}_\alpha\}\right)\cdot\nabla_\gamma\Psi\left(\{\mathbf{r}_i\};\{\mathbf{r}_\alpha\}\right) \\ = \; & -\sum_\gamma\int\prod_\beta \mathrm{d}\mathbf{r}_\beta\Phi^*\left(\{\mathbf{r}_\alpha\}\right)\nabla_\gamma\Phi\left(\{\mathbf{r}_\alpha\}\right)\cdot\left[\int\prod_j \mathrm{d}\mathbf{r}_j\Psi^*\left(\{\mathbf{r}_i\};\{\mathbf{r}_\alpha\}\right)\nabla_\gamma\Psi\left(\{\mathbf{r}_i\};\{\mathbf{r}_\alpha\}\right)\right]\end{aligned} \tag{2.21}$$

and the term in square brackets can be rewritten

$$\begin{aligned}\int\prod_j \mathrm{d}\mathbf{r}_j\Psi^*\left(\{\mathbf{r}_i\};\{\mathbf{r}_\alpha\}\right)\nabla_\gamma\Psi\left(\{\mathbf{r}_i\};\{\mathbf{r}_\alpha\}\right) &= \tfrac{1}{2}\nabla_\gamma\int\prod_j \mathrm{d}\mathbf{r}_j\left|\Psi\left(\{\mathbf{r}_i\};\{\mathbf{r}_\alpha\}\right)\right|^2 \\ &= \tfrac{1}{2}\nabla_\gamma(1) = 0,\end{aligned} \tag{2.22}$$

since the normalisation of the electronic wave-function does not change when the nuclei move, so that the first order contribution vanishes. The second-order shift due to this term does not vanish and gives rise to transitions between electronic states as the ions move, otherwise known as the electron-phonon interaction, which will modify the energy.

The second non-adiabatic term in the final term of equation 2.20 will be largest when the electrons labelled i are tightly bound to the nuclei labelled α in which case $\Psi(\{\mathbf{r}_i\};\{\mathbf{r}_\alpha\}) = \Psi\left(\{\mathbf{u}_{(i,\alpha)}\}\right)$ where $\mathbf{u}_{(i,\alpha)} = \mathbf{r}_i - \mathbf{r}_\alpha$ and the first order correction from this term is

$$
\begin{aligned}
& -\int \prod_j \mathrm{d}\mathbf{r}_j \prod_\beta \mathrm{d}\mathbf{r}_\beta \Psi^*\left(\{\mathbf{u}_{(i,\alpha)}\}\right)\Phi^*\left(\{\mathbf{r}_\alpha\}\right)\sum_\gamma \frac{1}{2m_\gamma}\Big[\Phi\left(\{\mathbf{r}_\alpha\}\right)\nabla_\gamma^2\Psi\left(\{\mathbf{u}_{(i,\alpha)}\}\right)\Big] \\
= \; & -\sum_\gamma \frac{1}{2m_\gamma}\left[\int \prod_\beta \mathrm{d}\mathbf{r}_\beta \left|\Phi\left(\{\mathbf{r}_\alpha\}\right)\right|^2\right]\left[\int \prod_{(j,\beta)} \mathrm{d}\mathbf{u}_{(j,\beta)}\Psi^*\left(\{\mathbf{u}_{(i,\alpha)}\}\right)\nabla_\gamma^2\Psi\left(\{\mathbf{u}_{(i,\alpha)}\}\right)\right] \\
= \; & -\sum_{(k,\gamma)}\frac{1}{m_\gamma}\int \prod_{(j,\beta)} \mathrm{d}\mathbf{u}_{(j,\beta)}\Psi^*\left(\{\mathbf{u}_{(i,\alpha)}\}\right)\frac{1}{2}\nabla_{(k,\gamma)}^2\Psi\left(\{\mathbf{u}_{(i,\alpha)}\}\right),
\end{aligned} \tag{2.23}
$$

and this quantity is of the order of the electronic kinetic energy multiplied by the ratio of the electron and nuclear masses, typically a factor of the order of 10^{-4} or 10^{-5}, so that the contributions from this term to all orders can be neglected.

We therefore neglect the non-adiabatic terms and note that equation 2.20 is satisfied if $\Phi(\{\mathbf{r}_\alpha\})$ obeys a Schrödinger equation of the form

$$
\left[-\sum_\beta \frac{1}{2m_\beta}\nabla_\beta^2 + \mathcal{E}_{\mathrm{e}}(\{\mathbf{r}_\alpha\}) + \frac{1}{2}\sum_\beta\sum_{\gamma\neq\beta}\frac{Z_\beta Z_\gamma}{|\mathbf{r}_\beta - \mathbf{r}_\gamma|}\right]\Phi\left(\{\mathbf{r}_\alpha\}\right) = \mathcal{E}\Phi\left(\{\mathbf{r}_\alpha\}\right). \tag{2.24}
$$

This adiabatic principle is crucial because it allows us to separate the nuclear and electronic motion, leaving a residual electron-phonon interaction. From this point on it is assumed that the electrons respond instantaneously to the nuclear motion and always occupy the ground-state of that nuclear configuration. Varying the nuclear positions maps out a multi-dimensional ground-state potential energy surface, and the motion of the nuclei in this potential can then be solved. In practice Newtonian mechanics generally suffices for this part of the problem[7], and relaxation of the nuclear positions to the minimum-energy configuration or molecular dynamics [11, 12] can be performed. These aspects go beyond the scope of this dissertation so that from now on it is assumed that a system with a fixed nuclear configuration is to be treated, so that the electronic energy $\mathcal{E}_{\mathrm{e}}$ is a constant and the electronic wave-function $\Psi(\{\mathbf{r}_i\})$ obeys the Schrödinger equation 2.19. The dependence of the electronic wave-function on the nuclear positions $\{\mathbf{r}_\alpha\}$ is now suppressed.

[7] The most notable exception to this rule is the motion of hydrogen, which is often treated using the path-integral formulation of quantum mechanics [9, 10].

2.3 Identical particles

2.3.1 Symmetries

It is a consequence of quantum mechanics, usually expressed in the terms of the Heisenberg uncertainty principle that, in contrast to Newtonian mechanics, the trajectory of a particle is undefined. When dealing with identical particles this leads to complications, as illustrated in figure 2.1.

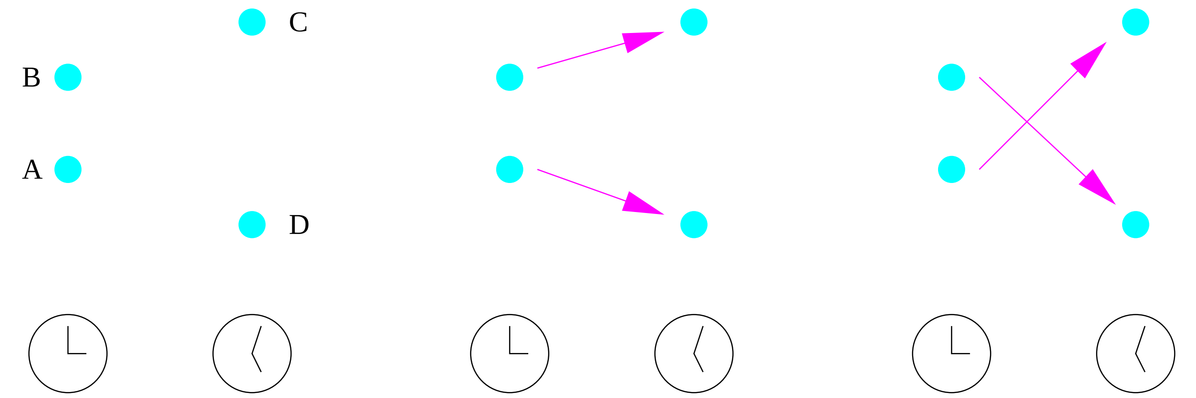

Figure 2.1: Indistinguishable particles in quantum mechanics: (left) initially there are two particles at A and B, later on two particles are found at C and D; (middle) but we cannot be certain whether the particles travelled from A to D and B to C or (right) from A to C and B to D, because they are identical.

Consider a system of two identical particles represented by the wave-function $\Psi(\mathbf{r}_1, \mathbf{r}_2)$ and a particle-exchange operator $\hat{P}_{12}$ which swaps the particles i.e.

$$\hat{P}_{12}\Psi(\mathbf{r}_1, \mathbf{r}_2) = \Psi(\mathbf{r}_2, \mathbf{r}_1). \tag{2.25}$$

However, since the system must be unchanged by such an exchange of identical particles, the two states appearing in equation 2.25 must be the same and hence differ only by a multiplicative complex constant;

$$\Psi(\mathbf{r}_2, \mathbf{r}_1) = c\Psi(\mathbf{r}_1, \mathbf{r}_2), \tag{2.26}$$

so that many-body wave-functions of identical particles must be eigenstates of the particle interchange operator. Performing the exchange twice clearly returns the system precisely to its original state and so leads to

$$\hat{P}_{12}^2\Psi(\mathbf{r}_1, \mathbf{r}_2) = c^2\Psi(\mathbf{r}_1, \mathbf{r}_2) = \Psi(\mathbf{r}_1, \mathbf{r}_2) \tag{2.27}$$

i.e. $c^2 = 1$ so $c = \pm 1$, and the many-body wave-function at most changes sign under particle exchange. This result is readily extended to systems of more than two identical particles, so that the wave-functions are either symmetric or antisymmetric under exchange of any two identical particles.

2.3.2 Spin and statistics

It is necessary to go to the full relativistic theory of quantum mechanics in order to ascertain which sign is appropriate to a system of particles, although the result itself is simple enough to express[8]. A result of the relativistic theory is that particles may possess intrinsic angular momentum known as *spin*, which is quantised in units of $\frac{1}{2}$. A brief outline of the relationship between spin and statistics follows.

We use the method of *second quantisation* of fields of particles with spin (see [14]). For a system of free non-interacting particles, the single-particle states are characterised by linear momentum $\mathbf{p}$ and spin σ. We denote the occupation numbers of these states $N_{\mathbf{p}\sigma}$, but for now we will only consider situations in which every single-particle state is either empty or singly occupied, and in addition will consider a system of at most two particles and focus on just two single-particle states. The state-vector is represented by a series of "slots", whose order is important at this stage, each containing an occupation number. Thus $|1_{\mathbf{p}\sigma}, 1_{\mathbf{p}'\sigma'}\rangle$ denotes a state in which a particle was put in state $(\mathbf{p}'\sigma')$ and then a second particle was added in state $(\mathbf{p}\sigma)$.

Annihilation and creation operators[9] $\hat{a}_{\mathbf{p}\sigma}$, $\hat{a}^\dagger_{\mathbf{p}\sigma}$ are introduced for each state which act in the following manner:

$$\hat{a}_{\mathbf{p}\sigma}|1_{\mathbf{p}\sigma}\rangle = |0\rangle, \tag{2.28}$$

$$\hat{a}^\dagger_{\mathbf{p}\sigma}|0\rangle = |1_{\mathbf{p}\sigma}\rangle. \tag{2.29}$$

In order that the sign of the state is unambiguously defined in this notation, it is necessary for consistency that creation operators act on the right-most void and annihilation operators act on the left-most appropriately-filled slot.

We now consider the state $|1_{\mathbf{p}\sigma}, 1_{\mathbf{p}'\sigma'}\rangle$ and use the exchange operator $\hat{a}^\dagger_{\mathbf{p}'\sigma'}\hat{a}^\dagger_{\mathbf{p}\sigma}\hat{a}_{\mathbf{p}\sigma}\hat{a}_{\mathbf{p}'\sigma'}$ to obtain the state $|1_{\mathbf{p}'\sigma'}, 1_{\mathbf{p}\sigma}\rangle$, in which particles have been exchanged between state $(\mathbf{p}\sigma)$ and $(\mathbf{p}'\sigma')$:

$$\hat{a}^\dagger_{\mathbf{p}'\sigma'}\hat{a}^\dagger_{\mathbf{p}\sigma}\hat{a}_{\mathbf{p}\sigma}\hat{a}_{\mathbf{p}'\sigma'}|1_{\mathbf{p}\sigma}, 1_{\mathbf{p}'\sigma'}\rangle = \hat{a}^\dagger_{\mathbf{p}'\sigma'}\hat{a}^\dagger_{\mathbf{p}\sigma}\hat{a}_{\mathbf{p}\sigma}|1_{\mathbf{p}\sigma}, 0\rangle = \hat{a}^\dagger_{\mathbf{p}'\sigma'}\hat{a}^\dagger_{\mathbf{p}\sigma}|0, 0\rangle$$

[8]Berry [13] has recently proposed a non-relativistic explanation involving a geometric phase.

[9]Neither the creation nor annihilation operators are Hermitian, and so they do not correspond to physical observables.

$$= \hat{a}^{\dagger}_{\mathbf{p}'\sigma'}|0, 1_{\mathbf{p}\sigma}\rangle = |1_{\mathbf{p}'\sigma'}, 1_{\mathbf{p}\sigma}\rangle. \tag{2.30}$$

The initial discussion in this section showed that under this exchange, the wave-function at most changes sign. This requires that the creation and annihilation operators obey one of two sets of commutation rules, as we will now show. The first set is due to Bose and can be summarised by:

$$\begin{aligned}
\left[\hat{a}^{\dagger}_{\mathbf{p}\sigma}, \hat{a}_{\mathbf{p}'\sigma'}\right] &= \delta_{\mathbf{p}\mathbf{p}'}\delta_{\sigma\sigma'}, && (2.31)\\
\left[\hat{a}_{\mathbf{p}\sigma}, \hat{a}_{\mathbf{p}'\sigma'}\right] &= 0, && (2.32)\\
\text{where } [\hat{p}, \hat{q}] &= \hat{p}\hat{q} - \hat{q}\hat{p}. && (2.33)
\end{aligned}$$

Under the Bose commutation rules, the two creation operators in the exchange operator, which refer to different states, commute and so can be swapped, and the result is that

$$\begin{aligned}
\hat{a}^{\dagger}_{\mathbf{p}'\sigma'}\hat{a}^{\dagger}_{\mathbf{p}\sigma}\hat{a}_{\mathbf{p}\sigma}\hat{a}_{\mathbf{p}'\sigma'}|1_{\mathbf{p}\sigma}, 1_{\mathbf{p}'\sigma'}\rangle &= |1_{\mathbf{p}'\sigma'}, 1_{\mathbf{p}\sigma}\rangle\\
= \hat{a}^{\dagger}_{\mathbf{p}\sigma}\hat{a}^{\dagger}_{\mathbf{p}'\sigma'}\hat{a}_{\mathbf{p}\sigma}\hat{a}_{\mathbf{p}'\sigma'}|1_{\mathbf{p}\sigma}, 1_{\mathbf{p}'\sigma'}\rangle &= |1_{\mathbf{p}\sigma}, 1_{\mathbf{p}'\sigma'}\rangle && (2.34)
\end{aligned}$$

i.e. states describing particles whose creation and annihilation operators obey the Bose commutation rules (*bosons*) must have symmetric wave-functions.

The second set of commutation rules, which is due to Fermi, describes *fermions*:

$$\begin{aligned}
\left\{\hat{a}^{\dagger}_{\mathbf{p}\sigma}, \hat{a}_{\mathbf{p}'\sigma'}\right\} &= \delta_{\mathbf{p}\mathbf{p}'}\delta_{\sigma\sigma'}, && (2.35)\\
\left\{\hat{a}_{\mathbf{p}\sigma}, \hat{a}_{\mathbf{p}'\sigma'}\right\} &= 0, && (2.36)\\
\text{where } \{\hat{p}, \hat{q}\} &= \hat{p}\hat{q} + \hat{q}\hat{p}, && (2.37)
\end{aligned}$$

and gives rise to antisymmetric wave-functions:

$$\begin{aligned}
\hat{a}^{\dagger}_{\mathbf{p}'\sigma'}\hat{a}^{\dagger}_{\mathbf{p}\sigma}\hat{a}_{\mathbf{p}\sigma}\hat{a}_{\mathbf{p}'\sigma'}|1_{\mathbf{p}\sigma}, 1_{\mathbf{p}'\sigma'}\rangle &= |1_{\mathbf{p}'\sigma'}, 1_{\mathbf{p}\sigma}\rangle\\
= -\hat{a}^{\dagger}_{\mathbf{p}\sigma}\hat{a}^{\dagger}_{\mathbf{p}'\sigma'}\hat{a}_{\mathbf{p}\sigma}\hat{a}_{\mathbf{p}'\sigma'}|1_{\mathbf{p}\sigma}, 1_{\mathbf{p}'\sigma'}\rangle &= -|1_{\mathbf{p}\sigma}, 1_{\mathbf{p}'\sigma'}\rangle. && (2.38)
\end{aligned}$$

In particular, note that the Fermi rules (equation 2.36 for $(\mathbf{p}\sigma) = (\mathbf{p}'\sigma')$) require that

$$\hat{a}_{\mathbf{p}\sigma}\hat{a}_{\mathbf{p}\sigma} = \hat{a}^{\dagger}_{\mathbf{p}\sigma}\hat{a}^{\dagger}_{\mathbf{p}\sigma} = 0 \tag{2.39}$$

i.e. it is impossible to put more than one fermion in any single-particle state. This result is known as the Pauli exclusion principle and it is ultimately responsible for the stability of matter. In an atom, for instance, the Pauli exclusion principle prevents all of the electrons from falling into the lowest-lying energy level.

Thus all systems of identical particles must subscribe to one of the sets of rules above: bosons have symmetric wave-functions and fermions antisymmetric wave-functions.

The second result of the relativistic theory which needs to be considered is the existence of *antiparticles*, which have the same mass but opposite charge to their corresponding particles. The antiparticles are assigned their own set of creation and annihilation operators, denoted $\hat{b}^{\dagger}_{\mathbf{p}\sigma}$ and $\hat{b}_{\mathbf{p}\sigma}$ respectively, which obey the same commutation rules as the particle operators.

The creation and annihilation operators can be combined to form a Hermitian product, the *number operator*, $\hat{N}_{\mathbf{p}\sigma} = \hat{a}^{\dagger}_{\mathbf{p}\sigma}\hat{a}_{\mathbf{p}\sigma}$, so-called because its action is simply to return the number of particles in state $(\mathbf{p}\sigma)$. For antiparticles, $\hat{\bar{N}}_{\mathbf{p}\sigma} = \hat{b}^{\dagger}_{\mathbf{p}\sigma}\hat{b}_{\mathbf{p}\sigma}$.

Using the method of second quantisation, the Hamiltonian can be written as (see [15]):

$$\hat{H} = \sum_{\mathbf{p}} \sum_{\sigma} \varepsilon(\mathbf{p}) \left(\hat{a}^{\dagger}_{\mathbf{p}\sigma}\hat{a}_{\mathbf{p}\sigma} \pm \hat{b}_{\mathbf{p}\sigma}\hat{b}^{\dagger}_{\mathbf{p}\sigma} \right) \tag{2.40}$$

where the $\varepsilon(\mathbf{p}) = \sqrt{\mathbf{p}^2 + m^2}$ are the energies of the single-particle states, and the plus sign occurs for particles of integral spin and the minus sign for particles with half-integral spin. We note that the particle creation and annihilation operators occur in the correct order to be rewritten as the particle number operator, whereas the antiparticle operators are in the wrong order, so we can use the appropriate set of commutation rules to reverse this order. The Hamiltonian for free particles must be positive-definite, and therefore turns out to be of the form

$$\hat{H} = \sum_{\mathbf{p}} \sum_{\sigma} \varepsilon(\mathbf{p}) \left(\hat{N}_{\mathbf{p}\sigma} + \hat{\bar{N}}_{\mathbf{p}\sigma} + 1 \right). \tag{2.41}$$

The constant $\sum_{\mathbf{p}} \sum_{\sigma} \varepsilon(\mathbf{p})$ in equation 2.41 represents the energy of the vacuum and is usually ignored. In order to obtain the Hamiltonian in this form, particles with half-integral spin (minus sign in 2.40) must have creation and annihilation operators which anticommute according to the Fermi rules, whereas particles with integral spin (plus sign in 2.40) must have operators which commute according to the Bose rules.

We thus come to the following conclusions:

- particles with half-integral spin are fermions and have antisymmetric wave-functions,
- particles with integral spin are bosons and have symmetric wave-functions.

In particular, electrons (which have spin $\frac{1}{2}$) are fermions with antisymmetric wave-functions and obey the Pauli exclusion principle. These consequences of relativistic quantum mechanics must be carried over by hand into the non-relativistic theory if we are to correctly describe nature.

In this dissertation we will not address the issues which arise in spin-polarised systems, in which the numbers of electrons in different spin states differ. In our case, it is only necessary to ensure that the many-body electronic wave-function is antisymmetric under exchange and that each single-particle state is never more than doubly-occupied (with one spin "up" electron and one spin "down").

2.4 Variational principles

In section 2.1 we outlined the basic principles of quantum mechanics, and in particular noted the rôle of the quantity $\langle\Psi|\hat{O}|\Psi\rangle$ as the expectation value of the observable corresponding to the operator $\hat{O}$. In that section, mention was briefly made of the relationship:

$$\langle\Psi|\Psi\rangle = \sum_n |\langle\chi_n|\Psi\rangle|^2 \tag{2.42}$$

which is simply derived from equations 2.5, 2.6 and 2.8. If we relax the restriction on orthonormalisation, the expression for the expectation value becomes

$$\langle O\rangle = \frac{\langle\Psi|\hat{O}|\Psi\rangle}{\langle\Psi|\Psi\rangle}. \tag{2.43}$$

We now consider the expectation value of the Hamiltonian operator for the electrons, defined in equation 2.19 and reproduced here:

$$\hat{H}|\Psi\rangle = \left[-\frac{1}{2}\sum_i \nabla_i^2 - \sum_i\sum_\alpha \frac{Z_\alpha}{|\mathbf{r}_i - \mathbf{r}_\alpha|} + \frac{1}{2}\sum_i\sum_{j\neq i}\frac{1}{|\mathbf{r}_i - \mathbf{r}_j|}\right]|\Psi\rangle = E|\Psi\rangle \tag{2.44}$$

in which the electronic energy is now labelled E, and the dependence on the nuclear coordinates is suppressed since the nuclei are assumed to be static following the conclusions of section 2.2. This equation is an eigenvalue equation for a linear Hermitian operator, and as such can always be recast in the form of finding the stationary points of a functional subject to a constraint.

Consider the expectation value of the Hamiltonian $\langle E\rangle = E[\Psi]$ which is a functional of the wave-function, and make a small variation to the state-vector: $|\Psi\rangle \to |\Psi\rangle + |\delta\Psi\rangle$. The change in $E[\Psi]$ is given by

$$\begin{aligned} \delta E[\Psi] &= E[\Psi+\delta\Psi] - E[\Psi] \\ &= \frac{\langle\Psi+\delta\Psi|\hat{H}|\Psi+\delta\Psi\rangle}{\langle\Psi+\delta\Psi|\Psi+\delta\Psi\rangle} - \frac{\langle\Psi|\hat{H}|\Psi\rangle}{\langle\Psi|\Psi\rangle} \end{aligned}$$

$$= \frac{\langle\delta\Psi|\hat{H}|\Psi\rangle + \langle\Psi|\hat{H}|\delta\Psi\rangle}{\langle\Psi|\Psi\rangle} - \frac{\langle\Psi|\hat{H}|\Psi\rangle}{(\langle\Psi|\Psi\rangle)^2}\left(\langle\delta\Psi|\Psi\rangle + \langle\Psi|\delta\Psi\rangle\right) + O\left(\delta\Psi^2\right)$$

$$= \frac{1}{\langle\Psi|\Psi\rangle}\left[\langle\delta\Psi|\left(\hat{H}|\Psi\rangle - E[\Psi]|\Psi\rangle\right) + \left\{\langle\delta\Psi|\left(\hat{H}|\Psi\rangle - E[\Psi]|\Psi\rangle\right)\right\}^*\right] \tag{2.45}$$

neglecting changes which are second-order or higher in $\delta\Psi$ in the last line. Thus the quantity $E[\Psi]$ is stationary ($\delta E[\Psi] = 0$) when $|\Psi\rangle$ is an eigenstate of $\hat{H}$ and the eigenvalue is $E[\Psi]$,

$$\hat{H}|\Psi\rangle = E[\Psi]|\Psi\rangle \tag{2.46}$$

and this equation is the time-independent Schrödinger equation. The eigenvalues of $\hat{H}$ can therefore be found by finding the stationary values of $E[\Psi]$ i.e. finding the stationary values of $\langle\Psi|\hat{H}|\Psi\rangle$ subject to the constraint that $\langle\Psi|\Psi\rangle$ is constant. In this procedure, the eigenvalue E plays the rôle of a Lagrange multiplier used to impose the constraint.

In this dissertation we will only be interested in finding the electronic ground-state $|\Psi_0\rangle$ which is the eigenstate of the Hamiltonian with the lowest eigenvalue E_0. Suppose that we have a state close to the ground-state, but with some small error. Since the eigenstates of the Hamiltonian form a complete set, the error can be expanded as a linear combination of the excited eigenstates. The whole state can thus be written as

$$|\Psi\rangle = |\Psi_0\rangle + \sum_{n=1}^{\infty} c_n|\Psi_n\rangle \tag{2.47}$$

where

$$\hat{H}|\Psi_n\rangle = E_n|\Psi_n\rangle. \tag{2.48}$$

We now calculate the value of $E[\Psi]$:

$$\begin{aligned}
E[\Psi] &= \frac{\langle\Psi|\hat{H}|\Psi\rangle}{\langle\Psi|\Psi\rangle} \\
&= \frac{\langle\Psi_0 + \sum_{n=1}^{\infty} c_n\Psi_n|\hat{H}|\Psi_0 + \sum_{n=1}^{\infty} c_n\Psi_n\rangle}{\langle\Psi_0 + \sum_{n=1}^{\infty} c_n\Psi_n|\Psi_0 + \sum_{n=1}^{\infty} c_n\Psi_n\rangle} \\
&= \frac{\langle\Psi_0 + \sum_{n=1}^{\infty} c_n\Psi_n|E_0\Psi_0 + \sum_{n=1}^{\infty} c_n E_n\Psi_n\rangle}{\langle\Psi_0 + \sum_{n=1}^{\infty} c_n\Psi_n|\Psi_0 + \sum_{n=1}^{\infty} c_n\Psi_n\rangle} \\
&= \frac{E_0 + \sum_{n=1}^{\infty} |c_n|^2 E_n}{1 + \sum_{n=1}^{\infty} |c_n|^2} \\
&= E_0 + \sum_{n=1}^{\infty} |c_n|^2 (E_n - E_0) + O\left(|c_n|^4\right).
\end{aligned} \tag{2.49}$$

By definition, $E_n > E_0$ for $n \geq 1$, so that we note two points:

- $E[\Psi] \geq E_0$, with equality only when $|\Psi\rangle = |\Psi_0\rangle$ (i.e. $c_n = 0$ for $n \geq 1$),
- the error in the estimate of E_0 is second-order in the error in the wave-function (i.e. c_n).

The importance of such a variational principle is now clear. To calculate the ground-state energy E_0, we can minimise the functional $E[\Psi]$ with respect to all states $|\Psi\rangle$ which are antisymmetric under exchange of particles. The value of this functional gives an upper bound to the value of E_0, and even a relatively poor estimate of the ground-state wave-function gives a relatively good estimate of E_0. Eigenstates corresponding to excited states of the Hamiltonian can be found by minimising the functional with respect to states which are constructed to be orthogonal to all lower-lying states (which is usually achieved by considering the symmetries of the states) but in this work we will only ever be interested in the ground-state, and so there are no restrictions on the states other than antisymmetry.

Chapter 3

Quantum Mechanics of the Electron Gas

In chapter 2, we showed that the quantum mechanics of the electrons and nuclei which make up real systems can be simplified using the Born-Oppenheimer approximation to separate the motion of the nuclei and electrons. It is therefore possible to treat the nuclei as stationary and reduce the problem to that of a gas of interacting electrons moving in a static external potential due to the nuclei. We also showed that the many-electron wave-function must be antisymmetric under exchange of particles, and outlined the powerful variational method for finding the energy eigenvalues of the Hamiltonian.

In this chapter, we will first show how the problem of finding the ground-state energy can be simplified considerably by the use of density-functional theory, in which the electronic density, rather than the many-electron wave-function, plays the central rôle. Furthermore, it is possible to make a mapping from the system of interacting electrons to a fictitious system of non-interacting particles which has the same ground-state density. Thus the difficult interacting problem can be transformed into a simpler non-interacting problem. We will outline the local density approximation for the effects of exchange and correlation, which allows the theorems of density-functional theory to be applied, and gives surprisingly good results.

Exploiting these results, we will then describe the treatment of periodic systems, and conclude the chapter with a discussion of the pseudopotential approximation which eliminates the core electrons and strong nuclear Coulomb potential from the problem.

3.1 Density-functional theory

In this section we will describe the remarkable theorems of density-functional theory (DFT) which allow us to find ground-state properties of a system without dealing directly with the many-electron state $|\Psi\rangle$. We deal with a system of N electrons moving in a static potential, and adopt a conventional normalisation in which $\langle\Psi|\Psi\rangle = N$.

3.1.1 The Hohenberg-Kohn theorems

As a result of the Born-Oppenheimer approximation, the Coulomb potential arising from the nuclei is treated as a static external potential $V_{\text{ext}}(\mathbf{r})$:

$$V_{\text{ext}}(\mathbf{r}) = -\sum_{\alpha} \frac{Z_\alpha}{|\mathbf{r} - \mathbf{r}_\alpha|}. \tag{3.1}$$

We define the remainder of the electronic Hamiltonian given in (2.19) as $\hat{F}$:

$$\hat{F} = -\frac{1}{2}\sum_i \nabla_i^2 + \frac{1}{2}\sum_i \sum_{j\neq i} \frac{1}{|\mathbf{r}_i - \mathbf{r}_j|} \tag{3.2}$$

such that $\hat{H} = \hat{F} + \hat{V}_{\text{ext}}$ where

$$\hat{V}_{\text{ext}} = \sum_i V_{\text{ext}}(\mathbf{r}_i). \tag{3.3}$$

$\hat{F}$ is the same for all N-electron systems, so that the Hamiltonian, and hence the ground-state $|\Psi_0\rangle$, are completely determined by N and $V_{\text{ext}}(\mathbf{r})$. The ground-state $|\Psi_0\rangle$ for this Hamiltonian gives rise to a ground-state electronic density $n_0(\mathbf{r})$

$$n_0(\mathbf{r}) = \langle\Psi_0|\hat{n}|\Psi_0\rangle = \int \prod_{i=2}^{N} \mathrm{d}\mathbf{r}_i \left|\Psi_0\left(\mathbf{r}, \mathbf{r}_2, \mathbf{r}_3 \ldots \mathbf{r}_N\right)\right|^2. \tag{3.4}$$

Thus the ground-state $|\Psi_0\rangle$ and density $n_0(\mathbf{r})$ are both functionals of the number of electrons N and the external potential $V_{\text{ext}}(\mathbf{r})$. Density-functional theory, introduced in 1964 by Hohenberg and Kohn [16], makes two remarkable statements.

- The external potential $V_{\text{ext}}(\mathbf{r})$ is uniquely determined by the corresponding ground-state electronic density, to within an additive constant.

  Proof by *reductio ad absurdum*: assume that a second different external potential $V'_{\text{ext}}(\mathbf{r})$ with ground-state $|\Psi'_0\rangle$ gives rise to the same density $n_0(\mathbf{r})$. The ground-state energies are $E_0 = \langle\Psi_0|\hat{H}|\Psi_0\rangle$ and $E'_0 = \langle\Psi'_0|\hat{H}'|\Psi'_0\rangle$ where $\hat{H} = \hat{F} + \hat{V}_{\text{ext}}$ and $\hat{H}' = \hat{F} + \hat{V}'_{\text{ext}}$. Taking $|\Psi'_0\rangle$ as a trial wave-function for the Hamiltonian $\hat{H}$, we obtain the strict inequality

$$\begin{aligned} E_0 < \langle \Psi_0'|\hat{H}|\Psi_0'\rangle &= \langle \Psi_0'|\hat{H}'|\Psi_0'\rangle + \langle \Psi_0'|\left(\hat{H} - \hat{H}'\right)|\Psi_0'\rangle \\ &= E_0' + \int \mathrm{d}\mathbf{r}\; n_0(\mathbf{r})\left[V_{\mathrm{ext}}(\mathbf{r}) - V_{\mathrm{ext}}'(\mathbf{r})\right], \end{aligned} \tag{3.5}$$

whereas taking $|\Psi_0\rangle$ as a trial wave-function for $\hat{H}'$ gives

$$\begin{aligned} E_0' < \langle \Psi_0|\hat{H}'|\Psi_0\rangle &= \langle \Psi_0|\hat{H}|\Psi_0\rangle + \langle \Psi_0|\left(\hat{H}' - \hat{H}\right)|\Psi_0\rangle \\ &= E_0 - \int \mathrm{d}\mathbf{r}\; n_0(\mathbf{r})\left[V_{\mathrm{ext}}(\mathbf{r}) - V_{\mathrm{ext}}'(\mathbf{r})\right] \end{aligned} \tag{3.6}$$

and adding these two equations together results in the contradiction

$$E_0 + E_0' < E_0 + E_0'.$$

Thus, at least in principle, the ground-state density determines (to within a constant) the external potential of the Schrödinger equation of which it is a solution. The external potential and number of electrons $N = \int \mathrm{d}\mathbf{r}\; n_0(\mathbf{r})$ determine all the ground-state properties of the system since the Hamiltonian and ground-state wave-function are determined by them.

So for all densities $n(\mathbf{r})$ which are ground-state densities for some external potential (v-representable) the functional $F[n] = \langle\Psi|\hat{F}|\Psi\rangle$ is unique and well-defined, since $n(\mathbf{r})$ determines the external potential and N (and therefore $\hat{F}$) and thence $|\Psi\rangle$. Now a functional for an arbitrary external potential $V(\mathbf{r})$ unrelated to the $V_{\mathrm{ext}}(\mathbf{r})$ determined by $n(\mathbf{r})$ can be defined:

$$E_V[n] = F[n] + \int \mathrm{d}\mathbf{r}\; V(\mathbf{r})n(\mathbf{r}). \tag{3.7}$$

- For all v-representable densities $n(\mathbf{r})$, $E_V[n] \geq E_0$ where E_0 is now the ground-state energy for N electrons in the external potential $V(\mathbf{r})$.

  Proof of this energy variational principle: by the first theorem, a given $n(\mathbf{r})$ determines its own external potential $V_{\mathrm{ext}}(\mathbf{r})$ and ground-state $|\Psi\rangle$. If this state is used as a trial state for the Hamiltonian with external potential $V(\mathbf{r})$, we have

$$\langle\Psi|\hat{H}|\Psi\rangle = \langle\Psi|\hat{F}|\Psi\rangle + \langle\Psi|\hat{V}|\Psi\rangle = F[n] + \int \mathrm{d}\mathbf{r}\; V(\mathbf{r})n(\mathbf{r}) = E_V[n] \geq E_0 \tag{3.8}$$

  by the variational principle. For non-degenerate ground-states, equality only holds if $|\Psi\rangle$ is the ground-state for potential $V(\mathbf{r})$.

Thus the problem of solving the Schrödinger equation for non-degenerate ground-states can be recast into a variational problem of minimising the functional $E_V[n]$ with respect to v-representable densities. It should be noted that simple counter-examples of v-representable densities have been found [17–19], but this restriction and the non-degeneracy requirement are overcome by the constrained search formulation.

3.1.2 The constrained search formulation

Following Levy [20,21] we define a functional of the density $n(\mathbf{r})$ for the operator $\hat{F}$ (defined above) as:

$$F[n] = \min_{|\Psi\rangle \to n} \langle \Psi | \hat{F} | \Psi \rangle \tag{3.9}$$

i.e. the functional takes the minimum value of the expectation value with respect to all states $|\Psi\rangle$ which give the density $n(\mathbf{r})$. For a system with external potential $V(\mathbf{r})$ and ground-state $|\Psi_0\rangle$ with energy E_0, consider a state $|\Psi_{[n]}\rangle$, an N-electron state which yields density $n(\mathbf{r})$ and minimises $F[n]$. Define $E_V[n]$ as:

$$E_V[n] = F[n] + \int \mathrm{d}\mathbf{r}\ n(\mathbf{r}) V(\mathbf{r}) = \langle \Psi_{[n]} | (\hat{F} + \hat{V}) | \Psi_{[n]} \rangle \tag{3.10}$$

but since $\hat{H} = \hat{F} + \hat{V}$, by the variational principle we obtain

$$E_V[n] \geq E_0 \tag{3.11}$$

with equality only if $|\Psi_{[n]}\rangle = |\Psi_0\rangle$. This holds for all densities which can be obtained from an N-electron wave-function (N-representable). But from the definition of $F[n]$ (3.9) we must also have

$$F[n_0] \leq \langle \Psi_0 | \hat{F} | \Psi_0 \rangle \tag{3.12}$$

since $|\Psi_0\rangle$ must be one of states which yields $n_0(\mathbf{r})$. Adding $\int \mathrm{d}\mathbf{r}\ n_0(\mathbf{r}) V(\mathbf{r})$ gives

$$E_V[n_0] \leq E_0 \tag{3.13}$$

which when combined with (3.11) gives the desired result that $E_V[n] \geq E_V[n_0] = E_0$.

Thus the ground-state density $n_0(\mathbf{r})$ minimises the functional $E_V[n]$ and the minimum value is the ground-state electronic energy. Note that the requirement for non-degeneracy of the ground-state has disappeared, and further that instead of considering only v-representable densities, we can now consider N-representable densities. The requirements of N-representability are much weaker and satisfied by any well-behaved density, indeed the only condition [22] is proper differentiability i.e. that the quantity

$$\int \mathrm{d}\mathbf{r} \left|\nabla n^{\frac{1}{2}}(\mathbf{r})\right|^2$$

is real and finite.

3.1.3 Exchange and correlation

The remarkable results of density-functional theory are the existence of the universal functional $F[n]$, which is independent of the external potential, and that instead of dealing with a function of $3N$ variables (the many-electron wave-function) we can instead deal with a function of only three variables (the density). The complexity of the problem has thus been much reduced, and we note here that this complexity now scales linearly with system-size N, so that quantum-mechanical calculations based on density-functional theory can in principle be performed with an effort which scales linearly with system-size.

The exact form of the universal functional $F[n]$ is unknown. The Thomas-Fermi functional [23–25]

$$F_{\mathrm{TF}}[n] = \frac{3}{10}\left(3\pi^2\right)^{\frac{2}{3}} \int \mathrm{d}\mathbf{r}\ n^{\frac{5}{3}}(\mathbf{r}) + \frac{1}{2}\int \mathrm{d}\mathbf{r}\ \mathrm{d}\mathbf{r}'\ \frac{n(\mathbf{r})n(\mathbf{r}')}{|\mathbf{r}-\mathbf{r}'|} \tag{3.14}$$

can, with hindsight, be viewed as a tentative approximation to this universal functional, but fails to provide even qualitatively correct predictions for systems other than isolated atoms [26,27] although recent, more accurate developments [28–32] have led to the implementation of linear-scaling orbital-free methods for nearly-free electron metals.

The failure to find accurate expressions for the density-functional is a result of the complexity of the many-body problem which is at the heart of the definition of the universal functional. For the electron gas, a system of many interacting particles, the effects of exchange and correlation are crucial to an accurate description of its behaviour. In a non-interacting system, the antisymmetry of the wave-function requires that particles with the same spin occupy distinct orthogonal orbitals, and this results in the particles becoming spatially separated. In an interacting system such as the electron gas in which all the particles repel each other, exchange will thus lead to a lowering of the energy. Moreover, the interactions cause the motion of the particles to become correlated to further reduce the energy of interaction. Thus it is impossible to treat the electrons as independent particles. These effects are completely neglected by the Thomas-Fermi model, and must in part account for its failure, the other source of error being the local approximation for the kinetic energy.

3.1.4 The Kohn-Sham equations

In order to take advantage of the power of DFT without sacrificing accuracy (i.e. including exchange and correlation effects) we follow the method of Kohn and Sham [33] to map the problem of the system of interacting electrons onto a fictitious system of non-interacting "electrons". We write the variational problem for the Hohenberg-Kohn density-functional, introducing a Lagrange multiplier μ to constrain the number of electrons to be N:

$$\delta \left[F[n] + \int \mathrm{d}\mathbf{r}\ V_{\mathrm{ext}}(\mathbf{r}) n(\mathbf{r}) - \mu \left(\int \mathrm{d}\mathbf{r}\ n(\mathbf{r}) - N \right) \right] = 0. \tag{3.15}$$

Kohn and Sham separated $F[n]$ into three parts

$$F[n] = T_{\mathrm{s}}[n] + \frac{1}{2} \int \mathrm{d}\mathbf{r}\ \mathrm{d}\mathbf{r}'\ \frac{n(\mathbf{r}) n(\mathbf{r}')}{|\mathbf{r} - \mathbf{r}'|} + E_{\mathrm{xc}}[n] \tag{3.16}$$

in which $T_{\mathrm{s}}[n]$ is defined as the kinetic energy of a non-interacting gas with density $n(\mathbf{r})$ (not the same as that of the interacting system, although we might hope that the two quantities were of the same order of magnitude), the second term is the classical electrostatic (Hartree) energy and the final term is an implicit definition of the exchange-correlation energy which contains the non-classical electrostatic interaction energy and the difference between the kinetic energies of the interacting and non-interacting systems. The aim of this separation is that the first two terms can be dealt with simply, and the last term, which contains the effects of the complex behaviour, is a small fraction of the total energy and can be approximated surprisingly well.

Using this separation, equation 3.15 can be rewritten:

$$\frac{\delta T_{\mathrm{s}}[n]}{\delta n(\mathbf{r})} + V_{\mathrm{KS}}(\mathbf{r}) = \mu \tag{3.17}$$

in which the Kohn-Sham potential $V_{\mathrm{KS}}(\mathbf{r})$ is given by

$$V_{\mathrm{KS}}(\mathbf{r}) = \int \mathrm{d}\mathbf{r}' \frac{n(\mathbf{r}')}{|\mathbf{r} - \mathbf{r}'|} + V_{\mathrm{xc}}(\mathbf{r}) + V_{\mathrm{ext}}(\mathbf{r}) \tag{3.18}$$

and the exchange-correlation potential $V_{\mathrm{xc}}(\mathbf{r})$ is

$$V_{\mathrm{xc}}(\mathbf{r}) = \frac{\delta E_{\mathrm{xc}}[n]}{\delta n(\mathbf{r})}. \tag{3.19}$$

The crucial point to note here is that equation 3.17 is precisely the same equation which would be obtained for a non-interacting system of particles moving in an external potential $V_{\mathrm{KS}}(\mathbf{r})$. To find the ground-state density $n_0(\mathbf{r})$ for this non-interacting system we simply solve the one-electron Schrödinger equations;

$$\left[-\tfrac{1}{2}\nabla^2 + V_{\mathrm{KS}}(\mathbf{r})\right]\psi_i(\mathbf{r}) = \varepsilon_i\psi_i(\mathbf{r}) \tag{3.20}$$

for $\frac{1}{2}N$ single-particle states[1] $|\psi_i\rangle$ with energies ε_i, constructing the density from

$$n(\mathbf{r}) = 2\sum_{i=1}^{N/2}|\psi_i(\mathbf{r})|^2 \tag{3.21}$$

(the factor 2 is for spin degeneracy – we assume the orbitals are singly-occupied) and the non-interacting kinetic energy $T_{\mathrm{s}}[n]$ from

$$T_{\mathrm{s}}[n] = -\sum_{i=1}^{N/2}\int \mathrm{d}\mathbf{r}\ \psi_i^*(\mathbf{r})\nabla^2\psi_i(\mathbf{r}). \tag{3.22}$$

Since the Kohn-Sham potential $V_{\mathrm{KS}}(\mathbf{r})$ depends upon the density $n(\mathbf{r})$ it is necessary to solve these equations self-consistently i.e. having made a guess for the form of the density, the Schrödinger equation is solved to obtain a set of orbitals $\{\psi_i(\mathbf{r})\}$ from which a new density is constructed, and the process repeated until the input and output densities are the same. In practice there is no problem converging to the ground-state minimum because of the convex nature of the density-functional [34].

The energy of the non-interacting system, the sum of one-electron eigenvalues, is

$$\begin{aligned} 2\sum_{i=1}^{N/2}\varepsilon_i &= T_{\mathrm{s}}[n] + \int \mathrm{d}\mathbf{r}\ n(\mathbf{r})V_{\mathrm{KS}}(\mathbf{r}) \\ &= T_{\mathrm{s}}[n] + \int \mathrm{d}\mathbf{r}\ \mathrm{d}\mathbf{r}'\ \frac{n(\mathbf{r})n(\mathbf{r}')}{|\mathbf{r}-\mathbf{r}'|} + \int \mathrm{d}\mathbf{r}\ n(\mathbf{r})V_{\mathrm{xc}}(\mathbf{r}) + \int \mathrm{d}\mathbf{r}\ n(\mathbf{r})V_{\mathrm{ext}}(\mathbf{r}) \end{aligned} \tag{3.23}$$

which, compared to the interacting system, double-counts the Hartree energy and over-counts the exchange-correlation energy so that the interacting energy is

$$E = 2\sum_{i=1}^{N/2}\varepsilon_i - \frac{1}{2}\int \mathrm{d}\mathbf{r}\ \mathrm{d}\mathbf{r}'\ \frac{n(\mathbf{r})n(\mathbf{r}')}{|\mathbf{r}-\mathbf{r}'|} - \int \mathrm{d}\mathbf{r}\ n(\mathbf{r})V_{\mathrm{xc}}(\mathbf{r}) + E_{\mathrm{xc}}[n]. \tag{3.24}$$

Direct solution of the Schrödinger equation for the extended non-interacting orbitals $\{\psi_i(\mathbf{r})\}$ requires a computational effort which scales as the cube of the system-size N, due to the cost of diagonalising the Hamiltonian or orthogonalising the orbitals, whereas the original complexity of finding a minimum of the Hohenberg-Kohn functional only required an effort which scaled linearly with N. Thus a linear-scaling method must modify this

[1] Our restriction to non-spin-polarised systems requires that N be even.

Kohn-Sham scheme.

3.1.5 The local density approximation

The results so far are exact, provided that the functional form of $E_{\mathrm{xc}}[n]$ is known. The problem of determining the functional form of the universal Hohenberg-Kohn density functional has now been transferred to this one term, and therefore this term is not known exactly. Remarkably, it is possible to make simple approximations for the exchange-correlation energy which work extremely well, and the simplest of these, which is the approximation adopted in this work, is the *local density approximation* (LDA).

In the LDA, the contribution to the exchange-correlation energy from each infinitesimal volume in space, $\mathrm{d}\mathbf{r}$, is taken to be the value it would have if the whole of space were filled with a homogeneous electron gas with the same density as is found in $\mathrm{d}\mathbf{r}$ i.e.

$$E_{\mathrm{xc}}[n] = \int \mathrm{d}\mathbf{r} \; \epsilon_{\mathrm{xc}}\left(n(\mathbf{r})\right) n(\mathbf{r}) \tag{3.25}$$

where $\epsilon_{\mathrm{xc}}\left(n(\mathbf{r})\right)$ is the exchange-correlation energy per electron in a homogeneous electron gas of density $n(\mathbf{r})$. The exchange-correlation potential $V_{\mathrm{xc}}(\mathbf{r})$ then takes the form

$$V_{\mathrm{xc}}(\mathbf{r}) = \frac{\delta E_{\mathrm{xc}}[n]}{\delta n(\mathbf{r})} = \epsilon_{\mathrm{xc}}\left(n(\mathbf{r})\right) + n(\mathbf{r}) \left.\frac{\mathrm{d}\epsilon_{\mathrm{xc}}\left(n\right)}{\mathrm{d}n}\right|_{n=n(\mathbf{r})} . \tag{3.26}$$

The exchange-correlation energy for the homogeneous electron gas has been calculated by Ceperley and Alder [35] using Monte Carlo methods and in this work we use a parameterisation by Perdew and Zunger [36]. The LDA is exact in the limit of slowly-varying densities, however, the density in systems of interest is generally rapidly varying, and the LDA would appear to be a crude approximation in these cases. Its use is justified *a posteriori* by its surprising success at predicting physical properties in real systems. This success may be due in part to the fact that the sum rule for the exchange-correlation hole, which must be obeyed by the real functional, is reproduced by the LDA [37]. We can connect the interacting and non-interacting systems using a variable coupling constant λ which varies between 0 and 1. We replace the Coulomb interaction by

$$\frac{\lambda}{|\mathbf{r} - \mathbf{r}'|}$$

and vary λ in the presence of an external potential $V_{\lambda}(\mathbf{r})$ so that the ground-state density for all values of λ is the same [38]. The Hamiltonian is therefore

$$\hat{H}_\lambda = -\frac{1}{2}\sum_i \nabla_i^2 + \frac{1}{2}\sum_i \sum_{j\neq i} \frac{\lambda}{|\mathbf{r}_i - \mathbf{r}_j|} + \hat{V}_{\text{ext}} + \hat{V}_\lambda. \tag{3.27}$$

The exchange-correlation hole $n_{\text{xc}}(\mathbf{r}, \mathbf{r}')$ is then defined in terms of a coupling-constant integration of the pair correlation function $g(\mathbf{r}, \mathbf{r}'; \lambda)$ of the system with density $n(\mathbf{r})$ and scaled Coulomb interaction [39, 40];

$$n_{\text{xc}}(\mathbf{r}, \mathbf{r}') = n(\mathbf{r}') \int_0^1 \mathrm{d}\lambda \, [g(\mathbf{r}, \mathbf{r}'; \lambda) - 1] \, . \tag{3.28}$$

The exchange-correlation energy can then be expressed in the form of a classical electrostatic interaction between the density $n(\mathbf{r})$ and the hole density $n_{\text{xc}}(\mathbf{r}, \mathbf{r}')$;

$$E_{\text{xc}}[n] = \frac{1}{2} \int \mathrm{d}\mathbf{r} \; \mathrm{d}\mathbf{r}' \; \frac{n(\mathbf{r}) n_{\text{xc}}(\mathbf{r}, \mathbf{r}')}{|\mathbf{r} - \mathbf{r}'|}. \tag{3.29}$$

The sum rule follows from the definition of the pair correlation function [41]

$$\int \mathrm{d}\mathbf{r}' \; n_{\text{xc}}(\mathbf{r}, \mathbf{r}') = -1, \tag{3.30}$$

which is interpreted by saying that the exchange-correlation hole excludes one electron as expected. It can also be shown that the exchange-correlation energy depends only weakly on the detailed shape of the exchange-correlation hole [42], and these two facts account, at least in part, for the success of the LDA. This view is supported by the fact that improvements to the LDA involving gradient expansions show no consistent improvement unless they enforce the sum rule obeyed by the LDA [43, 44].

3.2 Periodic systems

Exploiting the results of the previous section, we can now consider the motion of non-interacting particles in a static potential, which is described by the time-independent Schrödinger equation 3.20. In the study of bulk crystals, the system is infinite but periodic, and so it is necessary to be able to reduce this problem to the study of a finite system. This approach turns out to have several advantages so that it is often easiest to study even aperiodic systems by imposing some false periodicity. The system is contained within a *supercell* which is then replicated periodically throughout space (see figure 3.1). The supercell must be large enough so that the systems contained within each one, which in reality are isolated, do not interact significantly.

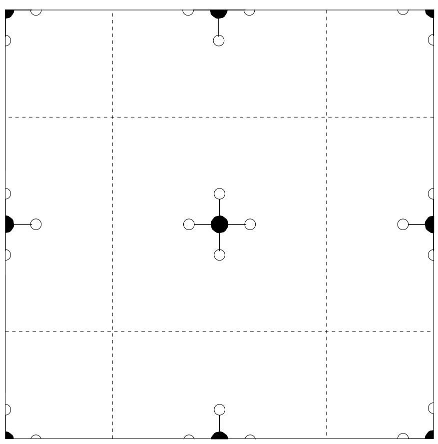

Figure 3.1: Using the supercell approximation, an isolated molecule can be studied using the same techniques which are usually applied to crystals.

3.2.1 Bloch's theorem

See [45] for a fuller discussion of the proof outlined here. We consider non-interacting particles moving in a static potential $V(\mathbf{r})$, which may be the Kohn-Sham effective potential $V_{\mathrm{KS}}(\mathbf{r})$ (3.18). In a perfect crystal, the nuclei are arranged in a regular periodic array described by a set of Bravais lattice vectors $\{\mathbf{R}\}$. The system, being infinite, is invariant under translation by any of these lattice vectors, and in particular the potential is also periodic i.e.

$$V(\mathbf{r}+\mathbf{R}) = V(\mathbf{r}) \tag{3.31}$$

for all Bravais lattice vectors $\mathbf{R}$.

The Schrödinger equation which describes the motion of a single particle in this potential is

$$\hat{H}|\psi\rangle = \left[-\tfrac{1}{2}\nabla^2 + V(\mathbf{r})\right]|\psi\rangle = \varepsilon|\psi\rangle \tag{3.32}$$

and we define translation operators $\hat{T}_{\mathbf{R}}$ for each lattice vector $\mathbf{R}$ which act in the following manner on any function of position $f(\mathbf{r})$:

$$\hat{T}_{\mathbf{R}} f(\mathbf{r}) = f(\mathbf{r}+\mathbf{R}). \tag{3.33}$$

Since the potential and hence the Hamiltonian are periodic i.e. $\hat{H}(\mathbf{r}+\mathbf{R}) = \hat{H}(\mathbf{r})$, these operators commute with the translation operators:

$$\hat{T}_{\mathbf{R}}\hat{H}(\mathbf{r})\psi(\mathbf{r}) = \hat{H}(\mathbf{r}+\mathbf{R})\psi(\mathbf{r}+\mathbf{R}) = \hat{H}(\mathbf{r})\psi(\mathbf{r}+\mathbf{R}) = \hat{H}(\mathbf{r})\hat{T}_{\mathbf{R}}\psi(\mathbf{r}) \tag{3.34}$$

i.e. $\left[\hat{H}, \hat{T}_{\mathbf{R}}\right] = 0$, and the translation operators commute with each other i.e. $\hat{T}_{\mathbf{R}}\hat{T}_{\mathbf{R}'} = \hat{T}_{\mathbf{R}'}\hat{T}_{\mathbf{R}} = \hat{T}_{\mathbf{R}+\mathbf{R}'}$.

There must, therefore, exist a good quantum number corresponding to each lattice vector $\mathbf{R}$, and it must also be possible to choose the eigenstates of the Hamiltonian to be simultaneous eigenstates of all the translation operators;

$$\hat{H}|\psi\rangle = \varepsilon|\psi\rangle, \tag{3.35}$$

$$\hat{T}_{\mathbf{R}}|\psi\rangle = c(\mathbf{R})|\psi\rangle. \tag{3.36}$$

From the commutation relations of the translation vectors it follows that the eigenvalues must satisfy

$$c(\mathbf{R}+\mathbf{R}') = c(\mathbf{R})c(\mathbf{R}'). \tag{3.37}$$

We can define the eigenvalues for the three primitive lattice vectors $\{\mathbf{a}_i\}$ in terms of three complex numbers $\{x_i\}$ by

$$c(\mathbf{a}_i) = \exp(2\pi \mathrm{i} x_i). \tag{3.38}$$

Since all lattice vectors can be expressed in the form $\mathbf{R} = n_1\mathbf{a}_1 + n_2\mathbf{a}_2 + n_3\mathbf{a}_3$, where the n_i are integers, it follows from equation 3.37 that

$$c(\mathbf{R}) = c(\mathbf{a}_1)^{n_1} c(\mathbf{a}_2)^{n_2} c(\mathbf{a}_3)^{n_3} \tag{3.39}$$

which is equivalent to

$$c(\mathbf{R}) = \exp(\mathrm{i}\mathbf{k}\cdot\mathbf{R}), \tag{3.40}$$

$$\mathbf{k} = x_1\mathbf{g}_1 + x_2\mathbf{g}_2 + x_3\mathbf{g}_3, \tag{3.41}$$

where the $\{\mathbf{g}_i\}$ are the reciprocal lattice vectors satisfying $\mathbf{g}_i \cdot \mathbf{a}_j = 2\pi\delta_{ij}$, and the $\{x_i\}$ are complex numbers in general.

Thus we have shown that

$$\hat{T}_{\mathbf{R}}\psi(\mathbf{r}) = \psi(\mathbf{r}+\mathbf{R}) = c(\mathbf{R})\psi(\mathbf{r}) = \exp(\mathrm{i}\mathbf{k}\cdot\mathbf{R})\psi(\mathbf{r}) \tag{3.42}$$

which is one statement of Bloch's theorem. Consider the function $u(\mathbf{r}) = \exp(-\mathrm{i}\mathbf{k}\cdot\mathbf{r})\psi(\mathbf{r})$.

$$u(\mathbf{r}+\mathbf{R}) = \exp(-\mathrm{i}\mathbf{k}\cdot[\mathbf{r}+\mathbf{R}])\psi(\mathbf{r}+\mathbf{R}) = \exp(-\mathrm{i}\mathbf{k}\cdot\mathbf{r})\psi(\mathbf{r}) = u(\mathbf{r}) \tag{3.43}$$

i.e. the function $u(\mathbf{r})$ also has the periodicity of the lattice, and so the wave-function $\psi(\mathbf{r})$ can also be expressed as

$$\psi(\mathbf{r}) = \exp(\mathrm{i}\mathbf{k}\cdot\mathbf{r})u(\mathbf{r}), \tag{3.44}$$

where $u(\mathbf{r})$ is a strictly cell-periodic function i.e. $u(\mathbf{r}+\mathbf{R}) = u(\mathbf{r})$.

We thus label the eigenstates of the Hamiltonian and the translation operators $|\psi_{n\mathbf{k}}\rangle$ where n is the good quantum number labelling different eigenstates of the Hamiltonian with the same good quantum vector $\mathbf{k}$, related to the translational symmetry.

At this point we note that a periodic function can always be expressed as a Fourier series i.e.

$$u(\mathbf{r}) = \sum_{\mathbf{G}} \tilde{u}_{\mathbf{G}} \exp(\mathrm{i}\mathbf{G}\cdot\mathbf{r}) \tag{3.45}$$

where $\mathbf{G}$ is reciprocal lattice vector $\mathbf{G} = m_1\mathbf{g}_1 + m_2\mathbf{g}_2 + m_3\mathbf{g}_3$ and the m_i are integers. Thus the state $|\psi_{n\mathbf{k}}\rangle$ can be expressed as a linear combination of plane-waves:

$$\begin{aligned}\psi_{n\mathbf{k}}(\mathbf{r}) &= \exp(\mathrm{i}\mathbf{k}\cdot\mathbf{r})u_{n\mathbf{k}}(\mathbf{r}) && (3.46)\\ &= \sum_{\mathbf{G}} c_{n\mathbf{k}}(\mathbf{G}) \exp[\mathrm{i}(\mathbf{k}+\mathbf{G})\cdot\mathbf{r}]. && (3.47)\end{aligned}$$

Instead of having to solve for a wave-function over all of (infinite) space, the problem now becomes one of solving for wave-functions only within a single (super)cell, albeit with an infinite number of possible values for $\mathbf{k}$. In order to simplify the problem to manageable proportions, it is necessary to impose some boundary conditions on the wave-function, which restrict the allowed values of $\mathbf{k}$.

3.2.2 Brillouin zone sampling

We choose to model the infinite periodic system by a large number of primitive cells $N_{\text{cells}} = N_1N_2N_3$ stacked together, with N_i cells along the $\mathbf{a}_i$ direction, and we apply periodic or generalised Born-von Karman boundary conditions to the wave-functions, which can be interpreted by saying that a particle which leaves one surface of the crystal simultaneously enters the crystal at the opposite surface. In fact it can be shown [46] that the choice of boundary conditions does not affect the bulk properties of the system. This condition is expressed mathematically as

$$\psi(\mathbf{r} + N_i\mathbf{a}_i) = \psi(\mathbf{r}), \qquad i = 1, 2, 3. \tag{3.48}$$

Applying Bloch's theorem (3.42) gives

$$\psi(\mathbf{r} + N_i\mathbf{a}_i) = \exp(\mathrm{i}N_i\mathbf{k}\cdot\mathbf{a}_i)\psi(\mathbf{r}) \tag{3.49}$$

so that the values of $\mathbf{k}$ are restricted such that

$$\exp(\mathrm{i}N_i\mathbf{k}\cdot\mathbf{a}_i) = \exp(2\pi\mathrm{i}N_i x_i) = 1, \qquad i = 1, 2, 3 \tag{3.50}$$

using equation 3.41. Therefore the values of the $\{x_i\}$ are required to be real and equal to

$$x_i = \frac{l_i}{N_i}, \qquad i = 1, 2, 3, \tag{3.51}$$

where the $\{l_i\}$ are integers, so that the general allowed form for the Bloch wave-vectors $\mathbf{k}$ is

$$\mathbf{k} = \sum_{i=1}^{3} \frac{l_i}{N_i}\mathbf{g}_i. \tag{3.52}$$

Taking the limit to the true infinite perfect crystal ($N_i \to \infty$) we see that there is still an infinite number of allowed $\mathbf{k}$-vectors, but that they are now members of a *countably* infinite set. Furthermore, we see that $\mathbf{k}$-vectors which differ only by a reciprocal lattice vector are in fact equivalent. Consider two such wave-vectors related by $\mathbf{k}' = \mathbf{k} + \mathbf{G}$, then the corresponding Bloch states are also related by

$$\begin{aligned} \psi_{n\mathbf{k}'}(\mathbf{r}) &= \exp(\mathrm{i}\mathbf{k}'\cdot\mathbf{r})u_{n\mathbf{k}'}(\mathbf{r}) = \exp(\mathrm{i}\mathbf{k}\cdot\mathbf{r})\left[u_{n\mathbf{k}'}(\mathbf{r})\exp(\mathrm{i}\mathbf{G}\cdot\mathbf{r})\right] \\ &= \exp(\mathrm{i}\mathbf{k}\cdot\mathbf{r})\tilde{u}(\mathbf{r}) = \psi_{n'\mathbf{k}}(\mathbf{r}). \end{aligned} \tag{3.53}$$

Since the expression in square brackets on the first line is a cell-periodic function the whole expression is a valid Bloch wave-function with wave-vector $\mathbf{k}$. Thus we can restrict our attention to those $\mathbf{k}$-vectors which lie within the *first Brillouin zone*, that volume of reciprocal-space enclosing the origin which is bounded by the planes which perpendicularly bisect lines from the origin to surrounding lattice points.

The situation now is that for each allowed $\mathbf{k}$-vector within the first Brillouin zone we must calculate the occupied Hamiltonian eigenstates in order to construct the density. However, the wave-functions and other properties such as Hamiltonian eigenvalues vary smoothly over the Brillouin zone [47] so that in practice only a finite set of points need to be chosen, and methods for making efficient choices have been developed [48–53]. From the calculation of the wave-functions at a certain set of $\mathbf{k}$-points, $\mathbf{k} \cdot \mathbf{p}$ perturbation theory [54, 55] can be used to approximate the wave-functions at other nearby $\mathbf{k}$-points.

In this work, we are interested in the behaviour of very large systems. The volume of the Brillouin zone Ω_{BZ} is related to the volume of the supercell Ω_{cell} by

$$\Omega_{\mathrm{BZ}} = \frac{(2\pi)^3}{\Omega_{\mathrm{cell}}} \tag{3.54}$$

so that for large systems, the Brillouin zone volume is very small and only a few $\mathbf{k}$-points need to be considered to describe the variation across the Brillouin zone accurately. In this work we therefore only calculate the wave-functions at the centre of the Brillouin zone, $\mathbf{k} = 0$, known as the Γ-point. This has the added advantage that at this $\mathbf{k}$-point the wave-functions can be chosen to be real (recall that there is always an arbitrary global phase factor) without loss of generality.

3.3 The pseudopotential approximation

In this section we outline a further approximation which is based upon the observation that the core electrons are relatively unaffected by the chemical environment of an atom. Thus we assume that their (large) contribution to the total binding energy does not change when isolated atoms are brought together to form a molecule or crystal. The actual energy differences of interest are the changes in valence electron energies, and so if the binding energy of the core electrons can be subtracted out, the valence electron energy change will be a much larger fraction of the total binding energy, and hence much easier to calculate accurately. We also note that the strong nuclear Coulomb potential and highly localised core electron wave-functions are difficult to represent computationally.

Since the atomic wave-functions are eigenstates of the atomic Hamiltonian, they must all be mutually orthogonal. Since the core states are localised in the vicinity of the nucleus, the valence states must oscillate rapidly in this core region in order to maintain this orthogonality with the core electrons. This rapid oscillation results in a large kinetic energy for the valence electrons in the core region, which roughly cancels the large potential energy due to the strong Coulomb potential. Thus the valence electrons are much more weakly bound than the core electrons.

It is therefore convenient to attempt to replace the strong Coulomb potential and core electrons by an effective *pseudopotential* which is much weaker, and replace the valence electron wave-functions, which oscillate rapidly in the core region, by *pseudo-wave-functions*, which vary smoothly in the core region [56, 57]. We outline two justifications for this approximation below; for further details see [58] and also [59, 60] for recent reviews.

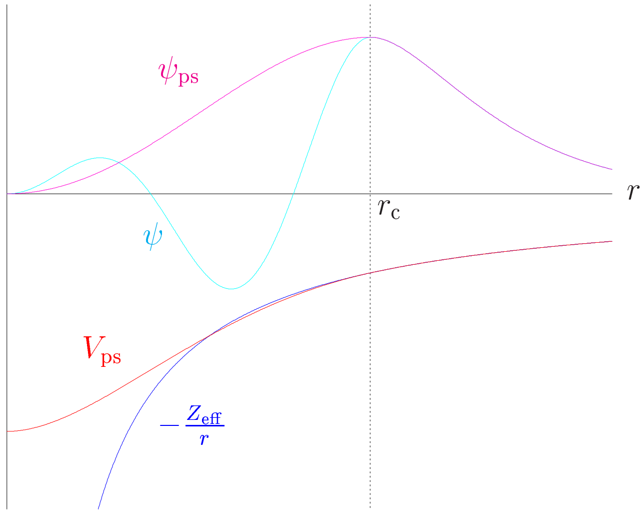

Figure 3.2: Schematic diagram of the relationship between all-electron and pseudo-potentials and wave-functions.

3.3.1 Operator approach

Following the orthogonalised plane-waves approach [61], we consider an atom with Hamiltonian $\hat{H}$, core states $\{|\chi_n\rangle\}$ and core energy eigenvalues $\{E_n\}$ and focus on one valence state $|\psi\rangle$ with energy eigenvalue E. From these states we attempt to construct a smoother pseudo-state $|\varphi\rangle$ defined by

$$|\psi\rangle = |\varphi\rangle + \sum_n^{\rm core} a_n |\chi_n\rangle. \tag{3.55}$$

The valence state must be orthogonal to all of the core states (which are of course mutually orthogonal) so that

$$\langle \chi_m|\psi\rangle = 0 = \langle \chi_m|\varphi\rangle + a_m \tag{3.56}$$

which fixes the expansion coefficients $\{a_n\}$. Thus

$$|\psi\rangle = |\varphi\rangle - \sum_n^{\rm core} |\chi_n\rangle\langle\chi_n|\varphi\rangle. \tag{3.57}$$

Substituting this expression in the Schrödinger equation $\hat{H}|\psi\rangle = E|\psi\rangle$ gives

$$\hat{H}|\varphi\rangle - \sum_n^{\text{core}} E_n|\chi_n\rangle\langle\chi_n|\varphi\rangle = E|\varphi\rangle - E\sum_n |\chi_n\rangle\langle\chi_n|\varphi\rangle \tag{3.58}$$

which can be rearranged in the form

$$\hat{H}|\varphi\rangle + \sum_n^{\text{core}}(E - E_n)|\chi_n\rangle\langle\chi_n|\varphi\rangle = E|\varphi\rangle \tag{3.59}$$

so that the smooth pseudo-state obeys a Schrödinger equation with an extra energy-dependent non-local potential $\hat{V}_{\text{nl}}$;

$$\left[\hat{H} + \hat{V}_{\text{nl}}\right]|\varphi\rangle = E|\varphi\rangle \tag{3.60}$$

$$\hat{V}_{\text{nl}} = \sum_n^{\text{core}}(E - E_n)|\chi_n\rangle\langle\chi_n|. \tag{3.61}$$

The energy of the smooth state described by the pseudo-wave-function is the same as that of the original valence state. The additional potential V_{nl}, whose effect is localised in the core, is repulsive and will cancel part of the strong Coulomb potential so that the resulting sum is a weaker pseudopotential. Of course, once the atom interacts with others, the energies of the eigenstates will change, but if the core states are reasonably far from the valence states in energy (i.e. $\delta E \ll E - E_n$) then fixing E in V_{nl} to be the atomic valence eigenvalue is a reasonable approximation. In fact we would like to make the behaviour of the pseudopotential follow that of the real potential to first order in E, and this can be achieved by constructing a *norm-conserving* pseudopotential (see section 3.3.3).

3.3.2 Scattering approach

For a fuller discussion of the theory of scattering see [62]. Consider a plane-wave with wave-vector $\mathbf{k}$ scattering from some spherically-symmetric potential localised within a radius r_{c} and centred at the origin. The incoming plane-wave can be decomposed into spherical-waves by the identity

$$\exp(\mathrm{i}\mathbf{k}\cdot\mathbf{r}) = 4\pi\sum_{\ell=0}^{\infty}\sum_{m=-\ell}^{\ell} \mathrm{i}^{\ell} j_{\ell}(kr) Y_{\ell m}^{*}(\hat{\mathbf{k}}) Y_{\ell m}(\hat{\mathbf{r}}) \tag{3.62}$$

where $\hat{\mathbf{k}}$ denotes a unit vector in the direction of $\mathbf{k}$. These spherical- or partial-waves are then elastically scattered by the potential which introduces a phase-shift δ_{ℓ}, which is related to the logarithmic derivative of the exact radial solution for given ℓ and energy

$E = \frac{1}{2}k^2$ within the core, evaluated on the surface of the core region:

$$L_\ell(E) = \left[\frac{\mathrm{d}}{\mathrm{d}r}\log[R_\ell(r,E)]\right]_{r=r_\mathrm{c}} = \frac{R_\ell{}'(r_\mathrm{c},E)}{R_\ell(r_\mathrm{c},E)} = k\,\frac{j_\ell{}'(kr_\mathrm{c}) - \tan(\delta_\ell)n_\ell{}'(kr_\mathrm{c})}{j_\ell(kr_\mathrm{c}) - \tan(\delta_\ell)n_\ell(kr_\mathrm{c})}. \tag{3.63}$$

j_ℓ and n_ℓ denote the spherical Bessel and von Neumann functions respectively, and the radial wave-function $R_\ell(r,E)$ is related to the solution of the Schrödinger equation with angular momentum state determined by the good quantum numbers ℓ and m, and energy E, within the core region, $\psi_{\ell m}(\mathbf{r},E)$ by

$$\psi_{\ell m}(\mathbf{r},E) = R_\ell(r,E)Y_{\ell m}(\hat{\mathbf{r}}). \tag{3.64}$$

The phase-shifted spherical-waves can then be recombined to form the total scattered wave. We can define a reduced phase-shift η_ℓ by

$$\delta_\ell = n_\ell\pi + \eta_\ell \tag{3.65}$$

which has the same effect (the scattering amplitude depends on $\exp(2\mathrm{i}\delta_\ell)$ so that factors of π in δ_ℓ have no effect) and fix n_ℓ by requiring η_ℓ to lie in the interval $0 \le \eta_\ell \le \pi$. The integer n_ℓ counts the number of radial nodes in $R_\ell(r,E)$, two in the case of figure 3.2, and is thus equal to the number of core states with angular momentum ℓ.

The pseudopotential is then defined as the potential whose complete phase-shifts are the reduced shifts η_ℓ so that the radial pseudo-wave-function has no nodes and thus the potential has no core states. The scattering effect of this potential is the same as the original potential. We note again the energy-dependence of the phase-shifts so that for a good approximation it will be necessary to match these phase-shifts to first order in the energy so that it is accurate over a reasonable range of energies, a property which results in good *transferability* of the pseudopotential i.e. it is accurate in a variety of different chemical environments. The non-local nature is also exhibited since different angular momentum states are scattered differently.

3.3.3 Norm conservation

The conditions of a good pseudopotential are that it reproduces the logarithmic derivative of the wave-function (and thus the phase-shifts) correctly for the isolated atom, and also that the variation of this quantity with respect to energy is the same to first order for pseudopotential and full potential[2]. Having replaced the full potential by a pseudopoten-

[2]The chemical hardness has been proposed as a quantity which gives a more reliable indication of pseudopotential transferability since it includes self-consistent effects [63, 64].

tial, we can once again solve the Schrödinger equation in the core region to obtain the pseudo-wave-function, with radial part $R_{\mathrm{ps},\ell}(r,E)$.

Pseudopotential generation has itself been the subject of a great deal of study in the past (see [65–73]) and in this work we have chosen to use those pseudopotentials generated by the method of Troullier and Martins [74]. With one notable exception [75], all of the recent methods have used norm-conservation to guarantee that the phase-shifts are correct to first order in the energy (correction to higher orders is also possible [76]).

Consider the following second-order ordinary differential equations which are eigenvalue equations for the same differential operator but with different eigenvalues:

$$\begin{aligned} {y_1}''(x) + p(x){y_1}'(x) + q(x)y_1(x) &= \lambda_1 y_1(x) \\ {y_2}''(x) + p(x){y_2}'(x) + q(x)y_2(x) &= \lambda_2 y_2(x). \end{aligned} \tag{3.66}$$

In the context of homogeneous differential equations, the quantity known as the Wronskian is defined by

$$W(x) = y_1(x){y_2}'(x) - y_2(x){y_1}'(x) \tag{3.67}$$

and can be calculated according to

$$W(x) = W_0 \exp\left[-\int^x \mathrm{d}x' p(x')\right] \tag{3.68}$$

in which the constant W_0 is arbitrary and of no consequence.

Following a similar analysis which leads to equation 3.68 for the quantity defined in equation 3.67 but for the functions which solve equations 3.66 we obtain

$$W(x) = \left[(\lambda_2 - \lambda_1)\int^x \mathrm{d}x' y_1(x')y_2(x') \exp\left[\int^{x'} \mathrm{d}x'' p(x'')\right] + W_0\right] \exp\left[-\int^x \mathrm{d}x' p(x')\right] \tag{3.69}$$

and note that the Wronskian can also be rewritten in terms of logarithmic derivatives:

$$W(x) = y_1(x)y_2(x)\frac{\mathrm{d}}{\mathrm{d}x}\Big\{\log[y_2(x)] - \log[y_1(x)]\Big\}. \tag{3.70}$$

Using equations 3.69 and 3.70 in the case of the Schrödinger equation for the radial wave-function $R_\ell(r,E)$, by making the replacements

$$x \to r \quad ; \quad p(x) \to \frac{2}{r} \quad ; \quad q(x) \to -2\left[V(r) + \frac{\ell(\ell+1)}{r^2}\right] \quad ; \quad \lambda \to -2E,$$

and using limits $r = 0, r_c$ we obtain

$$\left[r^2 R_{\ell,1}(r)R_{\ell,2}(r)\frac{\mathrm{d}}{\mathrm{d}r}\{\log[R_{\ell,2}(r)] - \log[R_{\ell,1}(r)]\}\right]_0^{r_c} = -2(E_2 - E_1)\int_0^{r_c} \mathrm{d}r\ r^2 R_{\ell,1}(r)R_{\ell,2}(r). \tag{3.71}$$

Rearranging, multiplying by -2π and noting that the lower limit on the left-hand side contributes nothing because of the r^2 factor:

$$-2\pi r_c^2 \frac{R_{\ell,1}(r_c)R_{\ell,2}(r_c)}{E_2 - E_1}\frac{\mathrm{d}}{\mathrm{d}r}\Big[\log[R_{\ell,2}(r)] - \log[R_{\ell,1}(r)]\Big]_{r=r_c} = 4\pi\int_0^{r_c} \mathrm{d}r\ r^2 R_{\ell,1}(r)R_{\ell,2}(r). \tag{3.72}$$

Finally, taking the limit $E_2 \to E_1$ so that $R_{\ell,2}(r) \to R_{\ell,1}(r)$ and interpreting the left-hand side as a derivative with respect to energy we obtain the desired result:

$$-2\pi r_c^2 R_\ell^2(r_c)\frac{\mathrm{d}}{\mathrm{d}E}\left[\frac{\mathrm{d}}{\mathrm{d}r}\log[R_\ell(r)]\right]_{r=r_c} = 4\pi\int_0^{r_c} \mathrm{d}r\ r^2 R_\ell^2(r) \tag{3.73}$$

i.e. the first energy-derivative of the logarithmic derivative evaluated at the core radius (and hence the phase-shift) is related directly to the norm of the radial wave-function within the core region. Thus if the pseudo-wave-function is norm-conserving such that

$$4\pi\int_0^{r_c} \mathrm{d}r\ r^2 R_\ell^2(r) = 4\pi\int_0^{r_c} \mathrm{d}r\ r^2 R_{\mathrm{ps},\ell}^2(r) \tag{3.74}$$

then the phase-shifts of the pseudopotential will be the same as those of the real potential to first order in energy, and this can be achieved by making the pseudo-wave-function identical to the original all-electron wave-function outside the core region.

3.3.4 Kleinman-Bylander representation

We have seen that it is necessary to use a non-local pseudopotential to accurately represent the combined effect of nucleus and core electrons, since different angular momentum states (partial waves) are scattered differently. In general we can express the non-local pseudopotential in *semi-local* form

$$\hat{V}_{\mathrm{ps}} = \hat{V}_{\mathrm{loc}} + \sum_\ell \sum_{m=-\ell}^{\ell} |\ell m\rangle \delta\hat{V}_\ell \langle \ell m| \tag{3.75}$$

in which $|\ell m\rangle$ denotes the spherical harmonic $Y_{\ell m}$. The choice of local potential $\hat{V}_{\mathrm{loc}}$ is arbitrary, but in general the sum over ℓ is truncated at a small value (e.g. $\ell = 2$) so that the local part is required to represent the potential which acts on higher angular momentum components.

This semi-local form suffers from the disadvantage that it is computationally very expensive to use, since the number of matrix elements which need to be calculated scales as the square of the number of basis states, and this is generally too costly. In section 5.6.1 we will describe how this problem can be overcome analytically with a certain set of localised basis functions, but the most common solution, and one which we have also implemented for consistency, is to use the Kleinman-Bylander separable form [77]

$$\hat{V}_{\mathrm{KB}} = \hat{V}_{\mathrm{loc}} + \sum_{\ell m} \frac{|\delta \hat{V}_\ell \phi_{\ell m}\rangle \langle \phi_{\ell m} \delta \hat{V}_\ell|}{\langle \phi_{\ell m} | \delta \hat{V}_\ell | \phi_{\ell m}\rangle} \tag{3.76}$$

where $|\phi_{\ell m}\rangle$ is an eigenstate of the atomic pseudo-Hamiltonian. This operator acts on this reference state in an identical manner to the original semi-local operator $\hat{V}_{\mathrm{ps}}$ so that it is conceptually well-justified, but now the number of projections which need to be performed scales only linearly with the number of basis states. This separable form can in fact be viewed as the first term of a complete series [78].

Chapter 4

Density-Matrix Formulation

Density-functional theory together with the pseudopotential approximation has established itself as the method of choice for performing large-scale *ab initio* quantum-mechanical calculations. In particular, the fact that the kinetic energy operator is diagonal in momentum-space, that the Hartree and local pseudopotential contributions are straightforward to calculate in momentum-space, the development of fast Fourier transforms (FFTs) to efficiently switch between momentum-space and real-space and their natural relation to periodic boundary conditions (3.47) has led the plane-wave basis set and momentum-space formalism to become the most widely accepted method for performing such calculations [79, 80].

Efficient methods to solve the Kohn-Sham equations have been developed [81–83] which iteratively diagonalise the Hamiltonian. All of these plane-wave methods require a computational effort which scales as the cube of the system-size, and an amount of memory which scales as the square. Although these methods have made first-principles quantum-mechanical calculations available as a tool to a wide range of scientists in a variety of disciplines, this scaling ultimately limits the maximum system-size which can be treated now and in the near future, despite the rapid development of computer technology. A method which requires an effort and amount of memory which scales linearly with system-size would push the boundaries back much further, and so it is to the development of such a method that we now turn our attention.

There has been a great deal of success in developing linear-scaling tight-binding methods [84–88], but full density-functional methods have proved far more elusive. The first approach was the "divide and conquer" method [89–91] in which the large system is partitioned into overlapping subsystems. The original formulation divides the electronic density between these subsystems, solving for each in turn until self-consistency is reached. More recently, the density-matrix has been divided instead of the density [92] and these methods have been applied to large molecular systems [93, 94]. The recursion method [95, 96] has been used in a linear-scaling scheme to determine the electronic density by calculating diagonal elements of the Green's function [97]. Still other methods focus on the density of states, which could be used to obtain total energies by integrating up to the chemical potential [98–101].

As already mentioned, attempts to construct approximations for the density-functional itself have led to linear-scaling methods for metals [29,31,32]. Electronic structure methods suitable for metallic systems based upon the multiple scattering method have also been proposed [102–104].

The Fermi operator expansion method calculates the density-matrix at finite temperature in terms of a Chebychev expansion [105–108] or a rational representation [106, 109–111]. The closely related kernel polynomial method [112, 113] expands the zero temperature Fermi distribution by integrating an expansion of the delta function in which damping factors are used to suppress Gibbs oscillations.

One method related to the density-matrix schemes discussed next is based on a formulation of Kohn-Sham theory in terms of non-orthogonal localised orbitals [114]. A new energy functional of these localised orbitals which naturally leads to orthogonal orbitals at its minimum (which is the same as the ground-state minimum of the conventional functional) is introduced [115–121] and allows a linear-scaling method to be constructed, which has been used to study extended defects in silicon [122]. For a review of these methods and an explanation of their relationship to the density-matrix schemes, see [123].

The method most closely related to the approach introduced in this dissertation is the density-matrix minimisation method. The total energy is minimised with respect to the density-matrix and the purifying transformation (section 4.4.4) is used to impose the idempotency constraint [124–129].

In this chapter we introduce the concept of the density-matrix and show how it can be applied to the system of non-interacting particles in density-functional theory. We then show how a linear-scaling method results naturally from the short-ranged nature of the density-matrix in real-space, and discuss the constraints which must be imposed in order to find the ground-state.

4.1 The density-matrix

In section 2.1 we laid down the fundamental principles of quantum mechanics in terms of wave-functions and operators. In practice, however, we often do not know the precise quantum-mechanical state of the system, but have some statistical knowledge about the probabilities for the system being in one of a set of states (note that these probabilities are completely distinct from the probabilities which arise when a measurement is made). For a fuller discussion of what follows, see [130].

Suppose that there is a set of orthonormal states $\{|\psi_i\rangle\}$ for our system, and that the probabilities that the system is in each of these states are $\{w_i\}$. The expectation value of an observable O is

$$\langle O\rangle_{\rm stat} = \sum_i w_i \langle\psi_i|\hat{O}|\psi_i\rangle \tag{4.1}$$

which is a quantum *and* statistical average.

We define the *density-operator* as

$$\hat{\rho} = \sum_i w_i |\psi_i\rangle\langle\psi_i| \tag{4.2}$$

and introduce a complete set of basis states $\{|\phi_i\rangle\}$, writing the $\{|\psi_i\rangle\}$ as linear combinations:

$$|\psi_i\rangle = \sum_j c_j^{(i)} |\phi_j\rangle. \tag{4.3}$$

Expressed in terms of this basis, the expectation value becomes

$$\begin{aligned}
\langle O\rangle_{\rm stat} &= \sum_i w_i \sum_j c_j^{(i)*} \langle\phi_j|\hat{O} \sum_k c_k^{(i)} |\phi_k\rangle \\
&= \sum_j \sum_k \left[\sum_i c_j^{(i)*} w_i c_k^{(i)}\right] \langle\phi_j|\hat{O}|\phi_k\rangle \\
&= \sum_j \sum_k \rho_{kj} O_{jk} = \mathrm{Tr}(\rho O)
\end{aligned} \tag{4.4}$$

in which the density-matrix ρ_{kj}, the matrix representation of the density-operator in this basis, is defined by

$$\rho_{kj} = \sum_i c_j^{(i)*} w_i c_k^{(i)} = \langle\phi_k|\hat{\rho}|\phi_j\rangle. \tag{4.5}$$

The fact that the probabilities must sum to unity is expressed by the fact that the trace of the density-matrix is also unity i.e. $\mathrm{Tr}(\rho) = 1$. A state of the system which corresponds to a single state-vector (i.e. when $w_i = 1$ and $w_j = 0 \;\; \forall \; j \neq i$) is known as a *pure state* and for such a state the density-matrix obeys a condition known as *idempotency* i.e. $\rho^2 = \rho$ which is only obeyed by matrices whose eigenvalues are all zero or unity. The more general state introduced above is known as a *mixed state* and does not obey the idempotency condition. Other properties of the density-matrix are that it is Hermitian, and that in all representations the diagonal elements are always real and lie in the interval $[0, 1]$.

4.2 Partial occupation of the Kohn-Sham orbitals

In the Kohn-Sham scheme, the single-particle orbitals $\{|\psi_i\rangle\}$ were either empty or doubly occupied (two spin states). It will prove to be useful if we now generalise to include partial occupation [131] so that each orbital contains $2f_i$ electrons where $0 \leq f_i \leq 1$. The electronic density is now defined as

$$n(\mathbf{r}) = 2\sum_i f_i \left|\psi_i(\mathbf{r})\right|^2 . \tag{4.6}$$

Following the constrained search formulation we now define a generalised non-interacting kinetic energy functional $T_{\mathrm{s}}^{\mathrm{J}}[n]$ as

$$T_{\mathrm{s}}^{\mathrm{J}}[n] = \min_{\{f_i\},\{|\psi_i\rangle\}\to n} 2\sum_i f_i \int \mathrm{d}\mathbf{r}\ \psi_i^*(\mathbf{r}) \left(-\tfrac{1}{2}\nabla^2\right) \psi_i(\mathbf{r}) \tag{4.7}$$

where the search is over all orthonormal orbitals $\{|\psi_i\rangle\}$ and occupation numbers $\{f_i\}$ which yield the density $n(\mathbf{r})$ (which implies that $2\sum_i f_i = N$).

Janak's functional is defined as

$$E_V^{\mathrm{J}}[\{f_i\},\{|\psi_i\rangle\}] = 2\sum_i f_i \int \mathrm{d}\mathbf{r}\ \psi_i^*(\mathbf{r}) \left(-\tfrac{1}{2}\nabla^2\right) \psi_i(\mathbf{r}) + E_{\mathrm{H}}[n] + E_{\mathrm{xc}}^{\mathrm{J}}[n] + \int \mathrm{d}\mathbf{r}\ n(\mathbf{r})V_{\mathrm{ext}}(\mathbf{r}). \tag{4.8}$$

The minimisation is now performed with respect to both the occupation numbers $\{f_i\}$ and the orbitals $\{|\psi_i\rangle\}$.

For a fixed set of occupation numbers, the Euler-Lagrange equations for the variation of the functional with respect to the orbitals again yield Schrödinger-like equations:

$$\left[-\tfrac{1}{2}f_i\nabla^2 + f_i V_{\mathrm{KS}}(\mathbf{r})\right]\psi_i(\mathbf{r}) = \lambda_i\psi_i(\mathbf{r}) \tag{4.9}$$

in which we can identify $\lambda_i = f_i\varepsilon_i$ to obtain the Kohn-Sham equations

$$\left[-\tfrac{1}{2}\nabla^2 + V_{\mathrm{KS}}(\mathbf{r})\right]\psi_i(\mathbf{r}) = \varepsilon_i\psi_i(\mathbf{r}). \tag{4.10}$$

Multiplying by $\psi_i^*(\mathbf{r})$ and integrating gives

$$\int \mathrm{d}\mathbf{r}\ \psi_i^*(\mathbf{r}) \left(-\tfrac{1}{2}\nabla^2\right) \psi_i(\mathbf{r}) + \int \mathrm{d}\mathbf{r}\ \left|\psi_i(\mathbf{r})\right|^2 V_{\mathrm{KS}}(\mathbf{r}) = \varepsilon_i. \tag{4.11}$$

We obtain the dependence of the energy functional on the occupation numbers by varying one of the $\{f_i\}$ while allowing the orbitals to relax (i.e. solving equations 4.6 and

4.10 self-consistently). We define the kinetic energy for orbital i, t_i, by

$$t_i = \int d\mathbf{r}\ \psi_i^*(\mathbf{r}) \left(-\tfrac{1}{2}\nabla^2\right) \psi_i(\mathbf{r}) \tag{4.12}$$

in terms of which the generalised kinetic energy functional $T_\mathrm{s}^\mathrm{J}[n]$ is

$$T_\mathrm{s}^\mathrm{J}[n] = 2\sum_i f_i\ t_i. \tag{4.13}$$

Then

$$\frac{\partial E_V^\mathrm{J}}{\partial f_i} = 2t_i + 2\sum_j f_j \frac{\partial t_j}{\partial f_i} + 2\int d\mathbf{r}\ V_\mathrm{KS}(\mathbf{r}) \left(|\psi_i(\mathbf{r})|^2 + \sum_j f_j \frac{\partial |\psi_j(\mathbf{r})|^2}{\partial f_i} \right). \tag{4.14}$$

Using equation 4.11 we can rewrite the terms not involving a summation over orbitals:

$$\frac{\partial E_V^\mathrm{J}}{\partial f_i} = 2\varepsilon_i + 2\sum_j f_j \left(\frac{\partial t_j}{\partial f_i} + \int d\mathbf{r}\ V_\mathrm{KS}(\mathbf{r}) \frac{\partial |\psi_j(\mathbf{r})|^2}{\partial f_i} \right). \tag{4.15}$$

From the definition of t_j (4.12) we obtain

$$\frac{\partial t_j}{\partial f_i} = \int d\mathbf{r} \left[\frac{\partial \psi_j^*(\mathbf{r})}{\partial f_i} \left(-\tfrac{1}{2}\nabla^2\right) \psi_j(\mathbf{r}) + \psi_j^*(\mathbf{r}) \left(-\tfrac{1}{2}\nabla^2\right) \frac{\partial \psi_j(\mathbf{r})}{\partial f_i} \right]. \tag{4.16}$$

Substituting this result in equation 4.15 we obtain for the second term on the right-hand side

$$2\sum_j f_j \int d\mathbf{r} \left[\frac{\partial \psi_j^*(\mathbf{r})}{\partial f_i} \left(-\tfrac{1}{2}\nabla^2 + V_\mathrm{KS}(\mathbf{r})\right) \psi_j(\mathbf{r}) + \psi_j^*(\mathbf{r}) \left(-\tfrac{1}{2}\nabla^2 + V_\mathrm{KS}(\mathbf{r})\right) \frac{\partial \psi_j(\mathbf{r})}{\partial f_i} \right]. \tag{4.17}$$

Now using equation 4.10 we find

$$\frac{\partial E_V^\mathrm{J}}{\partial f_i} = 2\varepsilon_i + 2\sum_j f_j \varepsilon_j \frac{\partial}{\partial f_i} \int d\mathbf{r}\ |\psi_j(\mathbf{r})|^2. \tag{4.18}$$

The second term on the right-hand side vanishes since the orbitals are normalised and so the final result is that

$$\frac{\partial E_V^\mathrm{J}}{\partial f_i} = 2\varepsilon_i. \tag{4.19}$$

Variation of the functional subject to the constraint of constant electron number (i.e. unconstrained variation of $E_V^\mathrm{J} - \mu N$) gives

$$\delta[E_V^\mathrm{J} - \mu N] = 2\sum_i (\varepsilon_i - \mu)\delta f_i. \tag{4.20}$$

This generalised functional is not variational with respect to arbitrary variations in the occupation numbers [132]. Objections have been raised [133] to considering occupation numbers other than zero or one in zero-temperature density-functional theory, but the conclusion is still that at self-consistency, orbitals above the Fermi energy are unoccupied and orbitals below are fully occupied, and we recall that this state of affairs corresponds to an idempotent density-matrix.

If the occupation numbers are allowed to vary in the interval $[0,1]$ we see that the lowest value of the generalised functional is obtained for the correct choice of occupation numbers outlined above. However, if the occupation numbers are allowed to vary outside this interval, this result no longer holds since the energy can be lowered by over-filling ($f_i \to \infty$) orbitals below the Fermi level, or negatively filling ($f_i \to -\infty$) orbitals above the Fermi level, while still keeping the sum of the occupation numbers correct. Constraining the occupation numbers to avoid these unphysical situations is discussed in section 4.4.

4.3 Density-matrix DFT

We consider a system with a set of orthonormalised orbitals $\{|\psi_i\rangle\}$ and occupation numbers $\{f_i\}$. The single-particle density-operator $\hat{\rho}$ is defined by

$$\hat{\rho} = \sum_i f_i |\psi_i\rangle\langle\psi_i| \tag{4.21}$$

and the density-matrix in the coordinate representation is

$$\rho(\mathbf{r},\mathbf{r}') = \langle\mathbf{r}|\hat{\rho}|\mathbf{r}'\rangle = \sum_i f_i \; \psi_i(\mathbf{r})\psi_i^*(\mathbf{r}'). \tag{4.22}$$

The diagonal elements of the density-matrix are thus related to the electronic density by

$$n(\mathbf{r}) = 2\rho(\mathbf{r},\mathbf{r}) \tag{4.23}$$

and the generalised non-interacting kinetic energy is

$$T_{\mathrm{s}}^{\mathrm{J}}[n] = 2\int \mathrm{d}\mathbf{r}' \left[-\tfrac{1}{2}\nabla_{\mathbf{r}}^2 \rho(\mathbf{r},\mathbf{r}')\right]_{\mathbf{r}=\mathbf{r}'} . \tag{4.24}$$

This expression can be written as a trace of the density-matrix and the matrix elements of the kinetic energy operator $\hat{T} = -\frac{1}{2}\nabla^2$ i.e. $T_{\mathrm{s}}^{\mathrm{J}}[n] = 2\mathrm{Tr}(\rho T)$. Similarly, for the energy of interaction of the electrons with the external (pseudo-) potential

$$E_{\mathrm{ps}} = 2\int \mathrm{d}\mathbf{r}\;\mathrm{d}\mathbf{r}'\; V_{\mathrm{ps}}(\mathbf{r}',\mathbf{r})\rho(\mathbf{r},\mathbf{r}') = 2\mathrm{Tr}(\rho V_{\mathrm{ps}}) \tag{4.25}$$

where $V_{\text{ps}}(\mathbf{r}', \mathbf{r}) = \langle \mathbf{r}' | \hat{V}_{\text{ps}} | \mathbf{r} \rangle$. The definitions of the Hartree and exchange-correlation energies in terms of the electronic density (now defined in terms of the density-matrix by equation 4.23) remain unchanged. Thus we can express the total energy of both interacting and non-interacting systems in terms of the density-matrix. By minimising the energy with respect to the density-matrix (subject to appropriate constraints to be discussed) we can thus find the ground-state properties of the system.

4.4 Constraints on the density-matrix

4.4.1 Trace

From the definitions so far, the trace of the density-matrix is defined to be

$$2\text{Tr}(\rho) = 2 \int \mathrm{d}\mathbf{r}\ \rho(\mathbf{r}, \mathbf{r}) = \int \mathrm{d}\mathbf{r}\ n(\mathbf{r}) = N. \tag{4.26}$$

This constraint may be applied explicitly, which is a simple matter given that this is a linear constraint, or we may prefer to make the Legendre transform to the zero-temperature grand canonical ensemble and work at fixed chemical potential and variable electron number, minimising the grand potential $\Omega = E - \mu N$ rather than the total energy E. For insulators, it is sufficient for the chemical potential μ to be between the energies of the highest occupied and lowest unoccupied states.

4.4.2 Idempotency

The self-consistent ground-state density-matrix must display the property of idempotency i.e. $\rho^2 = \rho$. Unless the eigenvalues of the density-matrix (occupation numbers) remain in the interval $[0, 1]$ the density-matrix will follow unphysical "run-away" solutions. Unfortunately it is not possible to work directly with the eigenvalues of the density-matrix[1] to constrain them to lie in this interval and together with the non-linearity of the idempotency condition, this constraint turns out to be the major problem to be tackled. We briefly outline three ways in which this constraint can be dealt with. The first two of these are related and all three are described in [134] in the context of Hartree-Fock calculations.

If we are considering m orbitals in our scheme, then the density-matrix in the representation of those orbitals, or of a linear combination of those orbitals, is an Hermitian $m \times m$ matrix of rank $n = \frac{1}{2}N$. The factorisation property of idempotent density-matrices

[1] The computational cost of diagonalising a sparse density-matrix scales as the square of the system-size.

is that an idempotent matrix P may always be written

$$P = TT^{\dagger} \tag{4.27}$$

where T is an $m \times n$ matrix whose columns are orthonormal i.e.

$$T^{\dagger}T = 1_n \tag{4.28}$$

in which 1_n denotes the $n \times n$ identity matrix.

Any Hermitian matrix can be diagonalised by some unitary matrix U such that the diagonal matrix $\tilde{P}$ is

$$\tilde{P} = U^{\dagger}PU. \tag{4.29}$$

As already observed, the property $P^2 = P$ implies $\tilde{P}^2 = \tilde{P}$ so that each diagonal element (eigenvalue) is zero or one. The rank of P is unchanged by the unitary transformation so that $\tilde{P}$ has n 1's and $(m-n)$ 0's on its diagonal. In this case,

$$P = U\tilde{P}U^{\dagger} = U\tilde{P}^2U^{\dagger} = U\tilde{P}U^{\dagger}U\tilde{P}U^{\dagger} = TT^{\dagger} \tag{4.30}$$

in which T is an $m \times n$ rectangular matrix whose n columns are selected from those of U. These columns possess the required orthonormality from the unitary property of U and the proof of the factorisation property is complete.

We also note that expressing the density-matrix in this way guarantees that it is positive semi-definite

$$\tilde{P}_{ij} = \sum_k (U^{\dagger}T)_{ik}(U^{\dagger}T)^{\dagger}_{kj} = \sum_k (U^{\dagger}T)_{ik}(U^{\dagger}T)^{*}_{jk} \tag{4.31}$$

so that the eigenvalues are (no summation convention)

$$\tilde{P}_{ii} = \sum_k \left|(U^{\dagger}T)_{ik}\right|^2 \geq 0. \tag{4.32}$$

4.4.3 Penalty functional

Consider a matrix R_0 which is not idempotent i.e. $R_0^2 \neq R_0$. To make it so, we need to reduce the matrix $(R_0^2 - R_0)$ to zero, which can be achieved by minimising the (positive semi-definite) scalar quantity $\mathrm{Tr}\left[(R_0^2 - R_0)^2\right]$, whose minimum value is zero, with respect to the individual elements. Since

$$\frac{\partial \mathrm{Tr}\left[(R_0^2 - R_0)^2\right]}{\partial (R_0)_{ij}} = \left[2R_0(R_0 - 1)(2R_0 - 1)\right]_{ji}\,, \tag{4.33}$$

this can be achieved by using the right-hand side of this equation as a search direction in a steepest descents or conjugate gradients scheme. This results in a rapidly convergent (second order) sequence R_0, R_1, R_2 etc. which in the steepest descents method is defined by

$$R_{n+1} = R_n^2(3 - 2R_n). \tag{4.34}$$

The limit R_∞ is a strictly idempotent matrix close to R_0 in the sense that the separation

$$\mathrm{Tr}\left[(R_\infty - R_0)^2\right] \ll \mathrm{Tr}(R_\infty) = n. \tag{4.35}$$

Kohn [135] has suggested the use of the square-root of this function as a penalty functional for the density-matrix:

$$\mathcal{P}[\rho] = \left[\int \mathrm{d}\mathbf{r} \left(\rho^2(1-\rho)^2\right)(\mathbf{r},\mathbf{r})\right]^{\frac{1}{2}} \tag{4.36}$$

and has proved that the minimum of the functional

$$2\mathrm{Tr}(\rho H_{\mathrm{KS}}) - \mu N + \alpha\mathcal{P}[\rho]$$

equals the ground-state grand potential (i.e. $\mathcal{P}[\rho] = 0$) for some $\alpha > \alpha_{\mathrm{c}}(\{\varepsilon_i\};\mu)$. In particular,

$$\alpha_{\mathrm{c}} > 2\left[\sum_{i,\varepsilon_i \leq \mu} (\varepsilon_i - \mu)^2\right]^{\frac{1}{2}} \tag{4.37}$$

although he does not prove that this is a lower bound. A practical scheme would increase the value of α until the minimum of the functional occurred for $\mathcal{P}[\rho] = 0$, and this is discussed more fully in section 6.1.

4.4.4 Purifying transformation

We consider the result of one steepest descent step i.e. one iteration of equation 4.34 which allows us to write the density-matrix ρ in terms of an auxiliary matrix σ as

$$\rho = 3\sigma^2 - 2\sigma^3. \tag{4.38}$$

The second order convergence is exhibited by

$$\rho^2 - \rho = 4(\sigma^2 - \sigma)^3 - 3(\sigma^2 - \sigma)^2 \tag{4.39}$$

so that if σ is a nearly idempotent matrix (in a manner to be defined below), then ρ constructed from σ by (4.38) is a more nearly idempotent matrix, with leading error second-order in the error of σ.

In the common diagonal representation of ρ and σ this relationship can be expressed in terms of the individual eigenvalues λ_ρ and λ_σ:

$$\lambda_\rho = 3\lambda_\sigma^2 - 2\lambda_\sigma^3. \tag{4.40}$$

Thus as long as all of the eigenvalues of σ lie in the interval $-\frac{1}{2} \leq \lambda_\sigma \leq \frac{3}{2}$ the eigenvalues

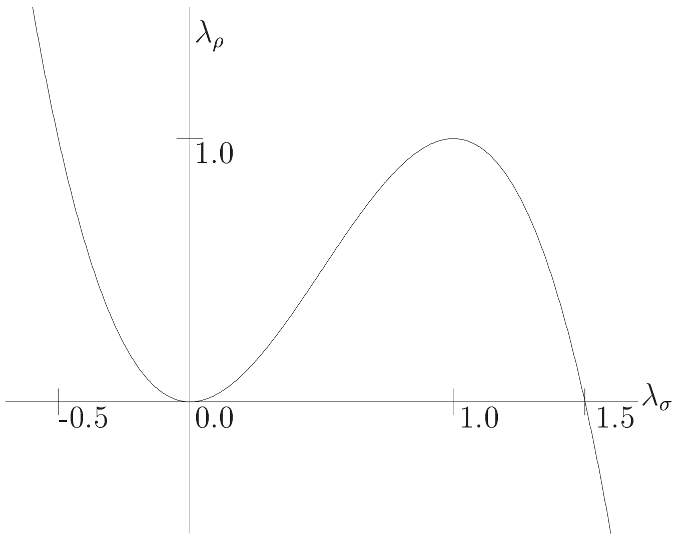

Figure 4.1: Behaviour of eigenvalues under the purifying transformation.

of ρ will lie in the interval $0 \leq \lambda_\rho \leq 1$ as required. If any of the eigenvalues of σ lie outside the interval $[\frac{1-\sqrt{5}}{2}, \frac{1+\sqrt{5}}{2}]$, then ρ as constructed by (4.38) will be *less* idempotent than σ, and this defines the meaning of "nearly idempotent" for σ. Run-away solutions are still possible when the purifying transformation is used to construct ρ, but at least there is now a metastable minimum at the ground-state, and variation of σ will implicitly drive ρ to idempotency.

4.4.5 Idempotency-preserving variations

Finally we consider the most general change which an idempotent $m \times m$ matrix of rank n can suffer, while maintaining that idempotency. Using the factorisation property we write

$R = TT^\dagger$ and consider changes in T i.e. $T \to T + \delta T$, where, without loss of generality,

$$\delta T = \Delta T \tag{4.41}$$

in which Δ is an arbitrary non-singular $m \times m$ matrix. Now the density-matrix R is a projection operator associated with an n-dimensional vector subspace (Γ_R) spanned by the columns of T. Any vector $\mathbf{x}$ may of course be uniquely decomposed into its components lying in the subspace Γ_R and in the complementary subspace Γ_{1-R}:

$$\mathbf{x} = \mathbf{x}_R + \mathbf{x}_{1-R} \tag{4.42}$$

where

$$\begin{aligned} \mathbf{x}_R &= R\mathbf{x}, & (4.43)\\ \mathbf{x}_{1-R} &= (1-R)\mathbf{x}. & (4.44) \end{aligned}$$

To define a new matrix R it is sufficient to define a new n-dimensional subspace. Since any vector can be decomposed according to equation 4.42, including the columns of T, any new vector (of arbitrary length) can be formed by adding a vector lying completely outside Γ_R. n arbitrary linearly-independent vectors of this kind are given by the columns of

$$\delta T = (1-R)\Delta T \tag{4.45}$$

in which the action of $(1-R)$ is to project out the part of ΔT lying in Γ_R. So $T + \delta T$ with δT defined by (4.45) defines a new subspace in a completely general way. However the columns of $T' = T + \delta T$ are no longer orthonormal and so it is necessary to orthonormalise the columns of T' to obtain a new set $\tilde{T}$ which defines the new projection operator

$$R + \delta R = \tilde{T}\tilde{T}^\dagger. \tag{4.46}$$

The metric associated with the vectors of T' is the $m \times m$ matrix $M = T'^\dagger T'$ and so a convenient orthonormalisation is

$$\tilde{T} = T' M^{-\frac{1}{2}}. \tag{4.47}$$

Defining $v = (1-R)\Delta R$ we note the following relations, following from $T^\dagger T = 1$ and $TT^\dagger = R$.

$$\begin{aligned} T^\dagger R &= T^\dagger(TT^\dagger) = (T^\dagger T)T^\dagger = T^\dagger & (4.48)\\ RT &= T & (4.49) \end{aligned}$$

$$
\begin{aligned}
T^\dagger v &= T^\dagger(1-R)\Delta R = 0 &(4.50)\\
v^\dagger T &= 0 &(4.51)
\end{aligned}
$$

Thus $R + \delta R$

$$
\begin{aligned}
&= \tilde{T}\tilde{T}^\dagger = T' M^{-\frac{1}{2}} (T' M^{-\frac{1}{2}})^\dagger = T' M^{-1} T'^\dagger = T'(T'^\dagger T')^{-1} T'^\dagger \\
&= [T + (1-R)\Delta T] \left[(T + (1-R)\Delta T)^\dagger (T + (1-R)\Delta T)\right]^{-1} [T + (1-R)\Delta T]^\dagger \\
&= (R+v)T \left[T^\dagger (1+v^\dagger)(1+v)T\right]^{-1} T^\dagger (R + v^\dagger) \\
&= (R+v) \left[1 + v^\dagger v\right]^{-1} (R + v^\dagger). &(4.52)
\end{aligned}
$$

When Δ represents a small change, then a convergent expansion for the inverse matrix in equation 4.52 can be used

$$
\left[1 + v^\dagger v\right]^{-1} = \sum_{n=0}^{\infty} (-1)^n (v^\dagger v)^n \qquad (4.53)
$$

to write down δR to any order

$$
\delta R = (v + v^\dagger) + (v v^\dagger - v^\dagger v) + \ldots \qquad (4.54)
$$

By taking the expansion to first order only, we make the change δR linear in Δ (which has certain advantages e.g. in implementing conjugate gradients) and see that this does indeed maintain idempotency to first order:

$$
\begin{aligned}
\delta R &= v + v^\dagger = (1-R)\Delta R + R\Delta^\dagger (1-R), &(4.55)\\
& &(4.56)\\
(R+\delta R)^2 - (R + \delta R) &= (R^2 - R) + R\delta R + (\delta R)R + (\delta R)^2 - \delta R \\
&= R(1-R)\Delta R + R^2 \Delta^\dagger (1-R) + (1-R)\Delta R^2 + R\Delta(1-R)R \\
&\quad -(1-R)\Delta R - R\Delta^\dagger(1-R) + (\delta R)^2 \\
&= (R^2 - R)\Delta^\dagger (1-R) + (1-R)\Delta(R^2 - R) + (\delta R)^2 \\
&= (\delta R)^2 &(4.57)
\end{aligned}
$$

which vanishes to first order in δR as required. Thus if we have the ground-state density-matrix and consider making variations consistent with idempotency to first order as described here, then the energy must increase, and again some stability against the run-away solutions is obtained.

4.5 Requirements for linear-scaling methods

We have shown how it is possible to reformulate density-functional theory in terms of the single-particle density-matrix, and the constraints which must be obeyed by ground-state density-matrices. However, in the coordinate representation, we note that the density-matrix is a function of two position variables $\rho(\mathbf{r}, \mathbf{r}')$ and thus contains an amount of information which scales as the square of the system-size (as of course it must since it contains all of the information in the Kohn-Sham orbitals, which are functions of one position but with the number of occupied orbitals also scaling linearly with system-size). To obtain a linear-scaling method, it is necessary to impose some further restrictions on the density-matrix.

4.5.1 Separability

In practice we do not wish to deal with a function of six variables (i.e. two three-dimensional positions). From the factorisation property of idempotent density-matrices, or the definition of the ground-state density-matrix in terms of the Kohn-Sham orbitals;

$$\rho(\mathbf{r}, \mathbf{r}') = \sum_i \psi_i(\mathbf{r}) f_i \ \psi_i^*(\mathbf{r}'), \tag{4.58}$$

we see that it is possible to consider separable density-matrices described in terms of some auxiliary orbitals. The general form of a separable density-matrix in terms of orbitals $\{\varphi_i\}$ is

$$\rho(\mathbf{r}, \mathbf{r}') = \sum_{ij} \varphi_i(\mathbf{r}) R_{ij} \varphi_j^*(\mathbf{r}'). \tag{4.59}$$

Although it is not necessary for the auxiliary orbitals to be orthonormal, in the case when they are, we can consider this general form as simply a unitary transformation of the Kohn-Sham expression (4.58):

$$\psi_i(\mathbf{r}) = \sum_j \varphi_j(\mathbf{r}) U_{ji} \tag{4.60}$$

where U is the unitary matrix which diagonalises R:

$$f_i = (U^\dagger R U)_{ii} \qquad \text{(no summation)}. \tag{4.61}$$

When the auxiliary orbitals are not orthonormal, then they can be viewed as a more general linear combination of the Kohn-Sham orbitals (involving both a unitary and Löwdin transformation) which is described in section 4.6. Whichever case applies, there is no loss of generality here as all idempotent matrices can always be expressed in this way, and these are the density-matrices of interest to us.

4.5.2 Spatial localisation

Kohn [136] has proved that in one-dimensional systems with a gap, a set of exponentially decaying Wannier functions can be found in the tight-binding limit, and that this localisation is related to the square-root of the gap. His method is not easily generalised to higher numbers of dimensions, and so until recently the exact nature of the Wannier functions in general three-dimensional systems was unknown, although it was anticipated that they would decay exponentially [137–139]. More recent numerical and analytical studies of the localisation of the density-matrix showed the decay to be exponential and again related to the square-root of the gap [140, 141], thus supporting the general validity of Kohn's result. Very recently, however, Ismail-Beigi and Arias [142] have argued that in the weak-binding limit the exponential decay varies linearly with the gap. What is now certain is that the Wannier functions and density-matrix decay exponentially in systems with a gap, and that this decay is more rapid in systems with larger gaps.

Wannier functions are simply a unitary transformation of Bloch wave-functions with respect to the complementary variables of Bloch wave-vector and lattice vector. Let $\psi_{n\mathbf{k}}(\mathbf{r})$ be the normalised Bloch wave-function for the nth band with wave-vector $\mathbf{k}$. Then the corresponding Wannier function for that band $w_{n\mathbf{R}}(\mathbf{r})$ is defined by [143]

$$w_{n\mathbf{R}}(\mathbf{r}) = \left(\frac{\Omega_{\text{cell}}}{(2\pi)^3}\right)^{\frac{1}{2}} \int_{1\text{BZ}} \mathrm{d}\mathbf{k}\ \psi_{n\mathbf{k}}(\mathbf{r}) \exp(-\mathrm{i}\mathbf{k}\cdot\mathbf{R}) \tag{4.62}$$

and naturally the inverse relation holds:

$$\psi_{n\mathbf{k}}(\mathbf{r}) = \left(\frac{\Omega_{\text{cell}}}{(2\pi)^3}\right)^{\frac{1}{2}} \sum_{\mathbf{R}} w_{n\mathbf{R}}(\mathbf{r}) \exp(\mathrm{i}\mathbf{k}\cdot\mathbf{R}). \tag{4.63}$$

The properties of Wannier functions are that they are localised in different cells (labelled by lattice vector $\mathbf{R}$) and are orthonormal:

$$\int \mathrm{d}\mathbf{r}\ w^*_{n\mathbf{R}}(\mathbf{r})\ w_{n\mathbf{R}'}(\mathbf{r}) = \delta_{\mathbf{R}\mathbf{R}'}. \tag{4.64}$$

The single-particle density-matrix in the case of full $\mathbf{k}$-point sampling $\varrho(\mathbf{r},\mathbf{r}')$ is given by

$$\varrho(\mathbf{r},\mathbf{r}') = \sum_i f_i \frac{1}{\Omega_{\text{BZ}}} \int \mathrm{d}\mathbf{k}\ \psi_{i\mathbf{k}}(\mathbf{r})\psi^*_{i\mathbf{k}}(\mathbf{r}') \tag{4.65}$$

(in which we have assumed that we are dealing with an insulator with completely full or empty bands) which is a trace over wave-vector $\mathbf{k}$ and thus invariant under unitary transformation so that it can also be written

$$\varrho(\mathbf{r},\mathbf{r}') = \sum_i f_i \sum_{\mathbf{R}} w_{i\mathbf{R}}(\mathbf{r}) w^*_{i\mathbf{R}}(\mathbf{r}'). \tag{4.66}$$

Thus if the Wannier function $w_{i\mathbf{R}}(\mathbf{r})$ is vanishing when $|\mathbf{r}-\mathbf{R}|$ is large, then when $|\mathbf{r}-\mathbf{r}'|$ is large the density-matrix must also vanish in the same way since it is impossible in that case for both $|\mathbf{r}-\mathbf{R}|$ and $|\mathbf{r}'-\mathbf{R}|$ to be small. Thus we expect that

$$\rho(\mathbf{r},\mathbf{r}') \to 0 \qquad \text{as } |\mathbf{r}-\mathbf{r}'| \to \infty \tag{4.67}$$

where at zero temperature the decay is exponential in insulators and algebraic in metals.

We can exploit this long-range behaviour to obtain a linear-scaling method: we introduce a spatial cut-off r_{cut} and require that the density-matrix be strictly zero when the separation of its arguments exceeds this cut-off;

$$\rho(\mathbf{r},\mathbf{r}') = 0, \qquad |\mathbf{r}-\mathbf{r}'| > r_{\text{cut}}, \tag{4.68}$$

so that the density-matrix now only contains an amount of information which scales linearly with system-size. Imposing this cut-off naturally restricts the variational freedom of the density-matrix, so it will be necessary to converge the ground-state energy with respect to this parameter in real calculations. Using the separable form above, we can impose this restriction by requiring the auxiliary orbitals to be localised in space (i.e. vanishing outside a certain region of space) and by making the matrix R sparse, so that elements of R corresponding to orbitals localised in regions separated by more than the spatial cut-off r_{cut} are automatically set to zero. The localised nature of the auxiliary orbitals requires a localised basis-set to describe them, and this is the subject of chapter 5.

4.6 Non-orthogonal orbitals

We conclude this chapter with a discussion about the representation of the density-matrix using non-orthogonal orbitals. We consider a set of non-orthogonal functions $\{\phi_\alpha(\mathbf{r})\}$ which we denote $\{|\phi_\alpha\rangle\}$, and introduce their dual functions defined by

$$|\phi^\alpha\rangle = |\phi_\beta\rangle S^{-1}_{\beta\alpha} \tag{4.69}$$

in which the summation convention is assumed and the matrix S^{-1} is the inverse of the overlap matrix S defined by

$$S_{\alpha\beta} = \langle \phi_\alpha | \phi_\beta \rangle = \int \mathrm{d}\mathbf{r}\ \phi_\alpha(\mathbf{r}) \phi_\beta(\mathbf{r}). \tag{4.70}$$

We have assumed from now on that we are only calculating wave-functions at the Γ-point and so can assume that everything is real. By construction, the dual states obey

$$\langle \phi^\alpha | \phi_\beta \rangle = \langle \phi_\alpha | \phi^\beta \rangle = \delta_\alpha^\beta \tag{4.71}$$

and the completeness relation is expressed as

$$|\phi^\alpha\rangle\langle\phi_\alpha| = |\phi_\alpha\rangle\langle\phi^\alpha| = |\phi_\alpha\rangle S^{-1}_{\alpha\beta}\langle\phi_\beta| = 1. \tag{4.72}$$

In general we will represent the density-matrix in the separable form

$$\rho(\mathbf{r}, \mathbf{r}') = \phi_\alpha(\mathbf{r}) K^{\alpha\beta} \phi_\beta(\mathbf{r}') \tag{4.73}$$

and note that the *density-kernel* $K^{\alpha\beta} \neq \langle \phi_\alpha | \hat{\rho} | \phi_\beta \rangle$ because of the non-orthogonality.

We can construct an orthonormalised set of orbitals $\{|\varphi_\alpha\rangle\}$ defined as linear combinations of the $\{|\phi_\alpha\rangle\}$ by the Löwdin transformation:

$$|\varphi_\alpha\rangle = |\phi_\beta\rangle S^{-\frac{1}{2}}_{\beta\alpha} \tag{4.74}$$

such that

$$\langle \varphi_\alpha | \varphi_\beta \rangle = S^{-\frac{1}{2}}_{\alpha\gamma} \langle \phi_\gamma | \phi_\delta \rangle S^{-\frac{1}{2}}_{\delta\beta} = S^{-\frac{1}{2}}_{\alpha\gamma} S_{\gamma\delta} S^{-\frac{1}{2}}_{\delta\beta} = \delta_{\alpha\beta}. \tag{4.75}$$

At the ground-state, these orthonormal orbitals $\{|\varphi_\alpha\rangle\}$ will be a unitary transformation of the Kohn-Sham orbitals $\{|\psi_i\rangle\}$, so that the density-kernel $\tilde{K}$ defined as the density-matrix in the representation of the orthonormalised orbitals $\{|\varphi_\alpha\rangle\}$,

$$\tilde{K}_{\alpha\beta} = \langle \varphi_\alpha | \hat{\rho} | \varphi_\beta \rangle, \tag{4.76}$$

can be diagonalised by a unitary transformation U as described in section 4.5.1 i.e. $f_i = (U^\dagger \tilde{K} U)_{ii}$ (no summation convention). The following relationship also holds;

$$|\psi_i\rangle = |\varphi_\alpha\rangle U_{\alpha i}, \tag{4.77}$$

and the relationship between the non-orthogonal orbitals $\{|\phi_\alpha\rangle\}$ and the Kohn-Sham orbitals $\{|\psi_i\rangle\}$ is of the general form

$$|\psi_i\rangle = |\varphi_\alpha\rangle U_{\alpha i} = |\phi_\beta\rangle S^{-\frac{1}{2}}_{\beta\alpha} U_{\alpha i} = |\phi_\beta\rangle V_{\beta i} \tag{4.78}$$

where the matrix $V = S^{-\frac{1}{2}}U$ and obeys

$$\begin{aligned} V^\dagger V &= U^\dagger S^{-1} U, && (4.79) \\ V V^\dagger &= S^{-1}. && (4.80) \end{aligned}$$

Using the completeness relation (4.72) we can now express the matrix K in terms of other quantities:

$$\begin{aligned} \rho(\mathbf{r}, \mathbf{r}') &= \phi_\alpha(\mathbf{r}) K^{\alpha\beta} \phi_\beta(\mathbf{r}') \\ &= \langle \mathbf{r}|\hat{\rho}|\mathbf{r}'\rangle = \langle \mathbf{r}|\phi_\alpha\rangle S^{-1}_{\alpha\gamma} \langle\phi_\gamma|\hat{\rho}|\phi_\delta\rangle S^{-1}_{\delta\beta} \langle\phi_\beta|\mathbf{r}'\rangle \\ &= \phi_\alpha(\mathbf{r}) S^{-1}_{\alpha\gamma} \langle\phi_\gamma|\hat{\rho}|\phi_\delta\rangle S^{-1}_{\delta\beta} \phi_\beta(\mathbf{r}') && (4.81) \end{aligned}$$

so that

$$\begin{aligned} K^{\alpha\beta} &= S^{-1}_{\alpha\gamma} \langle\phi_\gamma|\hat{\rho}|\phi_\delta\rangle S^{-1}_{\delta\beta}, && (4.82) \\ \langle\phi_\alpha|\hat{\rho}|\phi_\beta\rangle &= (SKS)_{\alpha\beta}. && (4.83) \end{aligned}$$

In fact, the density-kernel K contains the matrix elements of the density-operator in the representation of the dual vectors of the non-orthogonal functions:

$$K^{\alpha\beta} = S^{-1}_{\alpha\gamma} \langle\phi_\gamma|\hat{\rho}|\phi_\delta\rangle S^{-1}_{\delta\beta} = \langle\phi^\alpha|\hat{\rho}|\phi^\beta\rangle, \tag{4.84}$$

hence the superscript notation.

If we wish to obtain the occupation numbers, we must diagonalise the matrix $\tilde{K}$ which is given by

$$\begin{aligned} \tilde{K}_{\alpha\beta} &= \langle\varphi_\alpha|\hat{\rho}|\varphi_\beta\rangle \\ &= \langle\varphi_\alpha|\phi_\gamma\rangle S^{-1}_{\gamma\delta} \langle\phi_\delta|\hat{\rho}|\phi_\epsilon\rangle S^{-1}_{\epsilon\zeta} \langle\phi_\zeta|\varphi_\beta\rangle \\ &= S^{\frac{1}{2}}_{\alpha\gamma} S^{-1}_{\gamma\delta} (SKS)_{\delta\epsilon} S^{-1}_{\epsilon\zeta} S^{\frac{1}{2}}_{\zeta\beta} \\ &= (S^{\frac{1}{2}} K S^{\frac{1}{2}})_{\alpha\beta}. && (4.85) \end{aligned}$$

Thus the eigenvalues of $(S^{\frac{1}{2}} K S^{\frac{1}{2}})$ are the occupation numbers.

At the ground-state, the density-operator and Hamiltonian commute, and thus both the Hamiltonian and the density-matrix can be diagonalised simultaneously. The Hamiltonian is usually represented by its matrix elements in the representation of the non-orthogonal orbitals. Thus

$$H_{\alpha\beta} = \langle \phi_\alpha | \hat{H} | \phi_\beta \rangle \tag{4.86}$$

in contrast to the definition of K. In this case, to obtain the eigenvalues of the Hamiltonian $\{\varepsilon_i\}$ it is necessary to diagonalise the matrix $\tilde{H}$

$$\begin{aligned} \tilde{H}_{\alpha\beta} &= \langle \varphi_\alpha | \hat{H} | \varphi_\beta \rangle \\ &= \langle \varphi_\alpha | \phi_\gamma \rangle S^{-1}_{\gamma\delta} \langle \phi_\delta | \hat{H} | \phi_\epsilon \rangle S^{-1}_{\epsilon\zeta} \langle \phi_\zeta | \varphi_\beta \rangle \\ &= S^{\frac{1}{2}}_{\alpha\gamma} S^{-1}_{\gamma\delta} H_{\delta\epsilon} S^{-1}_{\epsilon\zeta} S^{\frac{1}{2}}_{\zeta\beta} \\ &= (S^{-\frac{1}{2}} H S^{-\frac{1}{2}})_{\alpha\beta} \end{aligned} \tag{4.87}$$

i.e. the eigenvalues of $(S^{-\frac{1}{2}} H S^{-\frac{1}{2}})$ are those of the Kohn-Sham Hamiltonian.

The advantage of representing the density-operator and Hamiltonian in different ways is that quantities such as the electron number and non-interacting energy can be expressed easily:

$$N = 2\mathrm{Tr}(\tilde{K}) = 2\mathrm{Tr}(KS) \tag{4.88}$$

$$E_{\mathrm{NI}} = 2\mathrm{Tr}(\tilde{K}\tilde{H}) = 2\mathrm{Tr}(KH) \tag{4.89}$$

since the factors of $S^{-\frac{1}{2}}$ and $S^{\frac{1}{2}}$ cancel.

In the language of tensor analysis, the functions $\{|\phi_\alpha\rangle\}$ are covariant vectors, and their duals the associated contravariant quantities. The overlap matrix $S_{\alpha\beta}$ plays the rôle of the metric tensor to convert between covariant and contravariant quantities. This is seen by verifying the relationship

$$S^{\alpha\beta} = S^{-1}_{\alpha\beta}. \tag{4.90}$$

For the orthogonal functions $\{|\varphi_\alpha\rangle\}$, the metric tensor is the identity and so there is no distinction between covariant and contravariant quantities.

In a linear-scaling scheme we will not be able to access the eigenvalues directly, since although H and K are sparse, $\tilde{H}$ and $\tilde{K}$ need not be, and in any case, the effort to diagonalise even a sparse matrix is $\mathcal{O}(N^2)$. However it is important to understand the different origins and rôles of these matrices in order to analyse the equations which result when we attempt to minimise the total energy to find the ground-state.

Chapter 5

Localised basis-set

One elegant and popular choice of basis in traditional calculations has been the plane-wave basis. However, because of the extended nature of these basis functions they cannot be used in linear-scaling calculations, and a different choice has to be made, in which the basis functions are localised in real-space. Gaussians [144] are a popular choice since many quantities can be calculated analytically [145], an advantage shared by the basis-set proposed here. Other choices include truncated atomic orbitals [146], B-splines or "blip" functions [147], wavelets [148] and real-space grids [149].

In this chapter we consider a localised spherical-wave basis set suitable for linear-scaling total-energy pseudopotential calculations. The basis-set is conveniently truncated using a single parameter, the kinetic energy cut-off used with the plane-wave basis. We present analytic results for the overlap integrals between any two basis functions centred on different sites, as well as for the kinetic energy matrix-elements which can, therefore, be evaluated accurately in real-space. Two methods for analytically performing the projection of the basis states onto angular momentum states required for the use of non-local pseudopotentials are also presented. This work has been published in [150].

5.1 Introduction

We present a set of localised functions which are related to the plane-wave basis set and share some of its attractive features. A significant problem associated with localised basis functions is that they are not in general orthogonal, so that as the size of the basis is increased, the overlap matrix becomes singular. We demonstrate that the basis functions introduced here are orthogonal, by construction, to others centred on the same site, and that the overlap matrix elements for functions centred on different sites can be calculated analytically, and hence evaluated efficiently and accurately when implemented computationally.

Another disadvantage of using basis functions localised in real-space arises in the calculation of the action of the kinetic energy operator. To take advantage of the localisation it is necessary to focus on real-space and calculate all quantities in that representation. However, since the kinetic energy operator is diagonal in reciprocal-space, the kinetic energy matrix elements are most naturally calculated in reciprocal-space. Methods to evaluate the kinetic energy using finite-difference schemes can be inaccurate when used with localised functions. It is particularly difficult to obtain accurate values for second derivatives in the vicinity of the support region boundaries so that this error is of the order of the surface area to volume ratio. For the one-centre integrals this is not significant, but for the two-centre integrals, the intersection of two spheres may have a large surface area to volume ratio and the error may therefore be large. Indeed, investigations show that the estimates of such integrals obtained by finite differences may often be of the wrong sign! With the new choice of basis, the matrix-elements of the kinetic energy operator between any two functions can also be calculated analytically, thereby overcoming this problem.

One final advantage arises in the inclusion of non-local pseudopotentials which traditionally required significant computational effort. We present two methods of obtaining the matrix-elements of the non-local pseudopotential operator by performing the projection of the basis function onto a core angular momentum state analytically.

5.2 Origin of the basis functions

As described in section 3.3, in the pseudopotential approximation, the core electrons and strong ionic potential of the atom are replaced by a much weaker potential in which the remaining pseudo-valence electrons move. The pseudo-valence states no longer have to be orthogonal to lower-lying core states and hence are much smoother than the all-electron valence states in the core region and have less kinetic energy. Thus the pseudo-valence states can be accurately represented by a much smaller set of plane-wave basis functions than the all-electron states.

The plane-wave basis state $\exp[i\mathbf{q}\cdot\mathbf{r}]$ is a solution of the Helmholtz equation (the time-independent free-electron Schrödinger equation)

$$\left(\nabla^2 + q^2\right)\psi(\mathbf{r}) = 0 \tag{5.1}$$

subject to periodic boundary conditions, with energy $E = \frac{1}{2}q^2$.

If instead we wish to localise the basis functions, say within spherical regions of radius a, so that the function vanishes outside these regions, then appropriate conditions would be to require the functions to be finite within the regions and to vanish on the boundary. The solutions to the Helmholtz equation 5.1 subject to these conditions are then truncated spherical-waves

$$\psi(\mathbf{r}) = \begin{cases} j_\ell(qr)\ Y_{\ell m}(\vartheta,\varphi), & r < a \\ 0, & r \geq a \end{cases} \tag{5.2}$$

where (r,ϑ,φ) are spherical polar coordinates with the origin at the centre of the spherical region, ℓ is a non-negative integer, m is an integer satisfying $-\ell \leq m \leq \ell$ and q is chosen to satisfy $j_\ell(qa) = 0$. j_ℓ denotes a spherical Bessel function and $Y_{\ell m}$ is a spherical harmonic. Solutions involving the spherical von Neumann function n_ℓ have been rejected because they are not finite at the centre of the sphere.

We note that these functions solve the same equation as the plane-wave basis functions, so that within the pseudopotential approximation the wave-functions will be well-described by a truncated set of these basis functions. Moreover, these functions are eigenstates of the kinetic energy operator within the localisation region $r < a$ (i.e. in the region in which they will be used to describe the wave-functions) with eigenvalue $\frac{1}{2}q^2$ so that the same kinetic energy cut-off used to truncate the plane-wave basis can be used here to restrict the values of ℓ and q.

Since the Laplacian is a self-adjoint operator under these boundary conditions, application of Sturm-Liouville theory proves that all states within the same spherical region are mutually orthogonal.

In a calculation, the electronic states are described by covering the simulation cell with overlapping spheres (known as support regions), usually chosen to be centred on the ions or bond-centres at positions $\mathbf{R}_\alpha$, and expanding the localised support functions ϕ_α within these spheres in this basis:

$$\phi_\alpha(\mathbf{r}) = \sum_{n\ell m} c_{(\alpha)}^{n\ell m}\ j_\ell(q_{n\ell}\,|\mathbf{r}-\mathbf{R}_\alpha|)\ Y_{\ell m}(\Omega_{\mathbf{r}-\mathbf{R}_\alpha}). \tag{5.3}$$

The notation $\Omega_{\mathbf{r}}$ is introduced as shorthand for the polar and azimuthal angles of the vector $\mathbf{r}$ used to represent that vector in spherical polar coordinates. We denote the radius of the sphere by r_α so that the $\{q_{n\ell}\}$ satisfy $j_\ell(q_{n\ell}r_\alpha) = 0$.

The expansion (5.3) is frequently written down formally, but rarely used computationally because of the inconvenience of using spherical Bessel functions in numerical work. However, the analytic results derived in the following sections offset this disadvantage.

As mentioned in section 3.2.2, linear-scaling methods are aimed at large systems, and so the Brillouin zone sampling of the electronic states is usually restricted to the states at the Γ-point only. The wave-functions can then be made real without loss of generality, and so in practice we use real linear combinations of the spherical harmonics defined below, which does not alter any of the analysis here.

$$\{Y_{\ell m}\} \rightarrow \left\{ \begin{array}{rcl} \bar{Y}_{\ell,0}(\Omega) & = & Y_{\ell,0}(\Omega) \\ \bar{Y}_{\ell,|m|}(\Omega) & = & \frac{1}{\sqrt{2}}\left[Y_{\ell,-|m|}(\Omega) + (-1)^m Y_{\ell,|m|}(\Omega)\right] \\ \bar{Y}_{\ell,-|m|}(\Omega) & = & \frac{\mathrm{i}}{\sqrt{2}}\left[Y_{\ell,-|m|}(\Omega) - (-1)^m Y_{\ell,|m|}(\Omega)\right] \end{array} \right\} \tag{5.4}$$

These real combinations of spherical harmonics, which we denote $\bar{Y}_{\ell m}$, can be written down as real functions of the variables $\left\{\frac{x}{r}, \frac{y}{r}, \frac{z}{r}\right\}$ where (x, y, z) are Cartesian coordinates with origin at the centre of the sphere, and are familiar as the angular components of s, p, d etc. orbitals.

We introduce $\chi_{\alpha,n\ell m}(\mathbf{r})$ to represent a truncated spherical-wave basis function centred at $\mathbf{R}_\alpha$ and confined to a sphere of radius r_α:

$$\chi_{\alpha,n\ell m}(\mathbf{r}) = \begin{cases} j_\ell(q_{n\ell}\,|\mathbf{r}-\mathbf{R}_\alpha|)\bar{Y}_{\ell m}(\Omega_{\mathbf{r}-\mathbf{R}_\alpha}), & |\mathbf{r}-\mathbf{R}_\alpha| \leq r_\alpha, \\ 0, & |\mathbf{r}-\mathbf{R}_\alpha| > r_\alpha. \end{cases} \tag{5.5}$$

Equation 5.3 can then be written:

$$\phi_\alpha(\mathbf{r}) = \sum_{n\ell m} c_{(\alpha)}^{n\ell m}\ \chi_{\alpha,n\ell m}(\mathbf{r}). \tag{5.6}$$

5.3 Fourier transform of the basis functions

We define the Fourier transform of a basis function $\chi_{\alpha,n\ell m}(\mathbf{r})$ by

$$\begin{aligned} \tilde{\chi}_{\alpha,n\ell m}(\mathbf{k}) &= \int_{\text{all space}} \mathrm{d}\mathbf{r}\ \exp[\mathrm{i}\mathbf{k}\cdot\mathbf{r}]\ \chi_{\alpha,n\ell m}(\mathbf{r}) \\ &= \exp\left[\mathrm{i}\mathbf{k}\cdot\mathbf{R}_\alpha\right] \int_0^{r_\alpha} \mathrm{d}r\ r^2\ j_\ell(q_{n\ell}r) \int \mathrm{d}\Omega_{\mathbf{r}}\ \exp[\mathrm{i}\mathbf{k}\cdot\mathbf{r}]\ \bar{Y}_{\ell m}(\Omega_{\mathbf{r}}). \end{aligned} \tag{5.7}$$

The angular integral is performed by using the expansion of $\exp[\mathrm{i}\mathbf{k}\cdot\mathbf{r}]$ into spherical-waves (A.3, appendix A) leaving the radial integral

$$\tilde{\chi}_{\alpha,n\ell m}(\mathbf{k}) = 4\pi\mathrm{i}^\ell\ \bar{Y}_{\ell m}(\Omega_{\mathbf{k}}) \exp\left[\mathrm{i}\mathbf{k}\cdot\mathbf{R}_\alpha\right] \int_0^{r_\alpha} \mathrm{d}r\ r^2\ j_\ell(q_{n\ell}r)\ j_\ell(kr). \tag{5.8}$$

The radial integral can now be calculated using equations A.4 and A.5 and the boundary conditions (that the basis functions are finite at $r = 0$ and vanish at $r = r_\alpha$) for the cases when $k \neq q_{n\ell}$ and $k = q_{n\ell}$ respectively. The final result for the Fourier transform of a basis function is then

$$\tilde{\chi}_{\alpha,n\ell m}(\mathbf{k}) = 4\pi \mathrm{i}^{\ell}\ \bar{Y}_{\ell m}(\Omega_{\mathbf{k}}) \exp\left[\mathrm{i}\mathbf{k}\cdot\mathbf{R}_{\alpha}\right] \begin{cases} \dfrac{q_{n\ell} r_{\alpha}^2}{k^2 - q_{n\ell}^2} j_{\ell}(kr_{\alpha}) j_{\ell-1}(q_{n\ell} r_{\alpha}), & k \neq q_{n\ell}, \quad (a) \\ \\ \dfrac{q_{n\ell} r_{\alpha}^3}{k + q_{n\ell}} j_{\ell-1}^2(q_{n\ell} r_{\alpha}), & k = q_{n\ell}. \quad (b) \end{cases} \tag{5.9}$$

Equation 5.9b is in fact a limiting case of (5.9a) which can therefore always be substituted for $\tilde{\chi}_{\alpha,n\ell m}(\mathbf{k})$ in an integral over reciprocal-space.

5.4 Overlap matrix elements

The overlap matrix for any two basis functions $\chi_{\alpha,n\ell m}$ and $\chi_{\beta,n'\ell' m'}$ centred at $\mathbf{R}_{\alpha}$ and $\mathbf{R}_{\beta}$ respectively is

$$\mathcal{S}_{\alpha,n\ell m;\beta,n'\ell' m'} = \int \mathrm{d}\mathbf{r}\ \chi_{\alpha,n\ell m}(\mathbf{r}) \chi_{\beta,n'\ell' m'}(\mathbf{r}). \tag{5.10}$$

Defining $\mathbf{R}_{\alpha\beta} = \mathbf{R}_{\beta} - \mathbf{R}_{\alpha}$, and using the result for the Fourier transform of the basis functions, the integral can be rewritten as

$$\mathcal{S}_{\alpha,n\ell m;\beta,n'\ell' m'} = \frac{1}{(2\pi)^3} \int \mathrm{d}\mathbf{k} \exp[-\mathrm{i}\mathbf{k}\cdot\mathbf{R}_{\alpha\beta}] \tilde{\chi}_{\alpha,n\ell m}(\mathbf{k}) \tilde{\chi}_{\beta,n'\ell' m'}(-\mathbf{k}). \tag{5.11}$$

Using equation 5.9a we obtain

$$\mathcal{S}_{\alpha,n\ell m;\beta,n'\ell' m'} = \left(q_{n\ell} r_{\alpha}^2\right) \left(q_{n'\ell'} r_{\beta}^2\right) j_{\ell-1}(q_{n\ell} r_{\alpha}) j_{\ell'-1}(q_{n'\ell'} r_{\beta})\ I_{\alpha,n\ell m;\beta,n'\ell' m'} \tag{5.12}$$

where $I_{\alpha,n\ell m;\beta,n'\ell' m'}$ is the integral

$$I_{\alpha,n\ell m;\beta,n'\ell' m'} = \frac{2}{\pi}\ \mathrm{i}^{(\ell-\ell')} \int \mathrm{d}\mathbf{k}\ \frac{\exp[-\mathrm{i}\mathbf{k}\cdot\mathbf{R}_{\alpha\beta}] j_{\ell}(kr_{\alpha})\ j_{\ell'}(kr_{\beta})}{(k^2 - q_{n\ell}^2)\,(k^2 - q_{n'\ell'}^2)} \bar{Y}_{\ell m}(\Omega_{\mathbf{k}}) \bar{Y}_{\ell' m'}(\Omega_{\mathbf{k}}). \tag{5.13}$$

Introducing differential operators $\hat{D}_{\ell m}$, obtained from $\bar{Y}_{\ell m}$ by making the replacement

$$\left\{\frac{x}{r}, \frac{y}{r}, \frac{z}{r}\right\} \longrightarrow \left\{\frac{\partial}{\partial x_{\alpha\beta}}, \frac{\partial}{\partial y_{\alpha\beta}}, \frac{\partial}{\partial z_{\alpha\beta}}\right\}$$

where $\mathbf{R}_{\alpha\beta} = (x_{\alpha\beta}, y_{\alpha\beta}, z_{\alpha\beta})$ in Cartesian coordinates, equation 5.13 becomes

$$I_{\alpha,n\ell m;\beta,n'\ell' m'} = 4(-1)^{\ell}\ \hat{D}_{\ell m} \hat{D}_{\ell' m'} \int_{-\infty}^{\infty} \mathrm{d}k\ \frac{j_{\ell}(kr_{\alpha})\ j_{\ell'}(kr_{\beta})\ j_0(kR_{\alpha\beta})}{k^{(\ell+\ell')}\,(k^2 - q_{n\ell}^2)\,(k^2 - q_{n'\ell'}^2)} \tag{5.14}$$

where we have used the fact that the integrand is an even function of k for all values of ℓ and ℓ' to change the limits of the integral. From equation 5.14 $I_{\alpha,n\ell m;\beta,n'\ell'm'}$ no longer appears manifestly symmetric with respect to swapping α and β (since there is no $(-1)^{\ell'}$ term). Nonetheless, it still is because under the swap $\{\alpha, n\ell m\} \leftrightarrow \{\beta, n'\ell'm'\}$, $\hat{D}_{\ell m} \rightarrow (-1)^{\ell'} \hat{D}_{\ell'm'}$ and $\hat{D}_{\ell'm'} \rightarrow (-1)^{\ell} \hat{D}_{\ell m}$.

The three spherical Bessel functions in equation 5.14 can all be expressed in terms of trigonometric functions and algebraic powers of the argument, using the recursion rules (A.1, A.2). The product of three trigonometric functions can always be expressed as a sum of four trigonometric functions with different arguments, using well-known identities. The result is to split the integrand up into terms of the following form:

$$\begin{aligned} &\frac{\sin k\,(r_\alpha \pm r_\beta \pm R_{\alpha\beta})}{k^p\,(k^2 - q_{n\ell}^2)\,(k^2 - q_{n'\ell'}^2)}, \qquad p \text{ always an odd integer,} \\ &\frac{\cos k\,(r_\alpha \pm r_\beta \pm R_{\alpha\beta})}{k^p\,(k^2 - q_{n\ell}^2)\,(k^2 - q_{n'\ell'}^2)}, \qquad p \text{ always an even integer.} \end{aligned} \tag{5.15}$$

These terms are individually singular and generally possess a pole of order p on the real axis at $k = 0$ and cannot be integrated. However, since we are integrating finite well-behaved functions over a finite volume of space, we know that the total integrand cannot contain any non-integrable singularities. Therefore we can add extra contributions to each term to cancel all the singularities except simple poles, in the knowledge that all these extra terms must cancel when the terms are added together to obtain the total integrand.

We shall evaluate the integrals using the calculus of residues so that the general integral to be performed is

$$I = \oint_C \mathrm{d}z\, \frac{\exp[\mathrm{i}Rz]}{z^p\,(z^2 - q_{n\ell}^2)\,(z^2 - q_{n'\ell'}^2)} \tag{5.16}$$

where $R = r_\alpha \pm r_\beta \pm R_{\alpha\beta}$ and the contour C runs along the real z-axis from $-\infty$ to $+\infty$, and is closed in either the upper or lower half z-plane, depending upon whether R is positive or negative respectively. Adding the extra terms to remove the non-integrable singularities we obtain the final form of the integral

$$I = \oint_C \mathrm{d}z\, \frac{\exp[\mathrm{i}Rz] - \sum_{m=0}^{p-2} \frac{(\mathrm{i}Rz)^m}{m!}}{z^p\,(z^2 - q_{n\ell}^2)\,(z^2 - q_{n'\ell'}^2)}. \tag{5.17}$$

This integrand has simple poles lying on the contour of integration at $z = 0, \pm q_{n\ell}, \pm q_{n'\ell'}$.

The residues of these poles are

$$\begin{aligned} &\frac{(\mathrm{i}R)^{p-1}}{(p-1)!\; q_{n\ell}^2\; q_{n'\ell'}^2}, && z=0, \\ &\frac{\exp[\pm\mathrm{i}q_{n\ell}R] - \sum_{m=0}^{p-2}\frac{(\pm\mathrm{i}q_{n\ell}R)^m}{m!}}{2\left(q_{n\ell}^2 - q_{n'\ell'}^2\right)\left(\pm q_{n\ell}\right)^{p+1}}, && z=\pm q_{n\ell} \quad \text{(similarly for } z=\pm q_{n'\ell'}\text{)}. \end{aligned} \tag{5.18}$$

Summing the residues to perform the Cauchy principal value integrals, and taking real or imaginary parts as appropriate, we obtain the following results:

$$\begin{aligned} &\int_{-\infty}^{\infty}\mathrm{d}k\;\frac{\sin kR + \text{(cancelling terms)}}{k^p\left(k^2-q_{n\ell}^2\right)\left(k^2-q_{n'\ell'}^2\right)} = \\ &\quad \frac{\pi\;\mathrm{sgn}R}{q_{n\ell}^2 - q_{n'\ell'}^2}\left[-\frac{(-1)^{\frac{p-1}{2}}\;R^{p-1}}{(p-1)!\;q_{n\ell}^2} + \frac{(-1)^{\frac{p-1}{2}}\;R^{p-1}}{(p-1)!\;q_{n'\ell'}^2} + \frac{\cos q_{n\ell}R}{q_{n\ell}^{p+1}}\right. \\ &\quad \left. -\frac{\cos q_{n'\ell'}R}{q_{n'\ell'}^{p+1}} - \sum_{m=0,\text{ even}}^{p-3}\left\{\frac{(-1)^{\frac{m}{2}}R^m}{m!\;q_{n\ell}^{p-m+1}} - \frac{(-1)^{\frac{m}{2}}R^m}{m!\;q_{n'\ell'}^{p-m+1}}\right\}\right], \end{aligned} \tag{5.19}$$

$$\begin{aligned} &\int_{-\infty}^{\infty}\mathrm{d}k\;\frac{\cos kR + \text{(cancelling terms)}}{k^p\left(k^2-q_{n\ell}^2\right)\left(k^2-q_{n'\ell'}^2\right)} = \\ &\quad \frac{\pi\;\mathrm{sgn}R}{q_{n\ell}^2 - q_{n'\ell'}^2}\left[-\frac{(-1)^{\frac{p}{2}}\;R^{p-1}}{(p-1)!\;q_{n\ell}^2} + \frac{(-1)^{\frac{p}{2}}\;R^{p-1}}{(p-1)!\;q_{n'\ell'}^2} - \frac{\sin q_{n\ell}R}{q_{n\ell}^{p+1}}\right. \\ &\quad \left. +\frac{\sin q_{n'\ell'}R}{q_{n'\ell'}^{p+1}} + \sum_{m=1,\text{ odd}}^{p-3}\left\{\frac{(-1)^{\frac{m-1}{2}}R^m}{m!\;q_{n\ell}^{p-m+1}} - \frac{(-1)^{\frac{m-1}{2}}R^m}{m!\;q_{n'\ell'}^{p-m+1}}\right\}\right] \end{aligned} \tag{5.20}$$

where

$$\mathrm{sgn}R = \begin{cases} -1, & R<0, \\ +1, & R\geq 0. \end{cases} \tag{5.21}$$

For the case when $q_{n\ell} = q_{n'\ell'}$, we note that since the integrand in equation 5.17 must still only have a simple pole at $z = \pm q_{n\ell}$ we obtain a simplified form in this special case by taking the limit $q_{n'\ell'} \to q_{n\ell}$ of equations 5.19 and 5.20.

$$\begin{aligned} &\int_{-\infty}^{\infty}\mathrm{d}k\;\frac{\sin kR + \text{(cancelling terms)}}{k^p\left(k^2-q_{n\ell}^2\right)^2} = \\ &\quad \pi\;\mathrm{sgn}R\;\frac{(-1)^{\frac{p-1}{2}}R^{p-1}}{(p-1)!\;q_{n\ell}^4} - \frac{(p+1)\cos q_{n\ell}R}{2q_{n\ell}^{p+3}} - \frac{R\sin q_{n\ell}R}{2q_{n\ell}^{p+2}} \\ &\quad + \sum_{m=0,\text{ even}}^{p-3}\frac{(-1)^{\frac{m}{2}}(p-m+1)R^m}{2(m!)q_{n\ell}^{p-m+3}}, \end{aligned} \tag{5.22}$$

$$\begin{aligned}
\int_{-\infty}^{\infty} \mathrm{d}k\ \frac{\cos kR + (\text{cancelling terms})}{k^p\left(k^2 - q_{n\ell}^2\right)^2} = \\
\pi\ \mathrm{sgn}R\ \frac{(-1)^{\frac{p}{2}} R^{p-1}}{(p-1)!\ q_{n\ell}^4} - \frac{(p+1)\sin q_{n\ell}R}{2q_{n\ell}^{p+3}} - \frac{R\cos q_{n\ell}R}{2q_{n\ell}^{p+2}} \\
+ \sum_{m=1,\ \text{odd}}^{p-3} \frac{(-1)^{\frac{m-1}{2}}(p-m+1)R^m}{2(m!)q_{n\ell}^{p-m+3}}.
\end{aligned} \tag{5.23}$$

The result for $\mathcal{S}_{\alpha,n\ell m;\beta,n'\ell'm'}$ is obtained by summing the results in equations 5.19, 5.20, 5.22 and 5.23 for all the terms in the expansion of the integrand (5.14) and then operating with the differential operators $\hat{D}_{\ell m}$.

A second special case occurs when $\mathbf{R}_{\alpha\beta} = 0$, and in this case it is simplest to perform the integral (5.10) in real-space using the generalised orthogonality relation for spherical Bessel functions (A.4) when $q_{n\ell} \neq q_{n'\ell'}$.

$$\mathcal{S}_{\alpha,n\ell m;\beta,n'\ell'm'} = \frac{1}{q_{n\ell}^2 - q_{n'\ell'}^2}\delta_{\ell\ell'}\delta_{mm'} \begin{cases} -q_{n\ell}r_\alpha^2 j_\ell(q_{n'\ell'}r_\alpha)j_{\ell-1}(q_{n\ell}r_\alpha), & r_\alpha < r_\beta, \\ q_{n'\ell'}r_\beta^2 j_\ell(q_{n\ell}r_\beta)j_{\ell-1}(q_{n'\ell'}r_\beta), & r_\alpha \geq r_\beta. \end{cases} \tag{5.24}$$

There is also the case when $\mathbf{R}_{\alpha\beta} = 0$ and $q_{n\ell} = q_{n'\ell'}$ which is calculated using equation A.5.

$$\mathcal{S}_{\alpha,n\ell m;\beta,n'\ell'm'} = \tfrac{1}{2}\delta_{\ell\ell'}\delta_{mm'} \begin{cases} r_\alpha^3 j_{\ell-1}^2(q_{n\ell}r_\alpha), & r_\alpha < r_\beta, \\ r_\beta^3 j_{\ell-1}^2(q_{n\ell}r_\beta), & r_\alpha \geq r_\beta. \end{cases} \tag{5.25}$$

Finally, it is obvious that the overlap matrix element must vanish when the separation of the the sphere centres exceeds the sum of their radii (i.e. $R_{\alpha\beta} > r_\alpha + r_\beta$) because then there is no region of space where both basis functions are non-zero. However, this is not obvious from the results presented above, but arises because of the change of sign of the residue sums in equations 5.19, 5.20, 5.22 and 5.23 (denoted by $\mathrm{sgn}R$) which occurs when $R_{\alpha\beta} = r_\alpha + r_\beta$ and results in the exact cancellation of all terms.

5.5 Kinetic energy matrix elements

The kinetic energy matrix elements for any two basis functions $\chi_{\alpha,n\ell m}$ and $\chi_{\beta,n'\ell'm'}$ centred at $\mathbf{R}_\alpha$ and $\mathbf{R}_\beta$ respectively are defined by

$$\begin{aligned}
\mathcal{T}_{\alpha,n\ell m;\beta,n'\ell'm'} &= -\tfrac{1}{2}\int \mathrm{d}\mathbf{r}\ \chi_{\alpha,n\ell m}(\mathbf{r})\nabla^2\chi_{\beta,n'\ell'm'}(\mathbf{r}) \\
&= \frac{1}{2(2\pi)^3}\int \mathrm{d}\mathbf{k}\ k^2 \exp[-\mathrm{i}\mathbf{k}\cdot\mathbf{R}_{\alpha\beta}]\tilde{\chi}_{\alpha,n\ell m}(\mathbf{k})\tilde{\chi}_{\beta,n'\ell'm'}(-\mathbf{k}).
\end{aligned} \tag{5.26}$$

Because of the discontinuity in the first derivatives of the basis functions at the sphere boundaries, a delta-function arises when the Laplacian operates on a basis function. This is integrated out when the matrix element is calculated and this contribution is included when transforming the real-space integral to reciprocal-space in equation 5.26.

The second line of equation 5.26 is identical to equation 5.11 apart from a factor of $\frac{1}{2}k^2$. The same separation into individually regular terms can be applied here, and the result is that we need to calculate the contour integral (5.17) as before, except that the integer p must be replaced by $(p-2)$ and a numerical factor of $\frac{1}{2}$ is introduced. The calculation of the residues is identical to that presented in the previous section, except that the integrand no longer *always* has a pole at $z=0$ in every term.

The results for $\mathcal{T}_{\alpha,n\ell m;\beta,n'\ell'm'}$ when $\mathbf{R}_{\alpha\beta}=0$ are

$$\begin{aligned}
&\frac{\frac{1}{2}\delta_{\ell\ell'}\delta_{mm'}}{q_{n\ell}^2-q_{n'\ell'}^2}\left\{\begin{array}{ll} -q_{n\ell}^3 r_\alpha^2 j_\ell(q_{n'\ell'}r_\alpha) j_{\ell-1}(q_{n\ell}r_\alpha), & r_\alpha < r_\beta \\ q_{n'\ell'}^3 r_\beta^2 j_\ell(q_{n\ell}r_\beta) j_{\ell-1}(q_{n'\ell'}r_\beta), & r_\alpha \geq r_\beta \end{array}\right\} q_{n\ell}\neq q_{n'\ell'}, \\
&\frac{1}{4}\delta_{\ell\ell'}\delta_{mm'}q_{n\ell}^2\left\{\begin{array}{ll} r_\alpha^3 j_{\ell-1}^2(q_{n\ell}r_\alpha), & r_\alpha < r_\beta \\ r_\beta^3 j_{\ell-1}^2(q_{n\ell}r_\beta), & r_\alpha \geq r_\beta \end{array}\right\} q_{n\ell}=q_{n'\ell'}.
\end{aligned} \tag{5.27}$$

The calculation of the kinetic energy has been checked by projecting a set of wave-functions expanded in the spherical-wave basis onto the plane-wave basis using equation 5.9a. As the kinetic energy cut-off for the plane-wave basis is increased, so the description of the wave-functions becomes more accurate. The kinetic energy calculated using the results above can then be compared against the kinetic energy calculated by the plane-wave $\mathcal{O}(N^3)$ CASTEP code [82].

From the asymptotic behaviour of the spherical Bessel functions, the Fourier transform (5.9a) for large k is

$$\tilde{\chi}_{\alpha,n\ell m}(\mathbf{k}) \propto \frac{\sin(kr_\alpha - \frac{\ell\pi}{2})}{k^3}\,\bar{Y}_{\ell m}(\Omega_{\mathbf{k}}) \tag{5.28}$$

and so the error in the kinetic energy due to truncating the plane-wave basis with cut-off $E_{\mathrm{cut}}=\frac{1}{2}k_{\mathrm{cut}}^2$ is

$$\Delta T \propto \int_{k_{\mathrm{cut}}}^{\infty} \mathrm{d}k\; k^2\left(\frac{1}{k^3}\right)k^2\left(\frac{1}{k^3}\right) = \frac{1}{k_{\mathrm{cut}}} \propto \frac{1}{\sqrt{E_{\mathrm{cut}}}}. \tag{5.29}$$

In figure 5.1 the kinetic energy as calculated by the plane-wave code has been plotted against $1/\sqrt{E_{\mathrm{cut}}}$ and yields a straight line as expected, which can then be extrapolated to obtain an estimate of the kinetic energy calculated for infinite cut-off: 60.66 ± 0.01 eV. This is in agreement with the value calculated analytically of 60.65 eV.

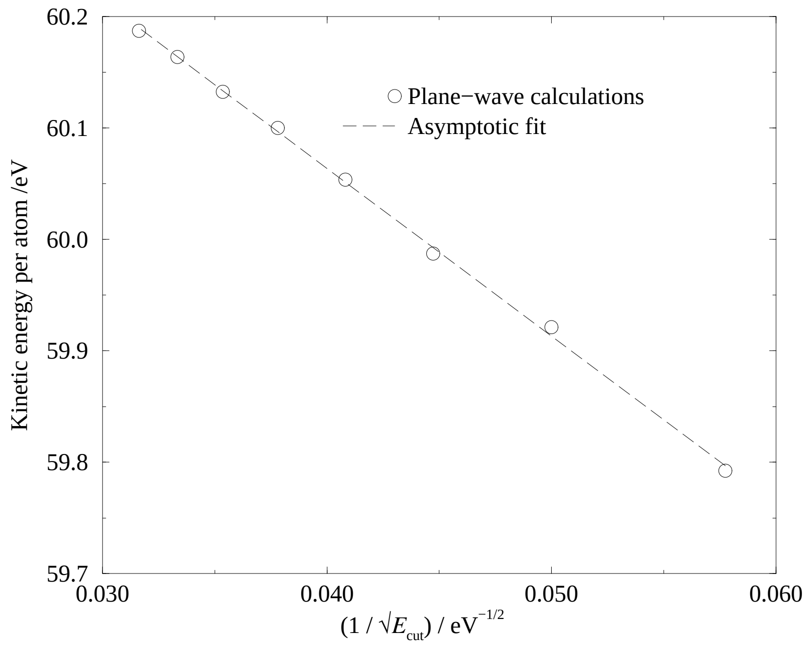

Figure 5.1: Plot of asymptotic fit to kinetic energy data.

5.6 Non-local pseudopotential

In this section we present two methods for obtaining the non-local pseudopotential matrix elements. The first constructs a Green's function in order to expand the basis functions on one site in terms of the same functions centred elsewhere. This method is particularly efficient, although it requires some restrictions to be made in the radial part of the support functions to give a variational method. The second method adopts the Kleinman-Bylander form and uses the results for the overlap matrix elements. This method is slower, but more robust numerically and allows direct comparison with existing pseudopotential codes.

5.6.1 Green's function method

The general form for a semi-local pseudopotential operator (i.e. one which is non-local in the angular but not radial coordinates) for an ion is

$$\hat{V}_{\mathrm{NL}} = \sum_{\ell m} |\ell m\rangle \delta \hat{V}_\ell \langle \ell m| \tag{5.30}$$

where $\langle \mathbf{r}|\ell m\rangle = \bar{Y}_{\ell m}(\Omega)$ and $\bar{Y}_{\ell m}$ is centred on the ion.

The pseudopotential components δV_ℓ are themselves short-ranged in real-space, and vanish beyond the core radius r_c. Therefore the action of the non-local pseudopotential depends only upon the form of the wave-functions within this core region. We require the matrix elements of the non-local pseudopotential between localised basis functions which are not necessarily centred on the ion.

We therefore need to find an expansion of the basis functions in terms of functions localised within the pseudopotential core. Since the basis functions are all solutions of the Helmholtz equation, we invoke the uniqueness theorem which states that the expansion we seek is uniquely determined by the boundary conditions on the surface of the core region and solve the Helmholtz equation subject to these inhomogeneous boundary conditions by the standard method using the formal expansion of the Green's function. We can write the basis function over all space using the Heaviside step function $H(x)$

$$H(x) = \begin{cases} 0, & x < 0, \\ 1, & x \geq 0, \end{cases} \tag{5.31}$$

so that a basis function centred in a sphere of radius r_α at the origin (i.e. for $\mathbf{R}_\alpha = 0$) is

$$\chi_{\alpha,n\ell m}(\mathbf{r}) = j_\ell(q_{n\ell} r)\bar{Y}_{\ell m}(\Omega_{\mathbf{r}})H(r_\alpha - r) \tag{5.32}$$

and therefore

$$(\nabla^2 + q_{n\ell}^2)\chi_{\alpha,n\ell m}(\mathbf{r}) = \left[j_\ell(q_{n\ell} r)\delta'(r_\alpha - r) - 2\left\{q_{n\ell} j'_\ell(q_{n\ell} r) + r^{-1} j_\ell(q_{n\ell} r)\right\}\delta(r_\alpha - r)\right]\bar{Y}_{\ell m}(\Omega_{\mathbf{r}}). \tag{5.33}$$

The terms on the right-hand side only contribute on the sphere boundary $r = r_\alpha$; everywhere else in space the basis function obeys the homogeneous Helmholtz equation (5.1). These terms will give rise to an extra term in the Green's function solution due to the discontinuity of the first radial derivative of the basis function at the sphere boundary. However, if the radial function for each angular momentum component has a continuous first derivative, then these contributions will cancel. In this case, we can proceed assuming that the basis function obeys the homogeneous equation everywhere. This condition is naturally obeyed by the support functions when the support regions are large enough, since there is a kinetic energy penalty associated with the same discontinuity in the radial wave-function, but in this case we would lose any variational principle if there was a discontinuity at any stage during the minimisation. A better solution is to impose a sum rule on the expansion coefficients in equation 5.3 to maintain a continuous radial derivative i.e.

$$\sum_n c_{(\alpha)}^{n\ell m} q_{n\ell} j'_\ell(q_{n\ell} r_\alpha) = 0 \tag{5.34}$$

which can be used to fix one coefficient in terms of the rest for each angular momentum component. This is the restriction mentioned above which must be imposed if the Green's function method is to be used. The basis function is assumed to obey the homogeneous Helmholtz equation throughout all space. In the original support region, homogeneous boundary conditions were applied. Now, in an overlapping region of radius r_c (the core region for the non-local pseudopotential), the basis function must still obey the same homogeneous Helmholtz equation, but it is now subject to *inhomogeneous* boundary conditions. Standard methods can be used to transform this problem into the solution of an inhomogeneous Helmholtz equation subject to homogeneous boundary conditions, and this new problem has a standard solution in terms of the Green's function, which can be formally expanded in terms of the eigenfunctions of an appropriate self-adjoint operator (here the operator on the left of the Helmholtz equation). The result is

$$\chi_{\alpha,n\ell m}(\mathbf{r}) = \sum_{\ell' m'} f_{\ell' m'}^{n\ell m} \left[1 + \sum_{n'} a_{n'\ell'}^{n\ell m} j_{\ell'}(q_{n'\ell'} r')\right] \bar{Y}_{\ell' m'}(\Omega_{\mathbf{r}'}) \tag{5.35}$$

and is valid for points $\mathbf{r}' = \mathbf{r} - \mathbf{R}_\mathrm{ion} + \mathbf{R}_\alpha$ within the core region (i.e. for $r' \leq r_\mathrm{c}$).

The coefficients $f_{\ell' m'}^{n\ell m}$ and $a_{n'\ell'}^{n\ell m}$ are defined by:

$$f_{\ell' m'}^{n\ell m} = \int_{r'=r_\mathrm{c}} \mathrm{d}\Omega_{\mathbf{r}'} \bar{Y}_{\ell' m'}(\Omega_{\mathbf{r}'})\ \chi_{\alpha,n\ell m}(\mathbf{r}' + \mathbf{R}_\mathrm{ion} - \mathbf{R}_\alpha), \tag{5.36}$$

$$a_{n'\ell'}^{n\ell m} = \frac{2}{r_\mathrm{c}^3\ j_{\ell'-1}^2(\lambda_{n'\ell'} r_\mathrm{c})} \left[\frac{\lambda_{n'\ell'}\ r_\mathrm{c}^2\ j_{\ell'-1}(\lambda_{n'\ell'} r_\mathrm{c})}{q_{n\ell}^2 - \lambda_{n'\ell'}^2} - \int_0^{r_\mathrm{c}} \mathrm{d}r\ r^2 j_{\ell'}(\lambda_{n'\ell'} r)\right]. \tag{5.37}$$

The $\{\lambda_{n\ell}\}$ are chosen by $j_\ell(\lambda_{n\ell} r_\mathrm{c}) = 0$ and play the same rôle as the $\{q_{n\ell}\}$ in the expansion of the wave-functions. The integral in equation 5.37 is straightforward to evaluate for given ℓ'.

The surface integral in equation 5.36 is evaluated by first rotating the coordinate system so that the new z-axis is parallel to $\mathbf{R}_\alpha - \mathbf{R}_\mathrm{ion}$, thus mixing the spherical harmonics [151]. The elements of the orthogonal spherical harmonic mixing matrices $C_{mm'}^{(\ell)}$ are defined by the elements of the rotation matrix for the coordinate system. In terms of the components (x, y, z) of the vector $\mathbf{R}_\alpha - \mathbf{R}_\mathrm{ion}$ of length $r = |\mathbf{R}_\alpha - \mathbf{R}_\mathrm{ion}|$, and $v^2 = r(z + r)$, the rotation matrix O is given by:

$$O = \frac{1}{v^2} \begin{pmatrix} v^2 - x^2 & -xy & -x(z+r) \\ -xy & v^2 - y^2 & -y(z+r) \\ x(z+r) & y(z+r) & z(z+r) \end{pmatrix} \tag{5.38}$$

The singularity which occurs when $z = -r$ i.e. when the ion is "vertically" above the support region, is avoided by inverting the calculation through the origin when $z < 0$. The spherical harmonic matrices $C^{(\ell)}_{mm'}$ can be written in terms of the elements of this matrix. Here we write them out explicitly for $\ell = 0, 1, 2$:

$$C^{(0)} = 1 \tag{5.39}$$

$$C^{(1)} = \begin{pmatrix} O_{22} & O_{32} & O_{12} \\ O_{23} & O_{33} & O_{13} \\ O_{21} & O_{31} & O_{11} \end{pmatrix} \tag{5.40}$$

$$C^{(2)} = \begin{pmatrix} O_{12}O_{21} + O_{11}O_{22} & O_{22}O_{31} + O_{21}O_{32} & \sqrt{3}O_{31}O_{32} & \dots \\ O_{13}O_{22} + O_{12}O_{23} & O_{23}O_{32} + O_{22}O_{33} & \sqrt{3}O_{32}O_{33} & \dots \\ \sqrt{3}O_{13}O_{23} & \sqrt{3}O_{23}O_{33} & \frac{1}{2}(3O_{33}^2 - 1) & \dots \\ O_{13}O_{21} + O_{11}O_{23} & O_{23}O_{31} + O_{21}O_{33} & \sqrt{3}O_{31}O_{33} & \dots \\ O_{11}O_{21} - O_{12}O_{22} & O_{21}O_{31} - O_{22}O_{32} & \frac{\sqrt{3}}{2}(O_{31}^2 - O_{32}^2) & \dots \end{pmatrix}$$
$$\begin{pmatrix} \dots & O_{12}O_{31} + O_{11}O_{32} & O_{11}O_{12} - O_{21}O_{22} \\ \dots & O_{13}O_{32} + O_{12}O_{33} & O_{12}O_{13} - O_{22}O_{23} \\ \dots & \sqrt{3}O_{33}O_{13} & \frac{\sqrt{3}}{2}(O_{13}^2 - O_{23}^2) \\ \dots & O_{13}O_{31} + O_{11}O_{33} & O_{11}O_{13} - O_{21}O_{23} \\ \dots & O_{11}O_{31} - O_{12}O_{32} & \frac{1}{2}(O_{11}^2 + O_{22}^2 - O_{12}^2 - O_{21}^2) \end{pmatrix} \tag{5.41}$$

In the new coordinate system, the surface integral is written in terms of a one-dimensional integral

$$K_{\ell' n\ell m}(u, q_{n\ell}) = \frac{1}{2u}\left[(2\ell'+1)(2\ell+1)\frac{(\ell'-|m|)!(\ell-|m|)!}{(\ell'+|m|)!(\ell+|m|)!}\right]^{\frac{1}{2}} \times$$
$$\int_{|u-1|}^{\min(u+1, r_\alpha/r_c)} \mathrm{d}z\ z P_{\ell'}^{|m|}\left(\frac{1+u^2-z^2}{2u}\right) j_\ell(q_{n\ell} r_c z) P_\ell^{|m|}\left(\frac{1-u^2-z^2}{2uz}\right) \tag{5.42}$$

in which the dimensionless variable $u = \frac{|\mathbf{R}_\alpha - \mathbf{R}_{\text{ion}}|}{r_c}$ is introduced. $P_\ell^{|m|}(x)$ denotes an associated Legendre polynomial, and these integrals can all be calculated indefinitely using elementary methods once the integrand is expanded into trigonometric functions.

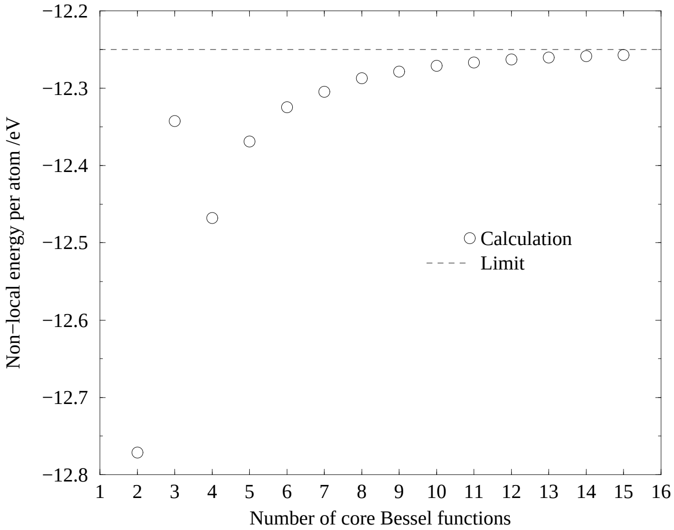

Figure 5.2: Non-local pseudopotential energy against number of Bessel functions used in Green's function expansion

The numerical evaluation of the analytic results for $K_{\ell' n\ell m}(u, q_{n\ell})$ is inaccurate when $u \ll 1$ and in this case it is necessary to employ Taylor expansions of the results. The two different cases for the upper limit of the integral also need to be treated separately, and this is one reason why the Kleinman-Bylander method described next is preferred.

The final result for $f^{n\ell m}_{\ell' m'}$ is then

$$f^{n\ell m}_{\ell' m'} = \sum_{M=-\min(\ell,\ell')}^{\min(\ell,\ell')} C^{(\ell')}_{Mm'} K_{\ell' n\ell m} C^{(\ell)}_{Mm}. \tag{5.43}$$

Defining the core matrix elements

$$\delta V^{\ell}_{nn'} = \begin{cases} \displaystyle\int_0^{r_c} \mathrm{d}r\ r^2\ j_\ell(\lambda_{n\ell} r)\delta V_\ell(r) j_\ell(\lambda_{n'\ell}) & n, n' \neq 0 \\ \displaystyle\int_0^{r_c} \mathrm{d}r\ r^2\ j_\ell(\lambda_{n\ell} r)\delta V_\ell(r) & n \neq 0, n' = 0 \\ \displaystyle\int_0^{r_c} \mathrm{d}r\ r^2\ \delta V_\ell(r) & n = n' = 0 \end{cases} \tag{5.44}$$

the matrix element of the non-local pseudopotential operator between any two basis functions overlapping the core ($\chi_{\alpha,n\ell m}$ and $\chi_{\beta,n'\ell' m'}$) can be written (defining $a^{n\ell m}_{0L} = 1$) as the sum:

$$\mathcal{V}_{\alpha,n\ell m;\beta,n'\ell'm'} = \sum_{LM} f_{LM}^{n\ell m} f_{LM}^{n'\ell'm'} \left[\sum_{i,j=0} a_{iL}^{n\ell m} \delta V_{ij}^{L} a_{jL}^{n'\ell'm'} \right]. \tag{5.45}$$

The non-local pseudopotential data is therefore stored in terms of the core matrix elements defined in equation 5.45. In figure 5.2 we plot the non-local pseudopotential energy against the number of core Bessel functions for an s-local silicon pseudopotential generated according to the scheme of Troullier and Martins [74]. We see that the energy converges rapidly with the number of core Bessel functions used (the dashed line is the energy calculated with fifty core functions.) Increasing the number of core functions only increases the number of $a_{n'\ell'}^{n\ell m}$ coefficients required, and the separable nature of the calculation means that even using fifty core functions requires very little computational effort.

5.6.2 Kleinman-Bylander form

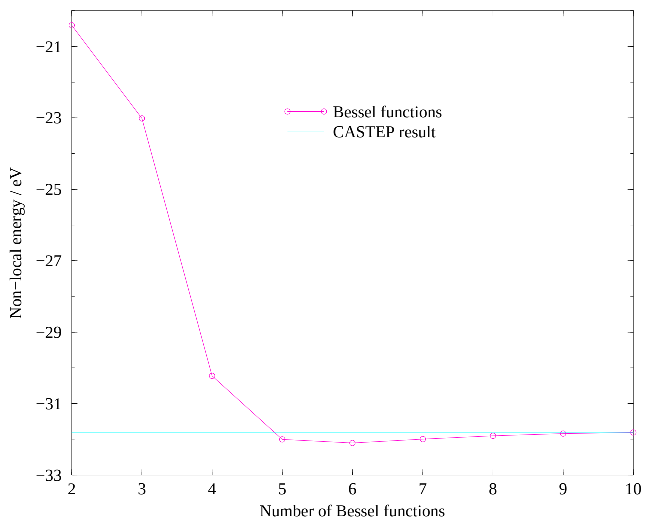

Figure 5.3: Non-local pseudopotential energy against number of Bessel functions used to describe Kleinman-Bylander projectors.

We reproduce equation 3.76 which demonstrates the Kleinman-Bylander form of the pseudopotential in terms of pseudo-atomic eigenstates $\{|\phi_{\ell m}\rangle\}$.

$$\hat{V}_{\mathrm{KB}} = \hat{V}_{\mathrm{loc}} + \sum_{\ell m} \frac{|\delta \hat{V}_\ell \phi_{\ell m}\rangle \langle \phi_{\ell m} \delta \hat{V}_\ell|}{\langle \phi_{\ell m} | \delta \hat{V}_\ell | \phi_{\ell m}\rangle} \tag{5.46}$$

For pseudopotentials whose non-local components $\{\delta V_\ell\}$ vanish at the core radius r_c, the projector states $\{|\delta\hat{V}_\ell\phi_{\ell m}\rangle\}$ can be expanded in the basis-states $\{|\chi_{n\ell m}\rangle\}$, and then the matrix-elements of the pseudopotential operator are straightforwardly obtained by applying the result for the overlap matrix elements, without resorting to the scheme by King-Smith *et al.* [152].

In figure 5.3 we show how the non-local pseudopotential energy rapidly converges as the number of Bessel functions used to expand the Kleinman-Bylander projectors is increased. This method is numerically more stable than the Green's function method, although slower, and has the added advantage that it allows a direct comparison to be made between the results calculated using this basis-set and traditional plane-wave codes. For these reasons the Kleinman-Bylander method has been used in computational implementations.

5.7 Computational implementation

The results in equations 5.19, 5.20, 5.22 and 5.23 have been written in a form which shows that in general each term can be represented by a real numerical prefactor, integers which are the powers of $\{R, q_{n\ell}, q_{n'\ell'}\}$ and one further integer to signify the presence of one of the terms $\{\sin q_{n\ell}R, \sin q_{n'\ell'}R, \cos q_{n\ell}R, \cos q_{n'\ell'}R\}$. When these terms are combined and differentiated by the $\hat{D}_{\ell m}$, the general term also needs integers to represent powers of $\{x_{\alpha\beta}, y_{\alpha\beta}, z_{\alpha\beta}, R_{\alpha\beta}, r_\alpha, r_\beta\}$. Therefore a general term in the expressions for $\mathcal{S}_{\alpha,n\ell m;\beta,n'\ell'm'}$ and $\mathcal{T}_{\alpha,n\ell m;\beta,n'\ell'm'}$ could be represented by a data structure consisting of one real variable g and ten integer variables I_{1-10} as follows:

$$g\frac{x_{\alpha\beta}^{I_1} y_{\alpha\beta}^{I_2} z_{\alpha\beta}^{I_3} R^{I_4} f(R)}{q_{n\ell}^{I_5} q_{n'\ell'}^{I_6} r_\alpha^{I_7} r_\beta^{I_8} R_{\alpha\beta}^{I_9}} \rightarrow \{g, I_1, I_2, I_3, I_4, I_5, I_6, I_7, I_8, I_9, I_{10}\} \tag{5.47}$$

with the following correspondence between $f(R)$ and I_{10}:

$$\begin{aligned} f(R) &= \{1, \sin q_{n\ell}R, \sin q_{n'\ell'}R, \cos q_{n\ell}R, \cos q_{n'\ell'}R\} \\ \rightarrow I_{10} &= \{0, 1, 2, 3, 4\}. \end{aligned} \tag{5.48}$$

A recursive function can be written to manipulate these encoded terms and perform the differentiation by the $\hat{D}_{\ell m}$, which can themselves be generated using the recursion rules for the associated Legendre polynomials. Thus it is straightforward to write a code which starts from equation 5.14 and generates the results up to arbitrary values of ℓ for $S_{\alpha\beta}$ and $T_{\alpha\beta}$ for the cases when $\mathbf{R}_{\alpha\beta} \neq 0$. The results for $\mathbf{R}_{\alpha\beta} = 0$ are simple enough to be coded within the program which uses this basis. For a given ionic configuration the matrix elements between the basis states can be calculated initially and stored on disk for use during the calculation.

The cost of calculating the analytic matrix elements increases dramatically as higher angular momentum components are included. In general, a much smaller value of ℓ_{max} is used than is "recommended" by the kinetic energy cut-off. However, these basis functions are being used to describe functions localised in *overlapping* regions, and in this instance, a degree of "under-completeness" is desirable. If the basis functions formed a complete set (up to a given kinetic energy cut-off) in each support region, then a variation which is confined to the overlapping region can be equally described by variations in either region. Symmetric and antisymmetric combinations of these variations can be formed, the antisymmetric variation vanishing and thus leaving the density-matrix invariant. Therefore this superposition results in directions in the parameter space with very small curvature which degrade the efficiency of minimisation algorithms (see section 6.2.3). When working with overlapping support functions, it is therefore better to treat ℓ_{max} as a convergence parameter along with, rather than derived from, E_{cut}.

Chapter 6

Penalty Functionals

In this chapter we first outline Kohn's derivation of a variational principle for a generalised energy functional which includes a penalty functional to impose the idempotency constraint. We show that this functional is non-analytic at its minimum and therefore incompatible with efficient minimisation algorithms, using conjugate gradients as an example.

We then outline an original scheme to use well-behaved penalty functionals to approximately impose the idempotency constraint. The density-matrix which minimises these generalised energy functionals is therefore only an approximation to the true ground-state density-matrix, but the resulting error in the total energy can be corrected to obtain accurate estimates of the true ground-state energy.

6.1 Kohn's method

6.1.1 Variational principle

As mentioned in section 4.4.3, Kohn [135] has suggested the use of a penalty functional to impose the idempotency condition, and has proved a variational principle based upon it. We consider trial density-matrices $\rho(\mathbf{r}, \mathbf{r}')$ expressed in diagonal form with real orthonormal extended orbitals $\{\varphi_i(\mathbf{r})\}$ and occupation numbers $\{f_i\}$:

$$\rho(\mathbf{r}, \mathbf{r}') = \sum_i f_i \; \varphi_i(\mathbf{r}) \varphi_i(\mathbf{r}'). \tag{6.1}$$

The functional $\mathcal{Q}[\rho; \mu, \alpha]$ is then formed:

$$\mathcal{Q}[\rho; \mu, \alpha] \equiv E_{\mathrm{NI}}[\rho^2] - \mu N[\rho^2] + \alpha \mathcal{P}[\rho] \tag{6.2}$$

in which

$$E_{\rm NI}[\rho^2] \;\equiv\; 2\int {\rm d}\mathbf{r}' \left\{ \left[-\tfrac{1}{2}\nabla_{\mathbf{r}}^2 \rho^2(\mathbf{r},\mathbf{r}') \right]_{\mathbf{r}=\mathbf{r}'} + \rho^2(\mathbf{r}',\mathbf{r}')V_{\rm KS}(\mathbf{r}') \right\} = 2\sum_i f_i^2\,\varepsilon_i, \tag{6.3}$$

$$N[\rho^2] \;\equiv\; 2\int {\rm d}\mathbf{r}\;\rho^2(\mathbf{r},\mathbf{r}) = 2\sum_i f_i^2, \tag{6.4}$$

$$\mathcal{P}[\rho] \;\equiv\; \left[\int {\rm d}\mathbf{r}\;\left(\rho^2(1-\rho)^2\right)(\mathbf{r},\mathbf{r}) \right]^{\frac{1}{2}} = \left[\sum_i f_i^2(1-f_i)^2 \right]^{\frac{1}{2}}, \tag{6.5}$$

and where μ is the chemical potential and α is a positive real parameter.

Kohn proves the following variational principle: that for some $\alpha > \alpha_{\rm c}$, the minimum value of $\mathcal{Q}[\rho;\mu,\alpha]$ is obtained for the idempotent ground-state density-matrix ρ_0 and that the minimum value is the ground-state grand potential i.e.

$$\min_\rho \mathcal{Q}[\rho;\mu,\alpha] = E_{\rm NI}[\rho_0^2] - \mu N[\rho_0^2] = \sum_{i,\varepsilon_i^{(0)}\le\mu} (\varepsilon_i^{(0)} - \mu) \tag{6.6}$$

in which the $\{\varepsilon_i^{(0)}\}$ are the exact eigenvalues of the self-consistent Hamiltonian, generated by the ground-state density-matrix ρ_0.

The critical value of α, denoted $\alpha_{\rm c}$, is given by

$$\alpha_{\rm c} = \max_{\mathcal{P}'} \left| \frac{{\rm d}\Omega(\mathcal{P}')}{{\rm d}\mathcal{P}'} \right| \tag{6.7}$$

in which $\Omega(\mathcal{P}')$ is the conditional minimum defined by

$$\Omega(\mathcal{P}') = \min_{\mathcal{P}[\rho]=\mathcal{P}'} \left(E_{\rm NI}[\rho^2] - \mu N[\rho^2] \right) \tag{6.8}$$

i.e. the minimum grand potential for all trial density-matrices which give a penalty functional value of $\mathcal{P}'$. Clearly

$$\alpha_{\rm c} \ge \left| \frac{{\rm d}\Omega(\mathcal{P}')}{{\rm d}\mathcal{P}'} \right|_{\mathcal{P}'=0} = 2\left[\sum_{i,\varepsilon_i^{(0)}\le\mu} (\varepsilon_i^{(0)} - \mu)^2 \right]^{\frac{1}{2}} \tag{6.9}$$

although this is only a lower bound on $\alpha_{\rm c}$.

Kohn's variational principle is based on the non-interacting energy $E_{\rm NI}[\rho^2]$. We now present a simple modification of this functional based upon self-consistent variation of the interacting energy. Consider the functional

$$\tilde{\mathcal{Q}}[\rho;\mu,\alpha] = E[\rho] - \mu N[\rho] + \alpha\mathcal{P}[\rho] \tag{6.10}$$

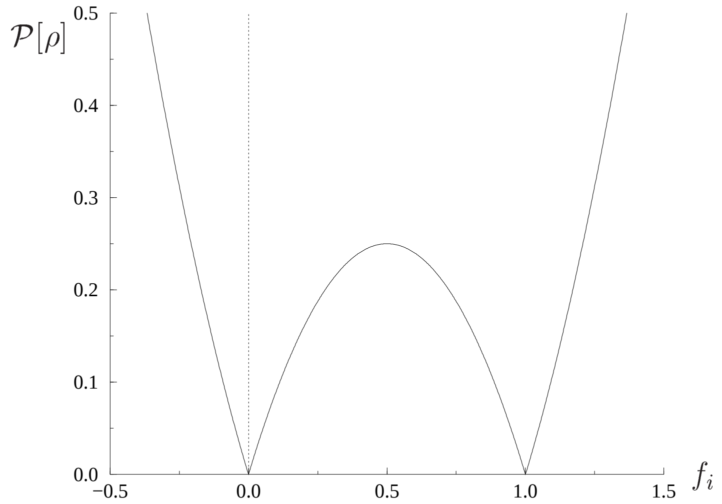

Figure 6.1: Behaviour of Kohn's penalty functional $\mathcal{P}[\rho]$ when a single occupation number f_i is varied and all others are zero or unity.

in which $E[\rho]$ is the interacting energy, and ρ is a positive semi-definite trial density-matrix. A given set of occupation numbers $\{f_i\}$ fixes the value of the penalty functional $\mathcal{P}[\rho]$ and variation of $\tilde{\mathcal{Q}}[\rho;\mu,\alpha]$ with respect to the orbitals $\{\varphi_i(\mathbf{r})\}$ at fixed occupation numbers and subject to the orthonormality constraint yields Kohn-Sham-like equations. Self-consistent variation of the occupation numbers $\{f_i\}$ (i.e. allowing the orbitals to relax, as in section 4.2) yields

$$\frac{\partial \tilde{\mathcal{Q}}[\rho;\mu,\alpha]}{\partial f_i} = 2(\varepsilon_i - \mu) + \frac{\alpha}{\mathcal{P}[\rho]} f_i(1-f_i)(1-2f_i). \tag{6.11}$$

In the case of idempotent density-matrices, for which $\mathcal{P}[\rho] = 0$, we obtain the special cases

$$\left.\frac{\partial \tilde{Q}[\rho;\mu,\alpha]}{\partial f_i}\right|_{f_i=(0^\pm,1^\pm)} = 2(\varepsilon_i - \mu) \pm \alpha. \tag{6.12}$$

For this functional the critical value of α, again denoted α_{c}, is given by

$$\alpha_{\mathrm{c}} = \max_{\rho} |2(\varepsilon_i - \mu)| \tag{6.13}$$

where the maximum is strictly over those density-matrices searched during the minimisation. For $\alpha > \alpha_{\mathrm{c}}$ the total functional $\tilde{\mathcal{Q}}[\rho;\mu,\alpha]$ takes its minimum value when $f_i = 0, 1$ for $\varepsilon_i > \mu$ and $\varepsilon_i < \mu$ respectively. In particular, for the ground-state density-matrix ρ_0, the functional is strictly increasing with respect to all variations in occupation numbers. The discontinuity in the occupation number derivative of the penalty functional at idempotency is required because of the non-variational behaviour of the total energy with respect to these variations (section 4.2). The behaviour of the penalty functional for unconstrained occupation number variation is plotted in figure 6.1, and in figure 6.2 the total functional is sketched schematically for several representative values of the parameter α. This demonstrates how the minimising density-matrix is idempotent only for $\alpha \geq \alpha_c$.

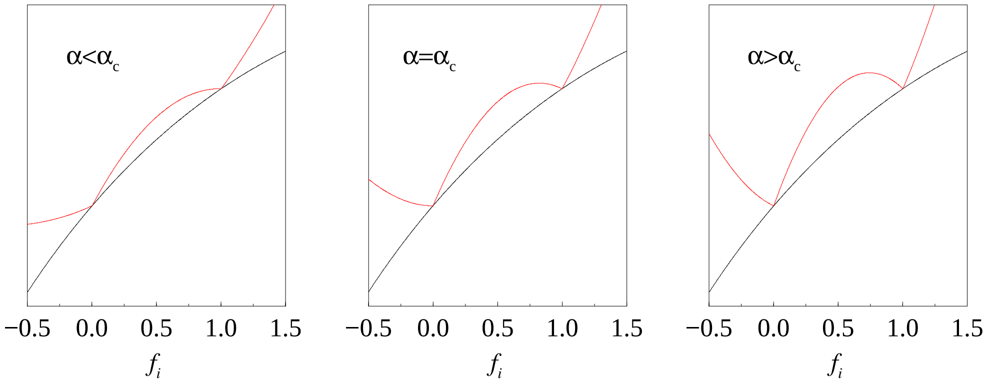

Figure 6.2: Schematic illustration of Kohn's variational principle: behaviour of the total energy (black) and total functional (red) for representative values of α.

6.1.2 Implementation problems

The conjugate gradients algorithm for minimising functions is described in appendix B. Throughout the lengthy derivation it is clear that the useful results obtained and the remarkably simple final result are due to the special properties of quadratic functions. Any function may be expanded in the form of a Taylor series about an analytic point, and around a minimum where the first order term from the gradient vanishes, a quadratic function is generally a good approximation. However, we note that the Kohn penalty functional has a branch point from the square-root function *exactly* at the ground-state minimum which we seek, and so the function cannot be Taylor-expanded there. Local information from the gradient cannot be used to infer the global shape of the function. This is illustrated in figure 6.3 for the case of a parabolic interpolation to find a line minimum based upon the gradient and a trial step, but the problem is even worse in the multi-dimensional space since the "conjugate" directions constructed from the gradients will not point in the direction of the ground-state minimum.

This problem is reflected in the very poor convergence when an attempt is made to minimise the functional using conjugate gradients: the steepest descents method actually

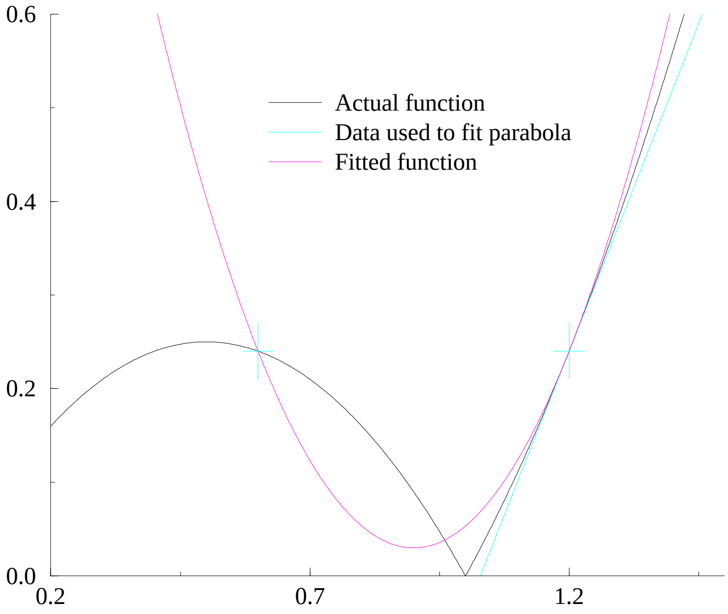

Figure 6.3: Failure of quadratic interpolation for Kohn's penalty functional.

performs better because it does not assume global quadratic behaviour. Also, the penalty functional does not vanish at the minimum sufficiently quickly as the parameter α is increased. However, the root-mean-square error in the occupation numbers $\overline{\delta f}$, given by

$$\overline{\delta f} = \frac{\mathcal{P}[\rho]}{\sqrt{N/2}} \tag{6.14}$$

in fact decays more rapidly, so that the total energy calculated at the minimum is quite accurate, although it is neither variational nor an upper bound. Also, although the total functional $\tilde{\mathcal{Q}}[\rho;\mu,\alpha]$ decreases monotonically, the total energy does not. Thus no advantage is gained by using the variational property, since it can only be applied to the total energy when $\mathcal{P}[\rho]=0$. The variational property of the total functional is that it is minimal at the ground-state, but this minimum is defined in terms of the functional taking its minimum value there, not in terms of a vanishing gradient (the gradient being undefined at the ground-state). Because of the non-variational behaviour of the total energy with respect to the occupation numbers at the ground-state, it is impossible to construct a penalty functional which has a continuous first derivative at the ground-state and also results in a variational principle for the total energy.

In figure 6.4 we present the results of tests on an 8-atom silicon cell to demonstrate

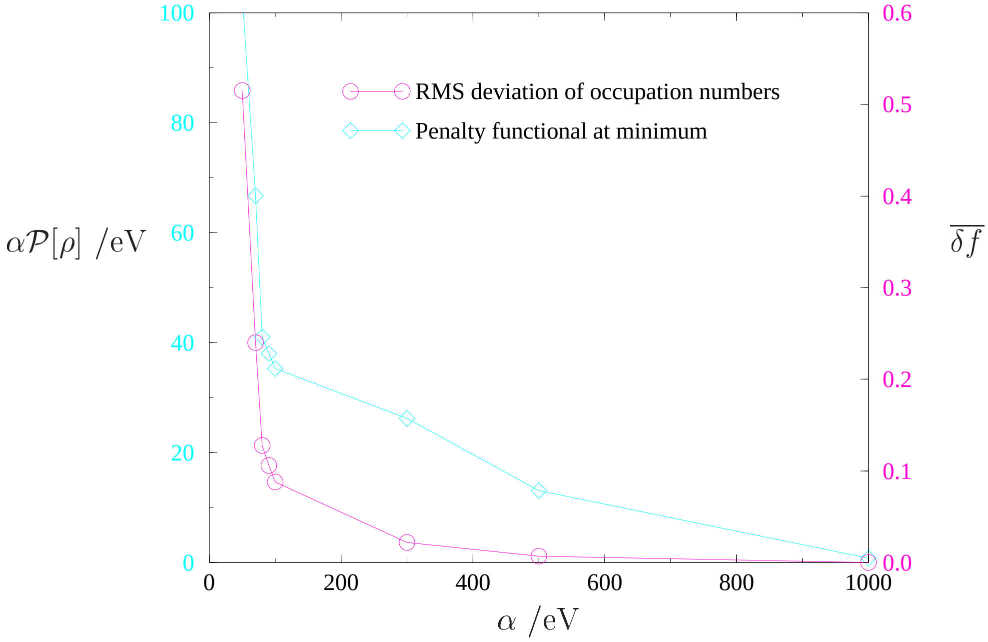

Figure 6.4: Convergence properties of Kohn's penalty functional: behaviour of penalty functional and occupation numbers with α.

the behaviour of the functional. As the penalty functional parameter α is increased, both the contribution of the penalty functional to the total functional $\alpha\mathcal{P}[\rho]$, and the root mean square error in the occupation numbers $\overline{\delta f}$ decrease, but not rapidly enough with α since the number of iterations required to reach convergence increases with α making the calculations too expensive for practical applications. For example, the number of iterations required to converge the total functional to 0.01 eV per atom increases by a factor of more than ten when α is increased from 100 eV to 1000 eV. Even with the smaller value for α, the rate of convergence is much slower than traditional methods, and this is due to the incompatibility of the functional with the conjugate gradients scheme.

6.2 Corrected penalty functional method

6.2.1 Derivation of the correction

In this section we present a new method to perform total energy calculations using a penalty functional to enforce idempotency approximately. We define a generalised energy functional $Q[\rho;\alpha]$ for trial density-matrices ρ by

$$Q[\rho;\alpha] = E[\rho] + \alpha P[\rho]. \tag{6.15}$$

$P[\rho]$ represents the penalty functional, which in this new method is required to be analytic at all points so that efficient minimisation schemes such as conjugate gradients may be applied. The simplest example is to take the square of Kohn's penalty functional i.e.

$$P[\rho] = \int \mathrm{d}\mathbf{r} \, \left[\rho^2 (1-\rho)^2\right](\mathbf{r},\mathbf{r}) = \sum_i f_i^2 (1-f_i)^2 , \tag{6.16}$$

but other choices are also possible (section 6.2.2). This penalty functional is sketched in figure 6.5. Since the penalty functional becomes large as the density-matrix becomes less

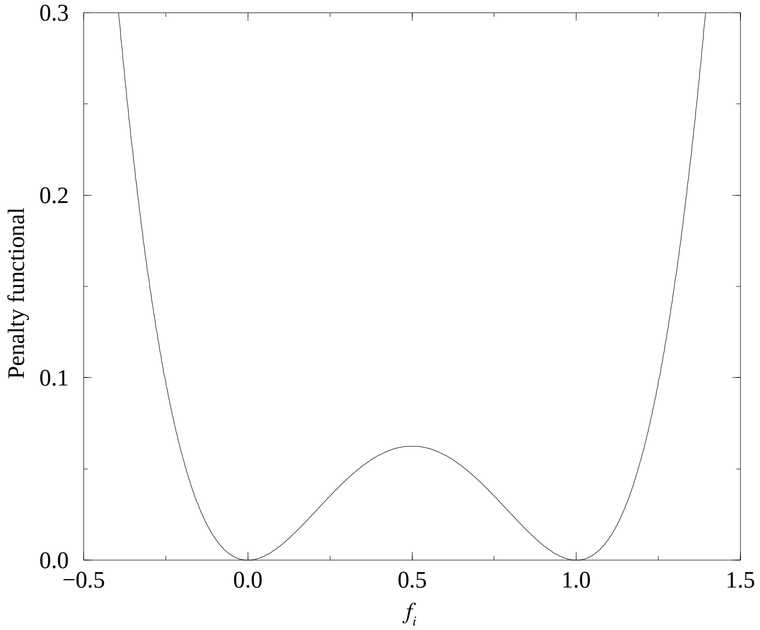

Figure 6.5: One possible choice of analytic penalty functional.

idempotent, minimisation of the total functional $Q[\rho;\alpha]$ is stable against run-away solutions in which $f_i \to \infty$ for occupied bands and $f_i \to -\infty$ for unoccupied bands. However, as illustrated in the sketch in figure 6.6, the minimising density-matrix is only approximately idempotent. In this particular case of an unoccupied band, the total functional is minimised when this band is negatively occupied i.e. for $f_i < 0$. In general the minimising density-matrix $\bar{\rho}$ will have eigenvalues lying outside the interval $[0,1]$, so that the energy calculated from such a density-matrix will be below the true ground-state energy.

We denote the set of occupation numbers which minimise the total functional $Q[\rho;\alpha]$

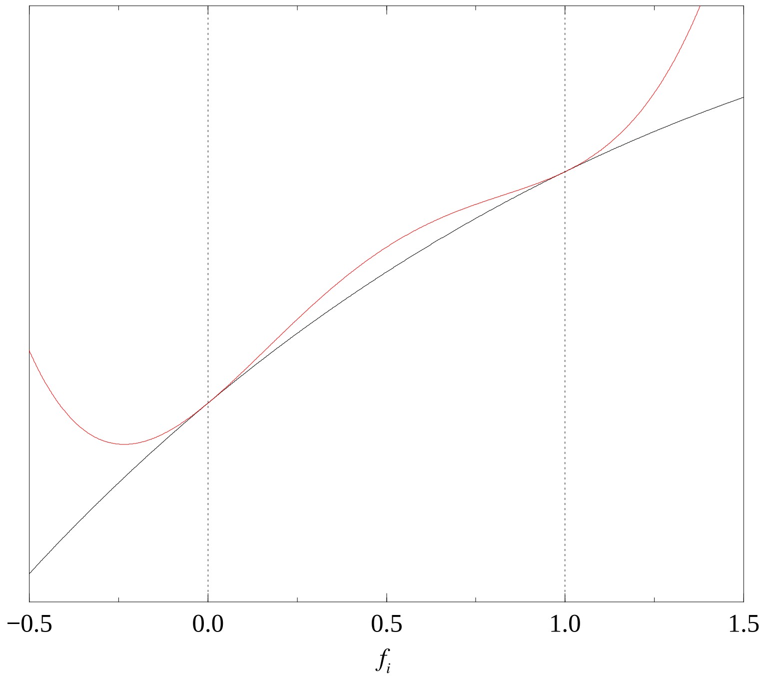

Figure 6.6: Schematic illustration of the analytic penalty functional: behaviour of the total energy (black) and total functional (red) with respect to a single occupation number for an unoccupied band.

by $\{\bar{f}_i\}$ and the errors in these occupation numbers with respect to idempotency by $\bar{f}_i = f_i^{(0)} + \delta f_i$ where $f_i^{(0)} = 1$ for occupied bands and $f_i^{(0)} = 0$ for unoccupied bands. Since $Q[\rho;\alpha]$ is minimised by $\bar{\rho}$, it is a minimum with respect to all changes in the occupation numbers which maintain the normalisation constraint

$$2\int d\mathbf{r}\ \rho(\mathbf{r},\mathbf{r}) = 2\sum_i f_i = N \tag{6.17}$$

which is imposed by introducing a Lagrange multiplier λ:

$$\frac{\partial}{\partial f_i}\left[Q[\rho;\alpha] - \lambda\left(2\sum_j f_j - N\right)\right]_{f_i=\bar{f}_i} = 0. \tag{6.18}$$

Using Janak's theorem for the derivative of the energy functional we obtain

$$\bar{\varepsilon}_i + \alpha\bar{f}_i\left(1-\bar{f}_i\right)\left(1-2\bar{f}_i\right) - \lambda = 0 \tag{6.19}$$

in which $\{\bar{\varepsilon}_i\}$ are the eigenvalues of the Hamiltonian obtained from the electronic density $\bar{n}(\mathbf{r}) = 2\bar{\rho}(\mathbf{r}, \mathbf{r})$ and are therefore different from the true ground-state eigenvalues. Assuming α to be sufficiently large so that the errors $\{\delta f_i\}$ are small,

$$\delta f_i \approx -\frac{\bar{\varepsilon}_i - \lambda}{\alpha}. \tag{6.20}$$

Application of the normalisation constraint 6.17 requires $\sum_i \delta f_i = 0$ from which we obtain the value of the Lagrange multiplier λ:

$$\lambda = \frac{2}{N} \sum_i \bar{\varepsilon}_i \tag{6.21}$$

which is the mean energy eigenvalue. The variance of the errors in the occupation numbers is thus related to the variance of the energy eigenvalues, scaled by the parameter α. Therefore, as is intuitively expected, the errors in the occupation numbers decrease as α is increased. More precisely, $\delta f_i \propto \alpha^{-1}$ and this behaviour is confirmed numerically in figure 6.7.

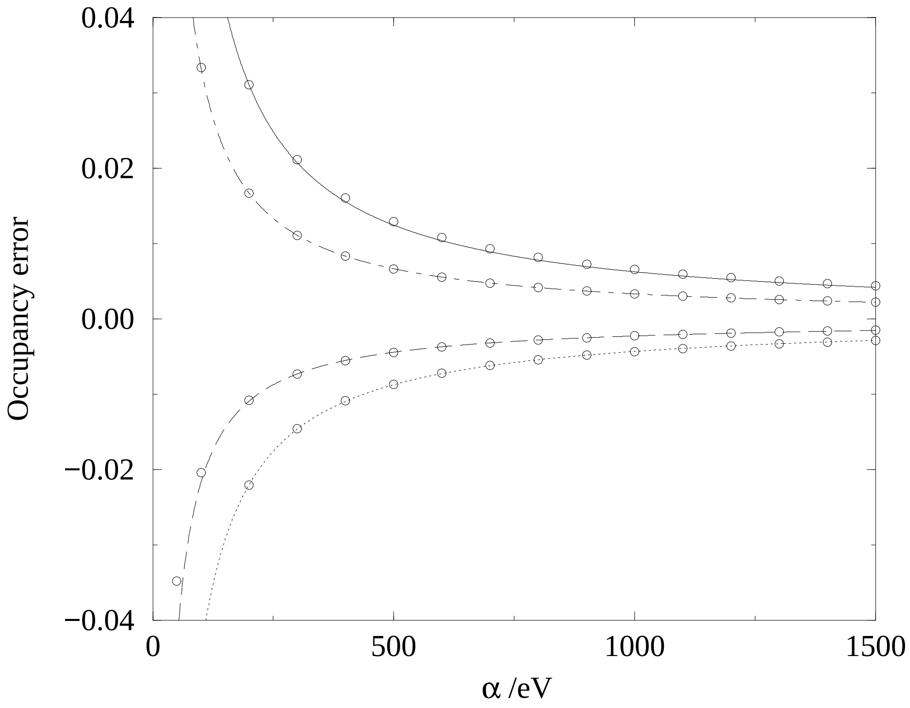

Figure 6.7: Variation of the occupation number errors with α. Lines show the best fit to α^{-1} behaviour.

For small deviations from idempotency, the penalty functional $P[\bar{\rho}] \approx \sum_i \delta f_i^2$ so that the penalty contribution to the minimised total functional, $\alpha P[\bar{\rho}]$ also decreases in proportion to α^{-1}. Hence the energy approaches the true ground-state energy as $\alpha \to \infty$, again with an error which decreases as α^{-1}. This α^{-1} convergence is unsatisfactory for practical applications, since it requires large values of α to obtain accurate estimates of the ground-state energy, and for large values of α the penalty term dominates the total functional and hinders efficient minimisation of the energy term. We now proceed to derive a correction to the estimated energy which allows accurate values for the ground-state energy to be obtained from the approximately idempotent density-matrices which minimise the total functional.

At the minimum of the total functional,

$$\left.\frac{\partial Q[\rho;\alpha]}{\partial f_i}\right|_{f_i=\bar{f}_i} = 0 = \left.\frac{\partial E[\rho]}{\partial f_i}\right|_{f_i=\bar{f}_i} + 2\alpha \bar{f}_i \left(1-\bar{f}_i\right)\left(1-2\bar{f}_i\right) \tag{6.22}$$

and this expression can be used to construct a first order Taylor expansion for the total energy with respect to the occupation numbers. We thus estimate the true ground-state energy E_0 to be

$$E_0 = E[\rho_0] \approx E[\bar{\rho}] + 2\alpha \sum_i \bar{f}_i \left(1-\bar{f}_i\right)\left(1-2\bar{f}_i\right)\delta f_i. \tag{6.23}$$

For occupied bands, $\delta f_i = \bar{f}_i - 1$ whereas for unoccupied bands $\delta f_i = \bar{f}_i$ so that

$$E_0 \approx E[\bar{\rho}] - 2\alpha \sum_i^{\text{all}} \bar{f}_i \left(1-\bar{f}_i\right)^2 \left(1-2\bar{f}_i\right) + 2\alpha \sum_i^{\text{unocc}} \bar{f}_i \left(1-\bar{f}_i\right)\left(1-2\bar{f}_i\right). \tag{6.24}$$

The first term of the correction has been written as a sum over all bands so that it can be expressed in terms of the trace $2\alpha\mathrm{Tr}\left[\bar{\rho}\left(1-\bar{\rho}\right)^2\left(1-2\bar{\rho}\right)\right]$ which can always be evaluated in $\mathcal{O}(N)$ operations. The second term only contributes when unoccupied bands are included in the calculation, which is not necessary for insulators. Since a single eigenvalue of the (sparse) density-matrix can always be obtained in $\mathcal{O}(N)$ operations, it is possible to evaluate the correction for a small number ($\ll N$) of unoccupied bands and retain the linear-scaling. However, we note that the correction need only be calculated once the minimum of the total functional has been found, so that a single $\mathcal{O}(N^2)$ step to obtain all of the occupation numbers will still be a tiny fraction of the total computational effort.

The error in a Taylor expansion is generally estimated by considering the lowest order term omitted, which in this case is

$$\frac{1}{2}\sum_{ij}\delta f_i \left.\frac{\partial^2 E[\rho]}{\partial f_i \partial f_j}\right|_{f_i=\bar{f}_i, f_j=\bar{f}_j} \delta f_j = \sum_{ij}\delta f_i \left.\frac{\partial \bar{\varepsilon}_i}{\partial f_j}\right|_{f_j=\bar{f}_j} \delta f_j \approx \sum_{ij}\delta f_i \mathcal{H}_{ij}\delta f_j \tag{6.25}$$

where $\mathcal{H}_{ij}$ is the chemical hardness matrix. Unfortunately this matrix is not guaranteed to be either positive or negative definite, and so the estimate of the ground-state energy 6.24 is not a strict upper or lower bound to the true energy. As will be seen shortly, this error is generally much smaller than other sources of error (such as the finite support region size, with respect to which the energy does behave variationally) so that this is not an issue in practice.

In figure 6.8 the energy, total functional and corrected energy are plotted for different values of the parameter α. These results confirm the α^{-1} behaviour of the energy and penalty functionals, and the error in the corrected energy even for $\alpha = 50$ eV is smaller than 10^{-4} eV per atom. Thus we have achieved our aim of being able to obtain accurate estimates of the ground-state energy from approximate density-matrices which minimise the total functional for values of α for which efficient minimisation is possible.

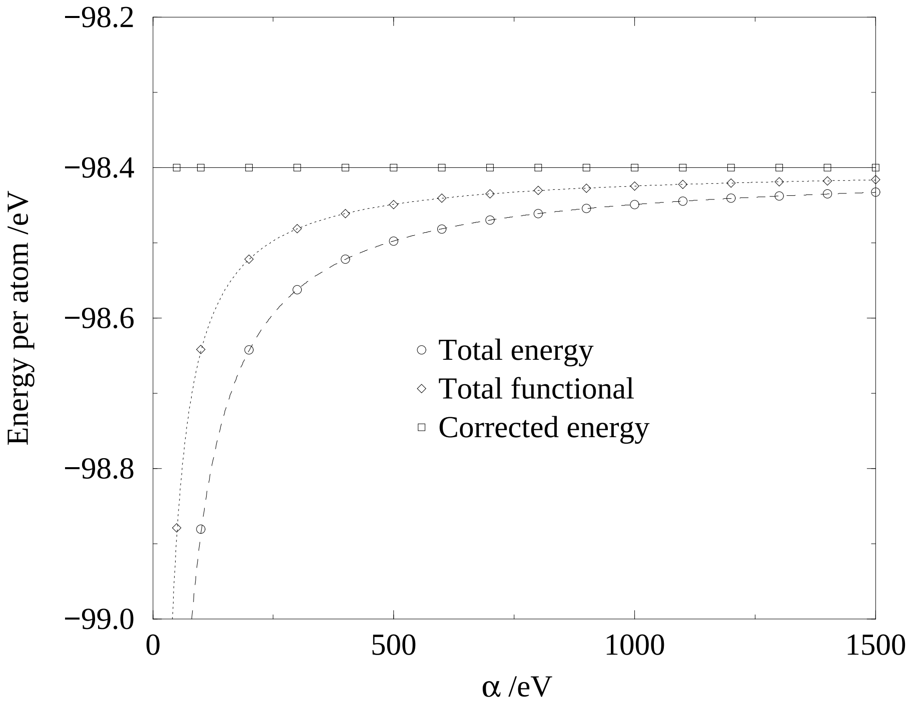

Figure 6.8: Total energy, total functional and corrected energy versus α. Lines are best fits to α^{-1} behaviour.

6.2.2 Further examples of penalty functionals

Before studying the efficiency of the minimisation procedure when applied to the total functional described above in section 6.2.1, we mention two further examples of penalty functionals which are suitable for this approach.

The first is applicable for positive semi-definite trial density-matrices. This requirement can be satisfied in practice by writing the density-kernel K in terms of an auxiliary matrix T as $K = TT^{\dagger}$ (see section 4.4.2). Since the eigenvalues of such a density-matrix must be non-negative, variation of the energy functional alone is sufficient to drive the occupation numbers of unoccupied bands to zero, and the penalty functional need only impose the occupation numbers of the occupied bands to lie close to unity. An appropriate penalty functional is then

$$P[\rho] = \int \mathrm{d}\mathbf{r} \left[\rho\,(1-\rho)^2\right](\mathbf{r},\mathbf{r}) = \sum_i f_i\,(1-f_i)^2\,, \tag{6.26}$$

and the corresponding energy correction is

$$E_0 \approx E[\bar{\rho}] - \alpha \sum_i^{\text{all}} (1-3\bar{f}_i)(1-\bar{f}_i)^2 + \alpha \sum_i^{\text{unocc}} (1-3\bar{f}_i)(1-\bar{f}_i). \tag{6.27}$$

Numerical investigation has shown that the occupation numbers of the unoccupied bands do indeed become very small but positive when this scheme is used.

The second penalty functional is applicable only when no unoccupied bands are included in the calculation. In this case, all of the occupation numbers should equal unity and so an appropriate penalty functional is

$$P[\rho] = \int \mathrm{d}\mathbf{r}\,(1-\rho)^2\,(\mathbf{r},\mathbf{r}) = \sum_i (1-f_i)^2\,. \tag{6.28}$$

The corresponding correction to the total energy in this case is

$$E_0 \approx E[\bar{\rho}] + 2\alpha \sum_i^{\text{all}} (1-\bar{f}_i)^2. \tag{6.29}$$

Both of these penalty functionals have been tested, and the results are very similar to those presented for the original functional in the previous section. These penalty functionals are plotted in figure 6.9.

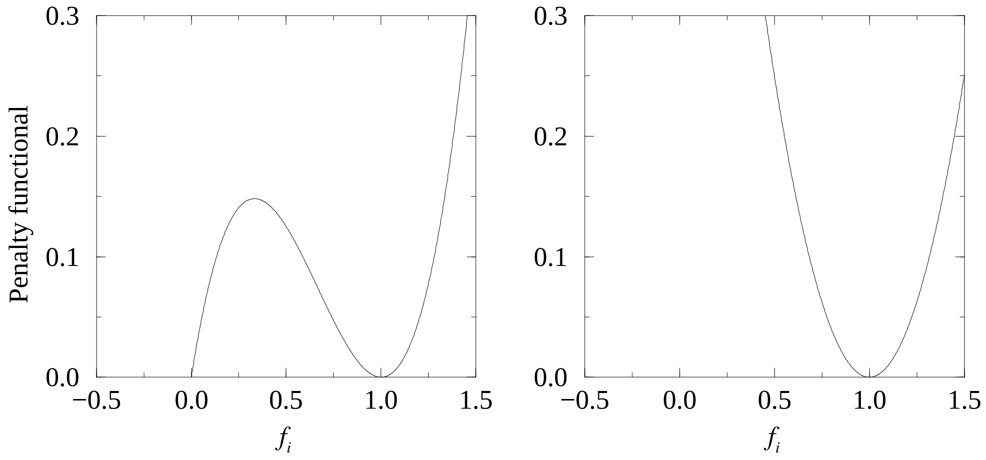

Figure 6.9: Two further examples of analytic penalty functionals.

6.2.3 Minimisation efficiency

In this section we discuss the efficiency of the conjugate gradients algorithm to minimise the total functional. We restrict the discussion to the penalty functional introduced in section 6.2.1. The total functional derived from this penalty functional appears to possess multiple local minima since the penalty functional itself is minimal for all idempotent density-matrices. However, most of these local minima do not correspond to density-matrices obeying the correct normalisation constraint and are therefore eliminated by imposing this constraint during the minimisation, as will be shown in chapter 7. Of the remaining minima, only one corresponds to the situation in which the lowest bands are occupied, and when the support functions are also varied, all other minima become unstable with respect to this one (i.e. these are minima with respect to occupation number variations but not orbital variations). Numerical investigations into this matter have been carried out and no problems arising from multiple minima have been observed (the minimised total functional has the same value independent of the starting point).

The efficiency with which the conjugate gradients scheme is able to minimise a function is known to depend upon the *condition number* κ, the ratio of the largest curvature to the smallest curvature at the minimum. The condition number may be calculated exactly by determining the Hessian matrix at the minimum, but may also be estimated as follows [153].

Consider the minimising density-matrix $\bar{\rho}$ expanded in terms of a set of orthonormal orbitals $\{\bar{\varphi}_i(\mathbf{r})\}$:

$$\bar{\rho}(\mathbf{r}, \mathbf{r}') = \sum_i \bar{f}_i \bar{\varphi}_i(\mathbf{r}) \bar{\varphi}_i(\mathbf{r}'). \tag{6.30}$$

Consider first perturbing the occupation numbers subject to the normalisation constraint i.e. increasing the occupation of some orbital labelled J by x at the expense of another orbital labelled I. The density-matrix becomes

$$\rho(\mathbf{r},\mathbf{r}') = \bar{\rho}(\mathbf{r},\mathbf{r}') - x\bar{\varphi}_I(\mathbf{r})\bar{\varphi}_I(\mathbf{r}') + x\bar{\varphi}_J(\mathbf{r})\bar{\varphi}_J(\mathbf{r}') \tag{6.31}$$

Defining $\bar{Q} = Q[\bar{\rho};\alpha]$ and using the orthonormality of the orbitals,

$$\begin{aligned} Q[\rho;\alpha] &= \bar{Q} + x(\bar{\varepsilon}_J - \bar{\varepsilon}_I) - \alpha[2x\{\bar{f}_I(1-2\bar{f}_I)(1-\bar{f}_I) + \bar{f}_J(1-2\bar{f}_J)(1-\bar{f}_J)\} \\ &- 2x^2\{1 - 3\bar{f}_I(1-\bar{f}_I) - 3\bar{f}_J(1-\bar{f}_J)\} - 4x^3(1-\bar{f}_I-\bar{f}_J) - 2x^4] \end{aligned} \tag{6.32}$$

and the curvature at the minimum is

$$\left.\frac{\partial^2 Q[\rho;\alpha]}{\partial x^2}\right|_{x=0} = 4\alpha\left[1 - 3\bar{f}_I(1-\bar{f}_I) - 3\bar{f}_J(1-\bar{f}_J)\right]. \tag{6.33}$$

Assuming that $\bar{\rho}$ is approximately idempotent so that both $\bar{f}_I$ and $\bar{f}_J$ are either roughly zero or unity,

$$\left.\frac{\partial^2 Q[\rho;\alpha]}{\partial x^2}\right|_{x=0} \approx 4\alpha \tag{6.34}$$

i.e. to first order, the curvature is independent of the choice of orbitals I and J so that the functional is spherical when this type of variation is considered, and the condition number is approximately unity.

The second type of variation is a unitary transformation of the orbitals i.e. $\varphi_I(\mathbf{r}) = (1-\frac{1}{2}x^2)\bar{\varphi}_I(\mathbf{r}) + x\bar{\varphi}_J(\mathbf{r})$ and $\varphi_J(\mathbf{r}) = (1-\frac{1}{2}x^2)\bar{\varphi}_J(\mathbf{r}) - x\bar{\varphi}_I(\mathbf{r})$, which maintains normalisation of the density-matrix to $\mathcal{O}(x^2)$. In this case

$$\begin{aligned} \rho(\mathbf{r},\mathbf{r}') &= \bar{\rho}(\mathbf{r},\mathbf{r}') + x(\bar{f}_I - \bar{f}_J)\bar{\varphi}_I(\mathbf{r})\bar{\varphi}_J(\mathbf{r}') + x(\bar{f}_I - \bar{f}_J)\bar{\varphi}_J(\mathbf{r})\bar{\varphi}_I(\mathbf{r}') \\ &+ x^2(\bar{f}_J - \bar{f}_I)\bar{\varphi}_I(\mathbf{r})\bar{\varphi}_I(\mathbf{r}') + x^2(\bar{f}_I - \bar{f}_J)\bar{\varphi}_J(\mathbf{r})\bar{\varphi}_J(\mathbf{r}') + \mathcal{O}(x^3) \end{aligned} \tag{6.35}$$

and similarly

$$Q[\rho;\alpha] = \bar{Q} + x^2(\bar{f}_I - \bar{f}_J)(\bar{\varepsilon}_J - \bar{\varepsilon}_I) + \mathcal{O}(x^3) \tag{6.36}$$

so that

$$\left.\frac{\partial^2 Q[\rho;\alpha]}{\partial x^2}\right|_{x=0} = 2(\bar{f}_I - \bar{f}_J)(\bar{\varepsilon}_J - \bar{\varepsilon}_I). \tag{6.37}$$

The maximum curvature is thus obtained when $\bar{f}_I \approx 1$ and $\bar{f}_J \approx 0$ and equals $2(\bar{\varepsilon}_{\max} - \bar{\varepsilon}_{\min})$ where $\bar{\varepsilon}_{\max}$ and $\bar{\varepsilon}_{\min}$ are the maximum and minimum energy eigenvalues of the orbitals

$\{\bar{\varphi}_i(\mathbf{r})\}$. The minimum curvature is obtained when $\bar{f}_I \approx \bar{f}_J$ and is therefore

$$2(\delta f_I - \delta f_J)(\bar{\varepsilon}_J - \bar{\varepsilon}_I) = \frac{2(\bar{\varepsilon}_J - \bar{\varepsilon}_I)^2}{\alpha} = \frac{2(\Delta\bar{\varepsilon})^2}{\alpha} \tag{6.38}$$

where $\Delta\bar{\varepsilon}$ is the minimum energy eigenvalue spacing. This curvature corresponds to unitary changes confined within the occupied or unoccupied subspaces with no mixing between, and the energy is indeed invariant under such changes. However, choosing to work with localised functions essentially defines a particular unitary transformation for the wave-functions, so that these variations are generally eliminated. If this is the case, then the minimum curvature will then be obtained in the same way as the maximum curvature, but seeking the minimum difference in energy eigenvalues between valence and conduction bands, which is the band gap $\bar{\varepsilon}_{\mathrm{g}}$. The minimum curvature is thus $2\bar{\varepsilon}_{\mathrm{g}}$ and the condition number is given by

$$\kappa = \frac{\bar{\varepsilon}_{\mathrm{max}} - \bar{\varepsilon}_{\mathrm{min}}}{\bar{\varepsilon}_{\mathrm{g}}}. \tag{6.39}$$

This is an encouraging result, since the condition number is independent of the system-size.

The length of the error vector after k iterations, η_k is related to κ by [154]

$$\eta_k \propto \left(\frac{\sqrt{\kappa} - 1}{\sqrt{\kappa} + 1} \right)^k \tag{6.40}$$

and the number of iterations required to converge to a given precision is therefore proportional to $\sqrt{\kappa}$ in the limit of large κ, and so independent of system-size.

Reviewing the results for both types of variation, we note that the minimisation with respect to occupation numbers (the first type) is very efficient, since $\kappa \approx 1$, whereas the minimisation with respect to orbitals is less efficient, depending upon the ratio of the total width of the eigenvalue spectrum to the band gap. Preconditioning schemes to compress the eigenvalue spectrum have been developed for use with plane-waves [81] and also with B-splines [155], and a similar scheme for the spherical-wave basis functions would also improve the rate of convergence. Nevertheless, we do not expect a significant change in the number of conjugate gradient steps required to converge to the minimum as the system-size increases. In practical implementations, discussed in chapter 7, these two types of variation are not strictly separated, both the occupation numbers and the orbitals being varied simultaneously, so that these results are hard to confirm numerically, although no significant increase in the number of iterations required to converge to a given accuracy is observed as the system-size increases.

Chapter 7

Computational implementation

In this chapter we describe how the corrected penalty functional method described in section 6.2 has been implemented in a total energy computer code to perform linear-scaling quantum-mechanical calculations on arbitrary systems.

As mentioned in section 4.6, the density-matrix is represented in the form

$$\rho(\mathbf{r},\mathbf{r}') = \phi_\alpha(\mathbf{r}) K^{\alpha\beta} \phi_\beta(\mathbf{r}'). \tag{7.1}$$

We refer to the contravariant quantity $K^{\alpha\beta}$ as the density-kernel, and the covariant quantities $\{\phi_\alpha(\mathbf{r})\}$ are localised non-orthogonal support functions, which are themselves expanded in terms of the spherical-wave basis-set of chapter 5:

$$\phi_\alpha(\mathbf{r}) = \sum_{n\ell m} c_{(\alpha)}^{n\ell m} \, \chi_{\alpha,n\ell m}(\mathbf{r}). \tag{7.2}$$

We now proceed to express the total energy and penalty functional in terms of these quantities, and also to calculate gradients with respect to the density-kernel and expansion coefficients $\{c_{(\alpha)}^{n\ell m}\}$. We will also discuss the implementation of the normalisation constraint and also how the convergence might be improved by the use of a preconditioning scheme for the gradients.

7.1 Total energy and Hamiltonian

A quantity which is frequently required is the overlap matrix $S_{\alpha\beta}$ defined by

$$S_{\alpha\beta} = \int \mathrm{d}\mathbf{r} \; \phi_\beta(\mathbf{r}) \phi_\alpha(\mathbf{r}). \tag{7.3}$$

The overlap matrix elements between the spherical-wave basis functions can be calculated analytically (section 5.4), and are denoted $\mathcal{S}_{\alpha,n\ell m;\beta,n'\ell'm'}$ where

$$\mathcal{S}_{\alpha,n\ell m;\beta,n'\ell'm'} = \langle \chi_{\alpha,n\ell m} | \chi_{\beta,n'\ell'm'} \rangle \tag{7.4}$$

so that the overlap matrix elements are given by

$$S_{\alpha\beta} = \sum_{n\ell m,n'\ell'm'} c_{(\alpha)}^{n\ell m} \mathcal{S}_{\alpha,n\ell m;\beta,n'\ell'm'} c_{(\beta)}^{n'\ell'm'} \tag{7.5}$$

recalling that the support functions may be assumed real in the case of Γ-point Brillouin zone sampling.

7.1.1 Kinetic energy

The kinetic energy of the non-interacting Kohn-Sham system is given by

$$T_{\mathrm{s}}^{\mathrm{J}} = -\int \mathrm{d}\mathbf{r}' \, \left[\nabla_{\mathbf{r}}^2 \rho(\mathbf{r},\mathbf{r}') \right]_{\mathbf{r}=\mathbf{r}'} = 2K^{\alpha\beta} T_{\beta\alpha} \tag{7.6}$$

in which

$$T_{\alpha\beta} = -\frac{1}{2} \int \mathrm{d}\mathbf{r} \, \phi_\alpha(\mathbf{r}) \nabla_{\mathbf{r}}^2 \phi_\beta(\mathbf{r}) \tag{7.7}$$

are the matrix elements of the kinetic energy operator in the representation of the support functions. Since all of the matrix elements between the spherical-wave basis functions can be calculated analytically,

$$T_{\alpha\beta} = \sum_{n\ell m,n'\ell'm'} c_{(\alpha)}^{n\ell m} \mathcal{T}_{\alpha,n\ell m;\beta,n'\ell'm'} c_{(\beta)}^{n'\ell'm'} \tag{7.8}$$

where $\mathcal{T}$ denotes matrix elements of the kinetic energy operator between spherical-wave basis functions.

7.1.2 Hartree energy and potential

The Hartree and exchange-correlation terms are calculated by determining the electronic density on a real-space grid $n(\mathbf{r})$, and Fast Fourier Transforms (FFTs) are used to transform between real- and reciprocal-space[1] to obtain $\tilde{n}(\mathbf{G})$. The Hartree energy is then given by

$$E_{\mathrm{H}} = \frac{1}{2}\int \mathrm{d}\mathbf{r}\ \mathrm{d}\mathbf{r}'\ \frac{n(\mathbf{r})n(\mathbf{r}')}{|\mathbf{r}-\mathbf{r}'|} = \frac{2\pi}{\Omega_{\mathrm{cell}}}\sum_{\mathbf{G}\neq 0}\frac{|\tilde{n}(\mathbf{G})|^2}{G^2} \tag{7.9}$$

where Ω_{cell} is the volume of the supercell and the (infinite) $\mathbf{G}=0$ term is omitted because the system is charge neutral overall. This term is therefore cancelled by similar terms in the ion-ion and electron-ion interaction energies. The Hartree potential in real-space is given by

$$V_{\mathrm{H}}(\mathbf{r}) = \int \mathrm{d}\mathbf{r}'\ \frac{n(\mathbf{r}')}{|\mathbf{r}-\mathbf{r}'|} \tag{7.10}$$

but is calculated in reciprocal-space as

$$\tilde{V}_{\mathrm{H}}(\mathbf{G}) = \frac{4\pi\tilde{n}(\mathbf{G})}{\Omega_{\mathrm{cell}}G^2} \tag{7.11}$$

and then transformed back into real-space by a FFT.

7.1.3 Exchange-correlation energy and potential

Having calculated the electron density on the grid points, the exchange-correlation energy is obtained by summing over those grid points

$$E_{\mathrm{xc}} = \delta\omega\sum_{\mathbf{r}} n(\mathbf{r})\epsilon_{\mathrm{xc}}(n(\mathbf{r})) \tag{7.12}$$

in the local density approximation. $\delta\omega$ is the volume of the supercell divided by the number of grid points. The exchange-correlation potential is similarly calculated at each grid point as

$$V_{\mathrm{xc}}(\mathbf{r}) = \left[\frac{\mathrm{d}}{\mathrm{d}n}\left\{n\epsilon_{\mathrm{xc}}(n)\right\}\right]_{n=n(\mathbf{r})}. \tag{7.13}$$

In practice, the values of $\epsilon_{\mathrm{xc}}(n)$ and $\frac{\mathrm{d}}{\mathrm{d}n}\left[n\epsilon_{\mathrm{xc}}(n)\right]$ are tabulated for various values of the electronic density n and then interpolated during the calculation.

[1] The conventions used here for discrete Fourier transforms are

$$\tilde{n}(\mathbf{G}) = \sum_{\mathbf{r}} n(\mathbf{r})\exp(-\mathrm{i}\mathbf{G}\cdot\mathbf{r}) \quad ; \quad n(\mathbf{r}) = \frac{1}{\Omega_{\mathrm{cell}}}\sum_{\mathbf{G}}\tilde{n}(\mathbf{G})\exp(\mathrm{i}\mathbf{G}\cdot\mathbf{r}).$$

7.1.4 Local pseudopotential

Like the Hartree potential, the local pseudopotential is also calculated in reciprocal-space as

$$\tilde{V}_{\mathrm{ps,loc}}(\mathbf{G}) = \sum_s \tilde{v}^s_{\mathrm{ps,loc}}(\mathbf{G}) \mathbb{S}^s(\mathbf{G}) \tag{7.14}$$

where the summation is over ionic species s, $\tilde{v}^s_{\mathrm{ps,loc}}(\mathbf{G})$ is the local pseudopotential for an isolated ion of species s in reciprocal-space and $\mathbb{S}^s(\mathbf{G})$ is the structure factor for species s defined by

$$\mathbb{S}^s(\mathbf{G}) = \sum_\alpha \exp[-\mathrm{i}\mathbf{G}\cdot\mathbf{r}^s_\alpha] \tag{7.15}$$

where the sum is over all ions α of species s with positions $\mathbf{r}^s_\alpha$. We note that in general the calculation of the structure factor is an $\mathcal{O}(N^2)$ operation, but since it only has to be calculated once for each atomic configuration, it is not a limiting factor of the overall calculation at this stage. Within the quantum chemistry community, work on generalised multipole expansions and new algorithms [156–162] has led to the development of methods to calculate Coulomb interaction matrix elements which scale linearly with system-size. The local pseudopotential energy can be calculated in reciprocal-space as

$$\begin{aligned} E_{\mathrm{ps,loc}} &= \int \mathrm{d}\mathbf{r}\ V_{\mathrm{ps,loc}}(\mathbf{r}) n(\mathbf{r}) \\ &= \sum_{\mathbf{G}\neq 0} \sum_s \tilde{v}^s_{\mathrm{ps,loc}}(\mathbf{G}) \mathbb{S}^s(\mathbf{G}) \tilde{n}^*(\mathbf{G}) + \sum_s N_s E^s_{\mathrm{ps,core}} \\ &= 2K^{\alpha\beta} V_{\mathrm{loc},\beta\alpha} \end{aligned} \tag{7.16}$$

where $E^s_{\mathrm{ps,core}}$ is the pseudopotential core energy, and $N_s = \mathbb{S}^s(\mathbf{G}=0)$ the number of ions of species s. The matrix elements $V_{\mathrm{loc},\alpha\beta}$ are defined by

$$V_{\mathrm{loc},\alpha\beta} = \int \mathrm{d}\mathbf{r}\ \phi_\alpha(\mathbf{r}) V_{\mathrm{ps,loc}}(\mathbf{r}) \phi_\beta(\mathbf{r}). \tag{7.17}$$

The Hartree potential and local pseudopotential can be summed and then transformed back together into real-space and added to the exchange-correlation potential to obtain the local part of the Kohn-Sham potential in real-space.

We note that the FFT is not strictly an $\mathcal{O}(N)$ operation but an $\mathcal{O}(N \log_m N)$ operation (where m is some small number which depends upon the prime factors of the number of grid points), but in practice (section 9.2) this scaling is not observed.

7.1.5 Non-local pseudopotential

The non-local pseudopotential energy is given by

$$E_{\mathrm{ps,NL}} = \int \mathrm{d}\mathbf{r}\ \mathrm{d}\mathbf{r}'\ \rho(\mathbf{r},\mathbf{r}')V_{\mathrm{ps,NL}}(\mathbf{r}',\mathbf{r}) = 2K^{\alpha\beta}V_{\mathrm{NL},\beta\alpha}. \tag{7.18}$$

The matrix elements of the non-local pseudopotential in the representation of the support functions $V_{\mathrm{NL},\alpha\beta}$ are calculated by summing over all ions whose cores overlap the support regions of ϕ_α and ϕ_β, and using the method described in section 5.6.2 to calculate the spherical-wave basis function matrix elements $\mathcal{V}_{\alpha,n\ell m;\beta,n'\ell'm'}$ analytically. The result is therefore

$$V_{\mathrm{NL},\alpha\beta} = \sum_{n\ell m,n'\ell'm'} c^{n\ell m}_{(\alpha)}\mathcal{V}_{\alpha,n\ell m;\beta,n'\ell'm'}c^{n'\ell'm'}_{(\beta)} \tag{7.19}$$

which is of exactly the same form as the kinetic energy, so that in practice the basis function matrix elements for the kinetic energy and non-local pseudopotential are summed and the two contributions to the energy combined.

7.2 Energy gradients

Having calculated the total energy, both the density-kernel $K^{\alpha\beta}$ and the expansion coefficients for the localised orbitals $\{c^{n\ell m}_{(\alpha)}\}$ are varied. Because of the non-orthogonality of the support functions, it is necessary to take note of the tensor properties of the gradients [163], as noted in section 4.6.

7.2.1 Density-kernel derivatives

The total energy depends upon $K^{\alpha\beta}$ both explicitly and through the electronic density $n(\mathbf{r})$. We use the result

$$\frac{\partial K^{ij}}{\partial K^{\alpha\beta}} = \delta^i_\alpha\delta^j_\beta. \tag{7.20}$$

Kinetic and pseudopotential energies

From equations 7.6, 7.16 and 7.18 we have that

$$E_{\mathrm{kin,ps}} = T^{\mathrm{J}}_{\mathrm{s}} + E_{\mathrm{ps,loc}} + E_{\mathrm{ps,NL}} = 2K^{ij}(T + V_{\mathrm{loc}} + V_{\mathrm{NL}})_{ji} \tag{7.21}$$

and therefore

$$\frac{\partial E_{\mathrm{kin,ps}}}{\partial K^{\alpha\beta}} = 2(T + V_{\mathrm{loc}} + V_{\mathrm{NL}})_{\beta\alpha}. \tag{7.22}$$

Hartree and exchange-correlation energies

The sum of the Hartree and exchange-correlation energies, E_{Hxc} depends only on the density so that

$$\frac{\partial E_{\mathrm{Hxc}}}{\partial K^{\alpha\beta}} = \int \mathrm{d}\mathbf{r}\ \frac{\delta E_{\mathrm{Hxc}}}{\delta n(\mathbf{r})} \frac{\partial n(\mathbf{r})}{\partial K^{\alpha\beta}}. \tag{7.23}$$

The functional derivative of the Hartree-exchange-correlation energy with respect to the electronic density is simply the sum of the Hartree and exchange-correlation potentials, $V_{\mathrm{Hxc}}(\mathbf{r})$. The electronic density is given in terms of the density-kernel by

$$n(\mathbf{r}) = 2\phi_i(\mathbf{r}) K^{ij} \phi_j(\mathbf{r}) \tag{7.24}$$

so that we obtain

$$\frac{\partial n(\mathbf{r})}{\partial K^{\alpha\beta}} = 2\phi_\alpha(\mathbf{r})\phi_\beta(\mathbf{r}). \tag{7.25}$$

Finally, therefore

$$\frac{\partial E_{\mathrm{Hxc}}}{\partial K^{\alpha\beta}} = 2\int \mathrm{d}\mathbf{r}\ \phi_\beta(\mathbf{r}) V_{\mathrm{Hxc}}(\mathbf{r}) \phi_\alpha(\mathbf{r}) = 2V_{\mathrm{Hxc},\beta\alpha}. \tag{7.26}$$

Total energy

Defining the matrix elements of the Kohn-Sham Hamiltonian in the representation of the support functions by

$$H_{\alpha\beta} = T_{\alpha\beta} + V_{\mathrm{Hxc},\alpha\beta} + V_{\mathrm{loc},\alpha\beta} + V_{\mathrm{NL},\alpha\beta} \tag{7.27}$$

the derivative of the total energy with respect to the density-kernel is simply

$$\frac{\partial E}{\partial K^{\alpha\beta}} = 2H_{\beta\alpha}. \tag{7.28}$$

7.2.2 Support function derivatives

Again we can treat the kinetic and pseudopotential energies together, and the Hartree and exchange-correlation energies together. We use the result that

$$\frac{\partial \phi_i(\mathbf{r})}{\partial \phi_\alpha(\mathbf{r}')} = \delta_i^\alpha \delta(\mathbf{r} - \mathbf{r}'). \tag{7.29}$$

Kinetic and pseudopotential energies

We define the kinetic energy operator $\hat{T} = -\frac{1}{2}\nabla^2$, whose matrix elements are

$$T_{ij} = \int \mathrm{d}\mathbf{r}\ \phi_i(\mathbf{r}) \hat{T} \phi_j(\mathbf{r}). \tag{7.30}$$

Since the operator is Hermitian,

$$\frac{\delta T_{ij}}{\delta\phi_\alpha(\mathbf{r})} = \delta_i^\alpha \hat{T}\phi_j(\mathbf{r}) + \delta_j^\alpha \hat{T}\phi_i(\mathbf{r}). \tag{7.31}$$

Therefore

$$\begin{aligned}\frac{\delta T_{\mathrm{s}}^{\mathrm{J}}}{\delta\phi_\alpha(\mathbf{r})} &= 2\frac{\delta}{\delta\phi_\alpha(\mathbf{r})}\left(K^{ij}T_{ji}\right) = 2K^{ij}\frac{\delta T_{ji}}{\delta\phi_\alpha(\mathbf{r})} \\ &= 4K^{\alpha\beta}\hat{T}\phi_\beta(\mathbf{r}). \end{aligned}\tag{7.32}$$

The derivation for the pseudopotential energy is identical with the replacement of $\hat{T}$ by the pseudopotential operator, and so the result for the sum of these energies is just

$$\frac{\delta E_{\mathrm{kin,ps}}}{\delta\phi_\alpha(\mathbf{r})} = 4K^{\alpha\beta}\left(\hat{T} + \hat{V}_{\mathrm{ps,tot}}\right)\phi_\beta(\mathbf{r}). \tag{7.33}$$

Hartree and exchange-correlation energies

Again this gradient is derived by considering the change in the electronic density.

$$\frac{\partial n(\mathbf{r}')}{\partial\phi_\alpha(\mathbf{r})} = 2\Big[K^{\alpha j}\delta(\mathbf{r}-\mathbf{r}')\phi_j(\mathbf{r}') + \phi_i(\mathbf{r}')\delta(\mathbf{r}-\mathbf{r}')K^{i\alpha}\Big]. \tag{7.34}$$

Therefore

$$\frac{\delta E_{\mathrm{Hxc}}}{\delta\phi_\alpha(\mathbf{r})} = \int \mathrm{d}\mathbf{r}'\ \frac{\delta E_{\mathrm{Hxc}}}{\delta n(\mathbf{r}')}\frac{\partial n(\mathbf{r}')}{\partial\phi_\alpha(\mathbf{r})} = \int \mathrm{d}\mathbf{r}'\ V_{\mathrm{Hxc}}(\mathbf{r}')\frac{\partial n(\mathbf{r}')}{\partial\phi_\alpha(\mathbf{r})} = 4K^{\alpha\beta}\hat{V}_{\mathrm{Hxc}}\phi_\beta(\mathbf{r}) \tag{7.35}$$

Total energy

The gradient of the total energy with respect to changes in the support functions is

$$\frac{\delta E}{\delta\phi_\alpha(\mathbf{r})} = 4K^{\alpha\beta}\hat{H}\phi_\beta(\mathbf{r}) \tag{7.36}$$

where $\hat{H}$ is the Kohn-Sham Hamiltonian which operates on $\phi_\beta(\mathbf{r})$.

7.3 Penalty functional and electron number

The penalty functional $P[\rho]$ is defined by

$$P[\rho] = \int \mathrm{d}\mathbf{r}\ \left(\rho^2(1-\rho)^2\right)(\mathbf{r},\mathbf{r})$$

$$\begin{aligned} &= \int \mathrm{d}\mathbf{r}_1 \mathrm{d}\mathbf{r}_2 \mathrm{d}\mathbf{r}_3 \mathrm{d}\mathbf{r}_4 \; \rho(\mathbf{r}_1, \mathbf{r}_2)\rho(\mathbf{r}_2, \mathbf{r}_3) \left[\delta(\mathbf{r}_3, \mathbf{r}_4) - \rho(\mathbf{r}_3, \mathbf{r}_4)\right] \left[\delta(\mathbf{r}_4, \mathbf{r}_1) - \rho(\mathbf{r}_4, \mathbf{r}_1)\right] \\ &= K^{ij} S_{jk} K^{kl} S_{lm} (\delta^m_p - K^{mn} S_{np})(\delta^p_i - K^{pq} S_{qi}). \end{aligned} \tag{7.37}$$

The derivative with respect to the density-kernel is then

$$\frac{\partial P[\rho]}{\partial K^{\alpha\beta}} = 2S_{\beta i} K^{ij} S_{jk} (\delta^k_m - K^{kl} S_{lm})(\delta^m_\alpha - 2K^{mn} S_{n\alpha}). \tag{7.38}$$

The penalty functional depends implicitly upon the support functions though the overlap matrix:

$$\frac{\delta S_{ij}}{\delta \phi_\alpha(\mathbf{r})} = \delta^\alpha_i \phi_j(\mathbf{r}) + \delta^\alpha_j \phi_i(\mathbf{r}) \tag{7.39}$$

so that

$$\frac{\delta P[\rho]}{\delta \phi_\alpha(\mathbf{r})} = 4K^{\alpha i} S_{ij} K^{jk} (\delta^m_k - S_{kl} K^{lm})(\delta^\beta_m - 2S_{mn} K^{n\beta})\phi_\beta(\mathbf{r}). \tag{7.40}$$

For the sake of completeness, we now describe the expressions for the electron number and its derivatives.

$$N = 2\int \mathrm{d}\mathbf{r} \; \rho(\mathbf{r}, \mathbf{r}) = 2K^{ij} S_{ji} \tag{7.41}$$

$$\frac{\partial N}{\partial K^{\alpha\beta}} = 2S_{\beta\alpha} \tag{7.42}$$

$$\frac{\delta N}{\delta \phi_\alpha(\mathbf{r})} = 2K^{\alpha\beta} \phi_\beta(\mathbf{r}) \tag{7.43}$$

7.4 Physical interpretation

At this stage we examine the energy gradients derived in section 7.2. At the minimum of the total functional $Q[\rho; \alpha]$,

$$\frac{\partial Q[\rho; \alpha]}{\partial K^{\alpha\beta}} = 0 = 2H_{\beta\alpha} + 2\alpha \left[SKS(1 - KS)(1 - 2KS)\right]_{\beta\alpha}. \tag{7.44}$$

Making the Löwdin transformation of this gradient into the representation of a set of orthonormal orbitals (using the results of section 4.6) yields

$$2S^{\frac{1}{2}} \left[\tilde{H} + \alpha\tilde{K}(1 - \tilde{K})(1 - 2\tilde{K})\right] S^{\frac{1}{2}} = 0 \tag{7.45}$$

which (pre- and post-multiplying by $S^{-\frac{1}{2}}$) simplifies to

$$\tilde{H} + \alpha\tilde{K}(1 - \tilde{K})(1 - 2\tilde{K}) = 0. \tag{7.46}$$

This result shows that at the minimum, $\tilde{K}$ and $\tilde{H}$ can be diagonalised simultaneously, and will therefore commute. The result of the variation of the density-kernel is to make the density-matrix commute with the Hamiltonian in the representation of the current support functions. Transforming to the diagonal frame by making a unitary transformation (the eigenvalues of $\tilde{K}$ being f_i and those of $\tilde{H}$ being ε_i) we obtain the following relationship:

$$\varepsilon_i + \alpha f_i(1 - f_i)(1 - 2f_i) = 0. \tag{7.47}$$

For the derivative with respect to the support functions we have

$$\frac{\delta Q[\rho;\alpha]}{\partial \phi_\alpha(\mathbf{r})} = 0 = 4\left\{K^{\alpha\beta}\hat{H} + \alpha[KSK(1-SK)(1-2SK)]^{\alpha\beta}\right\}\phi_\beta(\mathbf{r}) \tag{7.48}$$

which can again be transformed first into an orthonormal representation defined by the Löwdin transformation:

$$\varphi_\alpha(\mathbf{r}) = \phi_\beta(\mathbf{r})S^{-\frac{1}{2}}_{\beta\alpha} \tag{7.49}$$

to obtain

$$\begin{aligned}
\frac{\delta Q[\rho;\alpha]}{\delta \varphi_\alpha(\mathbf{r})} &= \int \mathrm{d}\mathbf{r}'\, \frac{\delta Q[\rho;\alpha]}{\delta \phi_\beta(\mathbf{r}')}\frac{\partial \phi_\beta(\mathbf{r}')}{\partial \varphi_\alpha(\mathbf{r})} = S^{\frac{1}{2}}_{\alpha\beta}\frac{\delta Q[\rho;\alpha]}{\delta \phi_\beta(\mathbf{r})} \\
&= 4S^{\frac{1}{2}}_{\alpha i}K^{ij}\left[\hat{H} + \alpha SK(1-SK)(1-2SK)\right]_j^{\,k} S^{\frac{1}{2}}_{kl}\varphi_l(\mathbf{r}) \\
&= 4\left[\tilde{K}\left\{\hat{H} + \alpha\tilde{K}(1-\tilde{K})(1-2\tilde{K})\right\}\right]_{\alpha\beta}\varphi_\beta(\mathbf{r}).
\end{aligned} \tag{7.50}$$

Assuming that we have performed the minimisation with respect to the density-kernel for the current support functions, transforming to the representation which simultaneously diagonalises the Hamiltonian and density-matrix, by the unitary transformation $\psi_i(\mathbf{r}) = \varphi_\alpha(\mathbf{r})U_{\alpha i}$, yields

$$\begin{aligned}
\frac{\delta Q[\rho;\alpha]}{\delta \psi_i(\mathbf{r})} &= U^\dagger_{i\alpha}\frac{\delta Q[\rho;\alpha]}{\delta \varphi_\alpha(\mathbf{r})} \\
&= 4U^\dagger_{ij}\left\{\hat{H}\delta_{jk} + \alpha\left[SK(1-SK)(1-2SK)\right]_{jk}\right\}U_{kl}\psi_l(\mathbf{r}) \\
&= 4f_i\left[\hat{H} + \alpha f_i(1-f_i)(1-2f_i)\right]\psi_i(\mathbf{r})
\end{aligned} \tag{7.51}$$

which is a Kohn-Sham-like equation, but where the energy eigenvalue ε_i does not explicitly appear since no orthonormalisation constraint is explicitly applied. Using equation 7.47, however, yields

$$\frac{\delta Q[\rho;\alpha]}{\delta \psi_i(\mathbf{r})} = 0 = 4f_i\left[\hat{H} - \varepsilon_i\right]\psi_i(\mathbf{r}) \tag{7.52}$$

and so, at least for $f_i \neq 0$, we see that the support function variations are equivalent to making the related wave-functions obey the Kohn-Sham equations. The factor of f_i will slow this convergence for unoccupied bands, since for $f_i \approx 0$ the gradient is small. In the next section (7.5) we therefore turn our attention to a potential method for eliminating this problem.

7.5 Occupation number preconditioning

The eigenvalues of the Hessian at a stationary point determine the nature and shape of that stationary point. Thus the shape of the ground-state minimum of an energy functional is determined by the eigenvalues of that functional. For the Kohn-Sham scheme these eigenvalues are the $\{\varepsilon_i\}$ and the narrower the eigenvalue spectrum, the more "spherical" the minimum, and the easier the functional is to minimise. From equation 4.9 we note that when partial occupation numbers are introduced, the relevant eigenvalue spectrum becomes $\{f_i \varepsilon_i\}$. When conduction bands are included in a calculation, their occupation numbers will be vanishingly small near the ground-state minimum, which will therefore be very aspherical, and convergence of these bands will become very slow. This problem has been addressed in the study of metallic systems [164,165] by the method of preconditioning which changes the metric of the parameter space to compress the eigenvalue spectrum and make the minimum more spherical.

With reference to the results in appendix B, we introduce a metric, represented by the matrix $\mathcal{M}$, such that a new set of variables (denoted by a tilde) is introduced:

$$\tilde{\mathbf{x}} = \mathcal{M} \cdot \mathbf{x} \tag{7.53}$$

and so that the new gradients are related to the old gradients by

$$\tilde{\mathbf{g}} = \mathcal{M}^{-1} \cdot \mathbf{g}. \tag{7.54}$$

In the new metric, the conjugate directions are defined (see appendix B) by

$$\tilde{\mathbf{p}}_{r+1} = -\tilde{\mathbf{g}}_{r+1} + \tilde{\beta}_r \tilde{\mathbf{p}}_r \tag{7.55}$$

$$\tilde{\beta}_r = \frac{\tilde{\mathbf{g}}_{r+1} \cdot \tilde{\mathbf{g}}_{r+1}}{\tilde{\mathbf{g}}_r \cdot \tilde{\mathbf{g}}_r} \tag{7.56}$$

where we have adopted the Fletcher-Reeves method (B.22) for calculating β_r. The line minimum is given by

$$\tilde{\mathbf{x}}_{r+1} = \tilde{\mathbf{x}}_r + \alpha_r \tilde{\mathbf{p}}_r \tag{7.57}$$

which can be rewritten in terms of the original variables as

$$\begin{aligned}\mathcal{M}\cdot\mathbf{x}_{r+1} &= \mathcal{M}\cdot\mathbf{x}_r+\alpha_r\tilde{\mathbf{p}}_r \\ \Rightarrow \mathbf{x}_{r+1} &= \mathbf{x}_r+\alpha_r\mathcal{M}^{-1}\cdot\tilde{\mathbf{p}}_r. \qquad (7.58)\end{aligned}$$

This identifies $\mathcal{M}^{-1}\cdot\tilde{\mathbf{p}}_r$ as the set of preconditioned conjugate gradients for the original variables in the original space. These directions $\{\mathbf{P}_r\}$ are thus given by

$$\mathbf{P}_{r+1}=\mathcal{M}^{-1}\cdot\tilde{\mathbf{p}}_{r+1}=-\mathcal{M}^{-1}\cdot\tilde{\mathbf{g}}_{r+1}+\tilde{\beta}_r\mathcal{M}^{-1}\cdot\tilde{\mathbf{p}}_r=-\mathcal{M}^{-2}\cdot\mathbf{g}_{r+1}+\tilde{\beta}_r\mathbf{P}_r \qquad (7.59)$$

so that the gradients to be used for the preconditioned search are

$$\mathbf{G}_r=\mathcal{M}^{-2}\cdot\mathbf{g}_r \qquad (7.60)$$

with mixing factor

$$\tilde{\beta}_r=\frac{\tilde{\mathbf{g}}_{r+1}\cdot\tilde{\mathbf{g}}_{r+1}}{\tilde{\mathbf{g}}_r\cdot\tilde{\mathbf{g}}_r}=\frac{\mathbf{g}_{r+1}\cdot\mathcal{M}^{-2}\cdot\mathbf{g}_{r+1}}{\mathbf{g}_r\cdot\mathcal{M}^{-2}\cdot\mathbf{g}_r}=\frac{\mathbf{G}_{r+1}\cdot\mathbf{g}_{r+1}}{\mathbf{G}_r\cdot\mathbf{g}_r}. \qquad (7.61)$$

It is observed that defining $\tilde{\beta}_r$ in terms of the preconditioned gradients alone does not interfere with the minimisation procedure, so that in practice

$$\tilde{\beta}_r=\frac{\mathbf{G}_{r+1}\cdot\mathbf{G}_{r+1}}{\mathbf{G}_r\cdot\mathbf{G}_r}. \qquad (7.62)$$

In order to apply this scheme here, we choose to make the metric $\mathcal{M}$ diagonal in the representation of the Kohn-Sham orbitals. In the original variables $\{x_i\}$ (the subscript i labels a component of a vector) the minimum can be expanded as $\sum_i f_i\varepsilon_i x_i^2$ so that the scaled variables $\{\tilde{x}_i\}$ defined by $\tilde{x}_i=m_{(i)}x_i=\sqrt{f_i}x_i$ (where $M_{ij}=m_{(i)}\delta_{ij}$) produce the desired compression since in terms of the new variables, the minimum has the form $\sum_i\varepsilon_i\tilde{x}_i^2$. In the representation of the Kohn-Sham orbitals, the gradient of the functional $Q[\rho;\alpha]$ (7.52) becomes

$$4m_{(i)}^{-2}\left[f_i\left\{\hat{H}-\varepsilon_i\right\}\right]\psi_i(\mathbf{r})=4\left[\hat{H}-\varepsilon_i\right]\psi_i(\mathbf{r}) \qquad (7.63)$$

in which we see that the factor of f_i in front of the $\hat{H}$ operator has been cancelled so that the effect of the gradient is now the same on both occupied and unoccupied bands, and these bands should now converge at the same rate.

We now transform the preconditioned gradient back to the support function representation using

$$\frac{\delta Q[\rho;\alpha]}{\delta\phi_\alpha(\mathbf{r})} = V_{\alpha i}\frac{\delta Q[\rho;\alpha]}{\delta\psi_i(\mathbf{r})} \tag{7.64}$$

where $V = S^{-\frac{1}{2}}U$ from 4.78 and U is a unitary matrix. Thus the preconditioned gradient we require is

$$4V_{\alpha i}\left[\hat{H} + \alpha f_i(1-f_i)(1-2f_i)\right]\psi_i(\mathbf{r}) = 4\left[S^{-1}_{\alpha\beta}\hat{H} + \alpha\left(K(1-SK)(1-2SK)\right)^{\alpha\beta}\right]\phi_\beta(\mathbf{r}) \tag{7.65}$$

from the properties of the matrix V (4.79, 4.80). We see that the gradient has thus been pre-multiplied by the matrix $(KS)^{-1}$ i.e. in the support function representation, the metric $\mathcal{M}$ is $(KS)^{\frac{1}{2}}$.

Although the overlap matrix S is a sparse matrix for localised support functions, its inverse S^{-1} is not sparse in general, so that this scheme is not straightforward to implement. For a sufficiently diagonally dominant overlap matrix, it is possible to approximate the inverse in the following manner. We write $S = D + E$ where D contains only the diagonal elements of S and E contains the off-diagonal elements. D is thus trivial to diagonalise. Writing $S = D(1 + D^{-1}E)$ we have $S^{-1} = (1 + D^{-1}E)^{-1}D^{-1}$ and if S is diagonally dominant, the elements of the matrix $D^{-1}E$ are small so that we can approximate the inverse of the term in brackets. If the elements of a matrix M are small then

$$\begin{aligned}(1+M)^{-1} &= 1 - M + M^2 - M^3 + \mathcal{O}(M^4) \\ &= \sum_{n=0}^{\infty}(-1)^n M^n.\end{aligned} \tag{7.66}$$

When the first few terms of equation 7.66 are applied to the inverse overlap matrix we obtain

$$\begin{aligned}S^{-1} &= (1 - D^{-1}E + D^{-1}ED^{-1}E - \ldots)D^{-1} \\ &= D^{-1} - D^{-1}ED^{-1} + D^{-1}ED^{-1}ED^{-1} - \ldots\end{aligned} \tag{7.67}$$

This expression could be used to obtain a good approximation to the inverse overlap matrix, which may be sufficient for preconditioning, but there is the danger that, particularly for large systems, the overlap matrix may become singular and the performance of the algorithm would deteriorate. In the following section, however, we show that the correct preconditioned gradient does not involve the inverse of the overlap matrix.

7.6 Tensor properties of the gradients

We have already noted that it is important to take note of the tensor properties of quantities when non-orthogonal functions are involved. In particular, the gradient of the scalar functional with respect to the contravariant density-kernel is a covariant quantity which should not be directly added to the contravariant density-kernel, but should first be converted into contravariant form using the metric tensor $S^{\alpha\beta} = S^{-1}_{\alpha\beta}$. Thus the correct search direction for the density-kernel variation is $\Lambda^{\alpha\beta}$ given by

$$\begin{aligned}
\Lambda^{\alpha\beta} &= S^{\alpha i} \frac{\partial Q[\rho;\alpha]}{\partial K^{ji}} S^{j\beta} \\
&= 2S^{-1}_{\alpha i} \left[H + \alpha SKS(1-KS)(1-2KS)\right]_{ij} S^{-1}_{j\beta} \\
&= 2(S^{-1}HS^{-1})_{\alpha\beta} + 2\alpha \left[K(1-SK)(1-2SK)\right]_{\alpha\beta}. \qquad (7.68)
\end{aligned}$$

While the penalty functional derivative is simplified, the energy derivative picks up two factors of the inverse overlap matrix, which, as in the case of occupation number preconditioning, makes this difficult to implement. Neglecting this conversion of the covariant gradient to its contravariant form corresponds to approximating the overlap matrix by the identity. Thus the covariant gradient corresponds to taking the first term only in the series expansion of the overlap matrix inverse in equation 7.66. Again, neglect of this correction may lead to a deterioration in the efficiency of the minimisation procedure as the system-size increases.

We now consider the contravariant gradient of the functional with respect to the covariant support functions. This is a first-rank tensor quantity whereas the density-kernel gradient is a second-rank tensor. The correct covariant gradient is thus $\delta\phi_\alpha(\mathbf{r})$ given by

$$\begin{aligned}
\delta\phi_\alpha(\mathbf{r}) &= S_{\alpha\beta} \frac{\delta Q[\rho;\alpha]}{\delta\phi_\beta(\mathbf{r})} \\
&= 4S_{\alpha\beta} \left[K^{\beta\gamma}\hat{H} + \alpha[KSK(1-SK)(1-2SK)]^{\beta\gamma}\right] \phi_\gamma(\mathbf{r}) \\
&= 4(SK)_\alpha^{\ \beta} \left\{\hat{H}\delta_\beta^\gamma + \alpha \left[SK(1-SK)(1-2SK)\right]_\beta^{\ \gamma}\right\} \phi_\gamma(\mathbf{r}). \qquad (7.69)
\end{aligned}$$

The covariant preconditioned gradient in particular turns out to be

$$\delta\phi_\alpha(\mathbf{r}) = 4\left\{\hat{H}\delta_\alpha^\beta + \alpha \left[SK(1-SK)(1-2SK)\right]_\alpha^{\ \beta}\right\} \phi_\beta(\mathbf{r}) \qquad (7.70)$$

so that the factor of the inverse overlap matrix is now eliminated.

7.7 Practical details

In this section we outline a number of details concerning the implementation of the penalty method. These concern the derivatives of the functional with respect to the expansion coefficients for the support functions $\{c^{n\ell m}_{(\alpha)}\}$, the imposition of the normalisation constraint and the general outline of the scheme.

7.7.1 Expansion coefficient derivatives

The support functions are expanded in spherical-wave basis functions:

$$\phi_\alpha(\mathbf{r}) = \sum_{n\ell m} c^{n\ell m}_{(\alpha)} \; \chi_{\alpha,n\ell m}(\mathbf{r}). \tag{7.71}$$

For a functional of the support functions $f[\{\phi_\alpha\}]$, the derivative with respect to the expansion coefficients is

$$\begin{aligned} \frac{\partial f[\{\phi_\alpha\}]}{\partial c^{n\ell m}_{(\beta)}} &= \sum_\gamma \int \mathrm{d}\mathbf{r} \; \frac{\delta f[\{\phi_\alpha\}]}{\delta \phi_\gamma(\mathbf{r})} \frac{\partial \phi_\gamma(\mathbf{r})}{\partial c^{n\ell m}_{(\beta)}} \\ &= \sum_\gamma \int \mathrm{d}\mathbf{r} \; \frac{\delta f[\{\phi_\alpha\}]}{\delta \phi_\gamma(\mathbf{r})} \delta^\beta_\gamma \chi_{\gamma,n\ell m}(\mathbf{r}) \\ &= \int \mathrm{d}\mathbf{r} \; \frac{\delta f[\{\phi_\alpha\}]}{\delta \phi_\beta(\mathbf{r})} \chi_{\beta,n\ell m}(\mathbf{r}). \end{aligned} \tag{7.72}$$

For example, for the derivative of the total energy,

$$\frac{\delta E[\rho]}{\delta \phi_\alpha(\mathbf{r})} = 4K^{\alpha\beta} \hat{H} \phi_\beta(\mathbf{r}), \tag{7.73}$$

we obtain

$$\begin{aligned} \frac{\partial E[\rho]}{\partial c^{n\ell m}_{(\beta)}} &= 4K^{\beta\gamma} \int \mathrm{d}\mathbf{r} \; \chi_{\beta,n\ell m}(\mathbf{r}) \hat{H} \phi_\gamma(\mathbf{r}) \\ &= 4K^{\beta\gamma} \sum_{n'\ell'm'} \langle \chi_{\beta,n\ell m} | \hat{H} | \chi_{\gamma,n'\ell'm'} \rangle c^{n'\ell'm'}_{(\gamma)} \end{aligned} \tag{7.74}$$

in which $\langle \chi_{\beta,n\ell m} | \hat{H} | \chi_{\gamma,n'\ell'm'} \rangle = \mathcal{H}_{\beta,n\ell m;\gamma,n'\ell' m}$ denotes the matrix element of the Kohn-Sham Hamiltonian with respect to the spherical-wave basis functions.

7.7.2 Normalisation constraint

We choose to minimise the total functional whilst constraining the normalisation of the density-matrix to the correct value. This is achieved firstly by projecting all gradients to be perpendicular to the gradient of the electron number, thus maintaining the electron number to first order, and secondly by re-converging the electron number to its correct value before each evaluation of the total functional.

Density-kernel variation

In section 7.3 the electron number gradient with respect to the density-kernel, which is here denoted $\varDelta$, is given as

$$\frac{\partial N}{\partial K^{\alpha\beta}} = 2S_{\beta\alpha} = \varDelta_{\alpha\beta}. \tag{7.75}$$

The density-kernel along this search direction $\varDelta$ is parameterised by λ as

$$K(\lambda) = K(0) + \lambda\varDelta \tag{7.76}$$

where $K(0)$ denotes the initial density-matrix. The electron number, given by $N = 2\mathrm{Tr}(KS)$ thus behaves linearly:

$$\begin{aligned} N(\lambda) &= N(0) + 2\lambda\mathrm{Tr}(\varDelta S) \\ &= N(0) + 4\lambda\mathrm{Tr}(S^2) \end{aligned} \tag{7.77}$$

and it is a trivial matter to calculate the required value of λ to return the electron number to its correct value.

In general during the minimisation, the search direction is $\varLambda$, and again this search can be parameterised by a single parameter λ:

$$K(\lambda) = K(0) + \lambda\varLambda. \tag{7.78}$$

We wish to project out from $\varLambda$ that component which is parallel to $\varDelta$. The modified search direction $\tilde{\varLambda}$ can be written as

$$\tilde{\varLambda} = \varLambda - \omega\varDelta. \tag{7.79}$$

The variation of the electron number along this modified direction is

$$N(\lambda) = N(0) + 2\lambda\mathrm{Tr}(\varLambda S) - 2\omega\lambda\mathrm{Tr}(\varDelta S) \tag{7.80}$$

and we wish the coefficient of the linear term in λ to vanish, which defines the required value of ω to be

$$\omega = \frac{\mathrm{Tr}(\varLambda S)}{\mathrm{Tr}(\varDelta S)} = \frac{\mathrm{Tr}(\varLambda S)}{2\mathrm{Tr}(S^2)}. \tag{7.81}$$

Since the electron number depends linearly upon the density-kernel, after this projection, the electron number is constant along the modified search direction, and the electron number need not be corrected after a trial step is taken.

Support function variation

The electron number gradient with respect to the support functions is given in section 7.3 and denoted by $\{\zeta^\alpha(\mathbf{r})\}$:

$$\frac{\delta N}{\delta\phi_\alpha(\mathbf{r})} = 2K^{\alpha\beta}\phi_\beta(\mathbf{r}) = \zeta^\alpha(\mathbf{r}). \tag{7.82}$$

The support function variation is again parameterised by the parameter λ:

$$\phi_\alpha(\mathbf{r};\lambda) = \phi_\alpha(\mathbf{r};\lambda=0) + \lambda\zeta^\alpha(\mathbf{r}) \tag{7.83}$$

and this results in the following quadratic variation of the overlap matrix

$$\begin{aligned} S_{\alpha\beta}(\lambda) &= S_{\alpha\beta}(0) + \lambda\langle\phi_\alpha(\lambda=0)|\zeta^\beta\rangle + \lambda\langle\zeta^\alpha|\phi_\beta(\lambda=0)\rangle + \lambda^2\langle\zeta^\alpha|\zeta^\beta\rangle \\ &= S_{\alpha\beta}(0) + \lambda S'_{\alpha\beta} + \lambda^2 S''_{\alpha\beta} \end{aligned} \tag{7.84}$$

which defines the matrices S' and S''. The variation of the electron number is therefore also quadratic

$$N(\lambda) = N(0) + 2\lambda\mathrm{Tr}(KS') + 2\lambda^2\mathrm{Tr}(KS'') \tag{7.85}$$

and the roots of this expression can be found to correct the electron number.

We consider a general search direction for the localised functions denoted $\{\xi^\alpha(\mathbf{r})\}$ and modify this search direction to obtain the direction which maintains the electron number to first order:

$$\tilde{\xi}^\alpha(\mathbf{r}) = \xi^\alpha(\mathbf{r}) - \omega\zeta^\alpha(\mathbf{r}). \tag{7.86}$$

Now varying the localised functions according to

$$\phi_\alpha(\mathbf{r};\lambda) = \phi_\alpha(\mathbf{r};\lambda=0) + \lambda\tilde{\xi}^\alpha(\mathbf{r}) \tag{7.87}$$

results in the following variation of the electron number:

$$N(\lambda) = N(0) + 2\lambda\mathrm{Tr}(K\tilde{S}') - 2\lambda\omega\mathrm{Tr}(KS') + \mathcal{O}(\lambda^2) \tag{7.88}$$

where $\tilde{S}'_{\alpha\beta} = \langle\phi_\alpha(\lambda=0)|\xi^\beta\rangle + \lambda\langle\xi^\alpha|\phi_\beta(\lambda=0)\rangle$. Thus to maintain the electron number to first order, we choose

$$\omega = \frac{\mathrm{Tr}(K\tilde{S}')}{\mathrm{Tr}(KS')}. \tag{7.89}$$

In this case, the electron number is not constant along the search direction, but will still vary quadratically, so that it is necessary to correct the density-matrix before evaluating the total functional.

7.7.3 General outline of the scheme

The initialisation of the density-matrix is described in chapter 8. The functional minimisation consists of two nested loops. The inner loop consists of the minimisation with respect to the density-kernel, while keeping the support functions constant. As shown in section 7.4, this corresponds to making the density-matrix commute with the Hamiltonian in the representation of the current support functions. The outer loop consists of the support function minimisations, which in section 7.4 were shown to correspond to solving the Kohn-Sham equations. In general, we find that two or three cycles of the inner loop for each cycle of the outer loop suffice, and this is demonstrated in figure 7.1 in which three cycles of the inner loop appears to give the best performance to computational cost ratio.

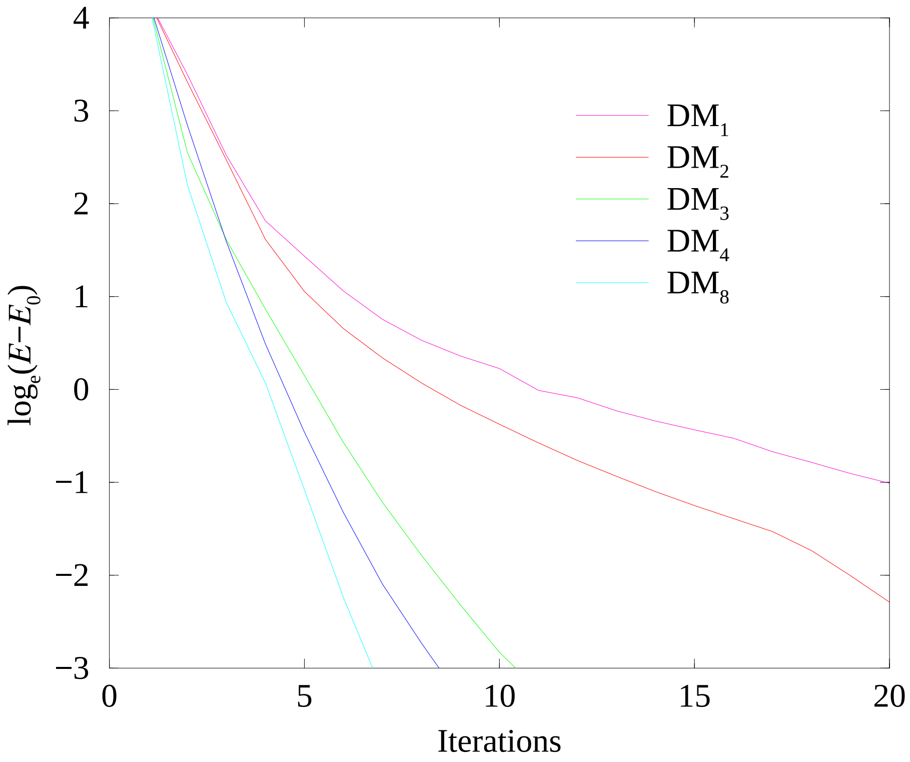

Figure 7.1: Rate of convergence for different numbers of inner cycles. In the legend, DM$_n$ corresponds to n cycles of the inner loop for each iteration of the outer loop (horizontal axis).

The conjugate gradients scheme is used to determine the search directions from the gradients, and these gradients are then projected perpendicular to the electron number gradient as described in section 7.7.2. We approximate the total functional by a parabola along the search direction, using the initial value of the functional, the first derivative of the functional at the initial position (which is simply the scalar product of the steepest descent and search directions) and the value of the functional at some trial position. The value of the functional at the predicted minimum is then evaluated. If this value deviates significantly from the value predicted by the quadratic fit, a cubic fit is constructed using this new value of the functional. In general, this is only necessary for the first few steps, and the parabolic fit is very good. In the case of the support function variation, the support functions are altered to give the correct number of electrons before each evaluation of the functional. The conjugate gradients procedure is reset after a finite number of steps, and this is illustrated in figure 7.2 for the inner and outer loops. In both cases, we see that there is little advantage in conjugating more than eight gradients before resetting.

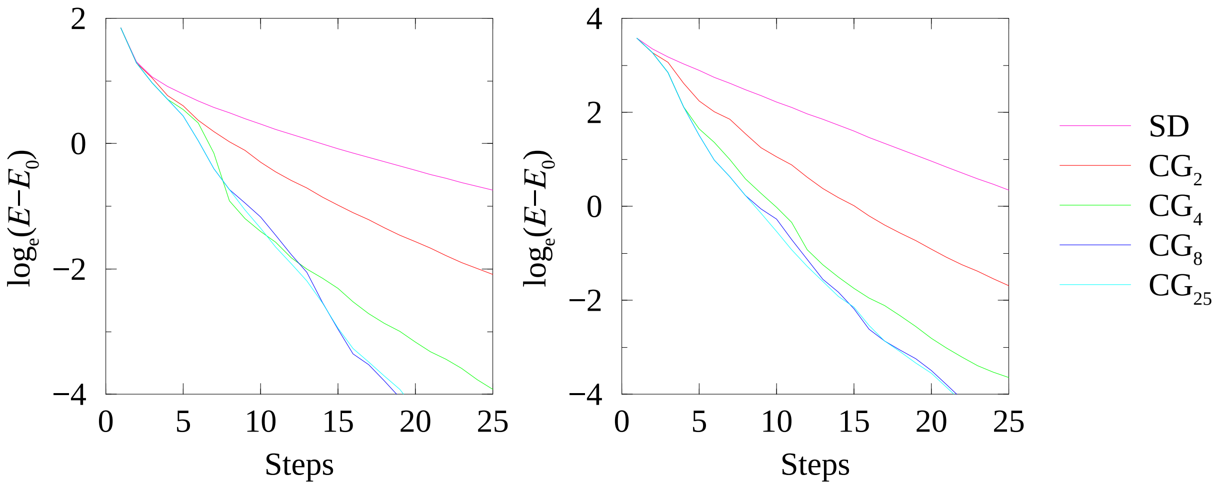

Figure 7.2: Performance of the conjugate gradients algorithm in the density-kernel variation (left) and the support function variation (right).

Once the functional has been minimised, the correction to the total energy is calculated. The whole calculation is generally repeated for a few different values of α to ensure that the corrected energy has indeed converged.

Chapter 8

Relating linear-scaling and plane-wave methods

For a number of reasons, it is useful to be able to convert the Kohn-Sham orbitals generated by traditional plane-wave codes into a set of support functions and a density-kernel which can be used as input in a linear-scaling code. One such reason is the need for careful density-matrix initialisation, discussed in section 8.3. For analysis it is also useful to be able to perform the reverse operation of extracting the Kohn-Sham orbitals and occupation numbers from the density-matrix. In this chapter we describe methods for performing both of these operations.

8.1 Wave-functions from density-matrices

In the linear-scaling method, we have a density-matrix represented in the form

$$\rho(\mathbf{r}, \mathbf{r}') = \phi_\alpha(\mathbf{r}) K^{\alpha\beta} \phi_\beta(\mathbf{r}'). \tag{8.1}$$

First we represent the localised support functions by linear combinations of plane-waves. For the analytic basis-set described in chapter 5 this is easily accomplished using equation 5.9 which gives the Fourier transform of the basis functions.

Having obtained an expansion for the support functions in a complete basis-set, it is now possible to orthogonalise the support functions by means of the Löwdin transformation to the set of orthonormal orbitals $\{\varphi_\alpha(\mathbf{r})\}$ given by

$$|\varphi_\alpha\rangle = |\phi_\beta\rangle S^{-\frac{1}{2}}_{\beta\alpha}. \tag{8.2}$$

Simultaneously transforming the matrix K into the matrix $\tilde{K}$ by

$$\tilde{K} = S^{\frac{1}{2}} K S^{\frac{1}{2}} \tag{8.3}$$

leaves the density-matrix invariant in the sense that

$$\rho(\mathbf{r},\mathbf{r}') = \phi_\alpha(\mathbf{r}) K^{\alpha\beta} \phi_\beta(\mathbf{r}') = \varphi_\alpha(\mathbf{r}) \tilde{K}_{\alpha\beta} \varphi_\beta(\mathbf{r}'). \tag{8.4}$$

To obtain the Kohn-Sham orbitals and occupation numbers it is necessary to diagonalise $\tilde{K}$. If this density-matrix is a ground-state density-matrix, then the density-operator and Hamiltonian commute so that they have the same diagonal representation, and therefore diagonalising $\tilde{K}$ is equivalent to diagonalising $\tilde{H} = S^{-\frac{1}{2}} H S^{-\frac{1}{2}}$. Thus the unitary transformation U which yields the occupation numbers $f_i = (U^\dagger \tilde{K} U)_{ii}$ (no summation convention) also yields the Kohn-Sham orbitals $|\psi_i\rangle = |\varphi_\alpha\rangle U_{\alpha i}$. This information can then be used in a traditional plane-wave code, and this is the method which was used to check the analytic results for the kinetic energy and non-local pseudopotential energy in chapter 5. The spatial cut-off of the support regions in real-space leads to algebraically-decaying oscillatory behaviour for large wave-vectors in reciprocal-space, so that a single basis function needs a high plane-wave energy cut-off to accurately describe this truncation. However, for support functions which decay smoothly to zero at the edge of the support region, the decay will be much faster, and the plane-wave cut-off comparable to the cut-off for the basis functions themselves.

8.2 Density-matrices from Kohn-Sham orbitals

This method is based upon work on the projection of plane-wave calculations onto atomic orbitals [166], which has been used to analyse atomic basis-sets [167] and obtain local atomic properties from the extended Kohn-Sham orbitals [168]. Here we review the method, for the special case of a Γ-point Brillouin zone sampling.

8.2.1 Projecting plane-wave eigenstates onto support functions

The plane-wave eigenstates are denoted $|\psi_i\rangle$ and the support functions are denoted $|\phi_\alpha\rangle$. The states obtained by projecting the plane-wave eigenstates onto the space spanned by the support functions are denoted $|\xi_\alpha\rangle$. As in section 4.6 we also introduce the dual states $|\phi^\alpha\rangle$ and $|\xi^\alpha\rangle$ with the properties outlined below.

$$S_{\alpha\beta} = \langle \phi_\alpha | \phi_\beta \rangle \qquad\qquad \Sigma_{\alpha\beta} = \langle \xi_\alpha | \xi_\beta \rangle \tag{8.5}$$

$$|\phi^\alpha\rangle = |\phi_\beta\rangle S^{-1}_{\beta\alpha} \qquad |\xi^\alpha\rangle = |\xi_\beta\rangle \Sigma^{-1}_{\beta\alpha} \tag{8.6}$$

$$\langle\phi^\alpha|\phi_\beta\rangle = \langle\phi_\alpha|\phi^\beta\rangle = \delta^\beta_\alpha \qquad \langle\xi^\alpha|\xi_\beta\rangle = \langle\xi_\alpha|\xi^\beta\rangle = \delta^\beta_\alpha \tag{8.7}$$

The projection operator onto the subspace spanned by the support functions is defined by

$$\hat{P} = |\phi_\alpha\rangle\langle\phi^\alpha| = |\phi_\alpha\rangle S^{-1}_{\alpha\beta}\langle\phi_\beta|. \tag{8.8}$$

A *spilling parameter* $\mathcal{S}$ can be defined to measure how much the subspace spanned by the plane-wave eigenstates falls outside the subspace spanned by the support functions. Minimising this quantity is one method of optimising the choice of support functions, and is described for the case of the spherical-wave basis (chapter 5) in section 8.2.3.

$$\mathcal{S} = \frac{1}{N_\mathrm{b}}\langle\psi_i|(1-\hat{P})|\psi_i\rangle \tag{8.9}$$

where N_b is the number of bands (labelled i) considered. The density-operator is then defined by

$$\hat{\rho} = \sum_\alpha^{\mathrm{occ}} |\xi_\alpha\rangle\langle\xi^\alpha| \tag{8.10}$$

where the sum is taken over occupied bands only. Substitution of the results given above then yields the following expression for the density-kernel:

$$K^{\alpha\beta} = \langle\phi^\alpha|\hat{\rho}|\phi^\beta\rangle = \sum_{ij}^{\mathrm{occ}} S^{-1}_{\alpha\lambda}\langle\phi_\lambda|\psi_i\rangle\Sigma^{-1}_{ij}\langle\psi_j|\phi_\mu\rangle S^{-1}_{\mu\beta}. \tag{8.11}$$

Defining the rectangular matrix L as

$$L_{\lambda i} = \langle\phi_\lambda|\psi_i\rangle \tag{8.12}$$

we give an expression for the matrix Σ in terms of L and S:

$$\Sigma_{\alpha\beta} = \langle\xi_\alpha|\xi_\beta\rangle = \langle\psi_\alpha|\phi_\kappa\rangle S^{-1}_{\kappa\lambda}\langle\phi_\lambda|\phi_\mu\rangle S^{-1}_{\mu\nu}\langle\phi_\nu|\psi_\beta\rangle = L^\dagger_{\alpha\kappa}S^{-1}_{\kappa\lambda}S_{\lambda\mu}S^{-1}_{\mu\nu}S_{\nu\beta} = (L^\dagger S^{-1} L)_{\alpha\beta}. \tag{8.13}$$

We can thus minimise the spilling parameter $\mathcal{S}$ to optimise our choice of support functions, and then calculate K to obtain all of the information required to start a linear-scaling calculation.

8.2.2 Obtaining auxiliary matrices

In the case when the density-kernel K is expanded in terms of an auxiliary matrix T e.g. in order to construct a positive semi-definite density-matrix, it is necessary to be able to calculate the auxiliary matrix T which corresponds to a given density-kernel K by

$$K = TT^{\dagger}. \tag{8.14}$$

This can be achieved by minimising the function $\mathcal{I}(T)$ given by

$$\mathcal{I}(T) = \mathrm{Tr}\left[(K - TT^{\dagger})^2\right] \tag{8.15}$$

whose derivative with respect to T is

$$\frac{\partial \mathcal{I}(T)}{\partial T^{\alpha\beta}} = -4\left[T^{\dagger}(K - TT^{\dagger})\right]_{\beta\alpha}. \tag{8.16}$$

This derivative vanishes at the minimum, and so we find that the matrix T which minimises $\mathcal{I}(T)$ is the desired auxiliary matrix (the solution $T = 0$ corresponds to a local maximum). We therefore choose to minimise $\mathcal{I}(T)$ by the conjugate gradients method to obtain the auxiliary matrix.

8.2.3 Optimising the support functions

As mentioned above, we can optimise our choice of support functions by minimising the spilling parameter $\mathcal{S}$. We describe this process here when the support functions are themselves described in terms of a localised basis:

$$|\phi_\alpha\rangle = \sum_{n\ell m} c^{n\ell m}_{(\alpha)} |\chi_{\alpha,n\ell m}\rangle. \tag{8.17}$$

The spilling parameter can be written in terms of the matrices L and S by:

$$\begin{aligned} \mathcal{S} &= \frac{1}{N_{\mathrm{b}}}\langle\psi_i|(1-\hat{P})|\psi_i\rangle = 1 - \frac{1}{N_{\mathrm{b}}}\langle\psi_i|\phi_\alpha\rangle\langle\phi^\alpha|\psi_i\rangle \\ &= 1 - \frac{1}{N_{\mathrm{b}}} L^{\dagger}_{i\alpha} S^{-1}_{\alpha\beta} L_{\beta i} = 1 - \frac{1}{N_{\mathrm{b}}}\mathrm{Tr}[L^{\dagger} S^{-1} L] \end{aligned} \tag{8.18}$$

and we wish to obtain the gradients of $\mathcal{S}$ with respect to the expansion coefficients $\{c^{n\ell m}_{(\alpha)}\}$.

$$\frac{\partial \mathcal{S}}{\partial c^{n\ell m}_{(\alpha)}} = -\frac{1}{N_{\mathrm{b}}}\left[\frac{\partial L^{\dagger}_{ij}}{\partial c^{n\ell m}_{(\alpha)}} S^{-1}_{jk} L_{ki} + L^{\dagger}_{ij}\frac{\partial S^{-1}_{jk}}{\partial c^{n\ell m}_{(\alpha)}} L_{ki} + L^{\dagger}_{ij} S^{-1}_{jk}\frac{\partial L_{ki}}{\partial c^{n\ell m}_{(\alpha)}}\right]. \tag{8.19}$$

We obtain the derivative of the inverse matrix by differentiating $S^{-1}S = 1$ i.e.

$$\frac{\partial (S^{-1}S)_{\alpha\beta}}{\partial x} = \frac{\partial S^{-1}_{\alpha\gamma}}{\partial x} S_{\gamma\beta} + S^{-1}_{\alpha\gamma} \frac{\partial S_{\gamma\beta}}{\partial x} = 0 \tag{8.20}$$

which can be rearranged to give

$$\frac{\partial S^{-1}_{\alpha\beta}}{\partial x} = -S^{-1}_{\alpha\gamma} \frac{\partial S_{\gamma\delta}}{\partial x} S^{-1}_{\delta\beta}. \tag{8.21}$$

Therefore (no summation over α)

$$\begin{aligned}
\frac{\partial \mathcal{S}}{\partial c^{n\ell m}_{(\alpha)}} &= -\frac{1}{N_{\mathrm{b}}} \Big[\langle \psi_i | \chi_{\alpha,n\ell m} \rangle S^{-1}_{\alpha k} L_{ki} - L^{\dagger}_{ij} S^{-1}_{j\beta} \left(\delta_{\beta\alpha} \langle \chi_{\alpha,n\ell m} | \phi_\gamma \rangle + \langle \phi_\beta | \chi_{\alpha,n\ell m} \rangle \delta_{\beta\gamma} \right) S^{-1}_{\gamma k} L_{ki} \\
&\qquad + L^{\dagger}_{ij} S^{-1}_{j\alpha} \langle \chi_{\alpha,n\ell m} | \psi_i \rangle \Big] \\
&= -\frac{2}{N_{\mathrm{b}}} \mathrm{Re} \left[L^{\dagger}_{\alpha\beta} S^{-1}_{\beta\gamma} \langle \chi_{\gamma,n\ell m} | \phi_\delta \rangle S^{-1}_{\delta\epsilon} L_{\epsilon\alpha} - \langle \psi_\alpha | \chi_{\beta,n\ell m} \rangle S^{-1}_{\beta\gamma} L_{\gamma\alpha} \right].
\end{aligned} \tag{8.22}$$

In the case of the set of basis functions introduced in chapter 5, the overlap between plane-wave eigenstates and localised basis functions, e.g. $\langle \psi_\alpha | \chi_{\beta,n\ell m} \rangle$, can be calculated using the expression for the basis function Fourier transform (5.9).

We can use these gradients to minimise the spilling parameter (by the conjugate gradients method) to obtain the set of optimal coefficients $\{c^{n\ell m}_{(\alpha)}\}$ which define the set of support functions which best span the space of the occupied plane-wave orbitals. The final minimum spilling parameter value also gives an estimate of the quality of the basis-set being used.

8.3 Density-matrix initialisation

Finally we discuss the subject of constructing an initial density-matrix for our calculations, which is related to the other work in this chapter. Although any linear-scaling method will obviously be more efficient than a traditional method for a sufficiently large system, the *cross-over* (i.e. the system-size at which the linear-scaling method beats the traditional method) may be very large. If it is larger than the largest system which can currently be simulated by traditional methods, then there is obviously little practical use for such a method. The methods described in this dissertation are not that inefficient, but neither is the cross-over sufficiently small that some advantage cannot be obtained by using some physical insight to assist the calculation e.g. by imposing appropriate symmetries (although we must take care not to impose symmetries which subsequently prevent the method from reaching the ground-state).

For example, consider a vacancy in an otherwise perfect crystal. Running a traditional calculation on the bulk crystal would allow us, using the methods in section 8.2, to obtain the density-matrix elements for the bulk crystal which could be used to initialise the density-matrix for a simulation of the large system with the vacancy. This would avoid wasting computational effort converging the density-matrix from a random position when the general form can be guessed from the bulk case.

A second example is that of a molecule interacting with a solid surface. In this case, the density-matrix for molecule and surface could be converged separately to obtain an estimate for the complete system. Obviously this method will be more successful the more weakly bound the molecule is to the surface.

The transferability of localised orbitals between closely-related systems has been studied in hydrocarbon chains [169] and methods have also been developed to calculate generalised Wannier functions [170, 171] which may also be transferred between systems [172].

One important consideration is that of local charge neutrality, often used as an approximation to self-consistency in non-self-consistent tight-binding calculations [173]. Because the density-matrix is truncated in real-space, long-wavelength fluctuations in the electronic density are suppressed. This has the advantage that it prevents "charge-sloshing" instabilities, so problematic in early traditional plane-wave methods on large systems. However, if the system is not initially charge neutral locally, it takes a very large number of iterations to transfer charge across the system, and this results in very poor convergence. We thus need to at least consider initialising our density-matrix to correspond to isolated atoms brought together, which are then allowed to interact and form bonds etc. This is simply achieved using the projection method described here and leads to a great improvement in performance.

Chapter 9

Results and discussion

In this chapter we present results obtained using the penalty functional method applied to bulk crystalline silicon. We show how the energy converges as the two spatial cut-offs; the support region radius and density-kernel cut-off, are increased and in particular that the estimate of the energy is variational with respect to these parameters. We also consider the difference in convergence of absolute energies and energy differences by calculating the energy-volume curve and comparing with the results obtained from the CASTEP plane-wave code [82] and from experiment. Finally we consider the scaling of the method with system-size (confirming that it is indeed linear) and the scaling with support region radius and density-kernel cut-off.

9.1 Bulk crystalline silicon

Calculations were performed for a cubic simulation cell containing 216 silicon atoms and using pseudopotentials generated according to the method of Troullier and Martins [74]. The kinetic energy cut-off for the basis-set was set at 200 eV and the FFT grid contained $72 \times 72 \times 72$ points. The basis-set contained spherical-waves with angular momentum components up to $\ell = 2$, and the support regions were chosen to be centred on the bonds, with one support function per region, so that no unoccupied bands were included in this calculation. The Brillouin zone was sampled using only the Γ-point. A value of 100 eV was used for the penalty functional prefactor α.

9.1.1 Convergence with density-matrix cut-off

In figure 9.1 we plot the total energy per atom against the support region radius r_{reg} for a density-kernel cut-off r_K of 4.0 Å. In figure 9.2 we plot the total energy per atom against the density-kernel cut-off r_K for a support region radius r_{reg} of 3.1 Å. In both cases, the

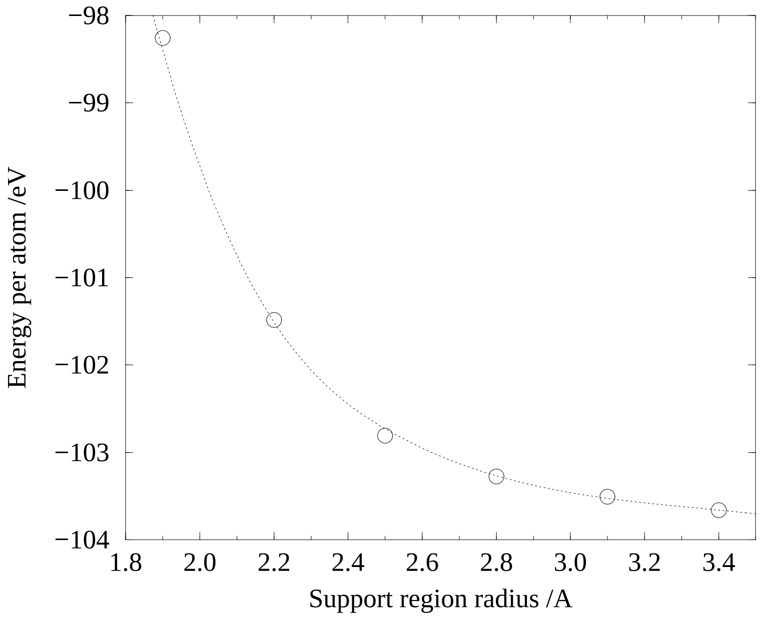

Figure 9.1: Convergence of total energy with respect to support region radius.

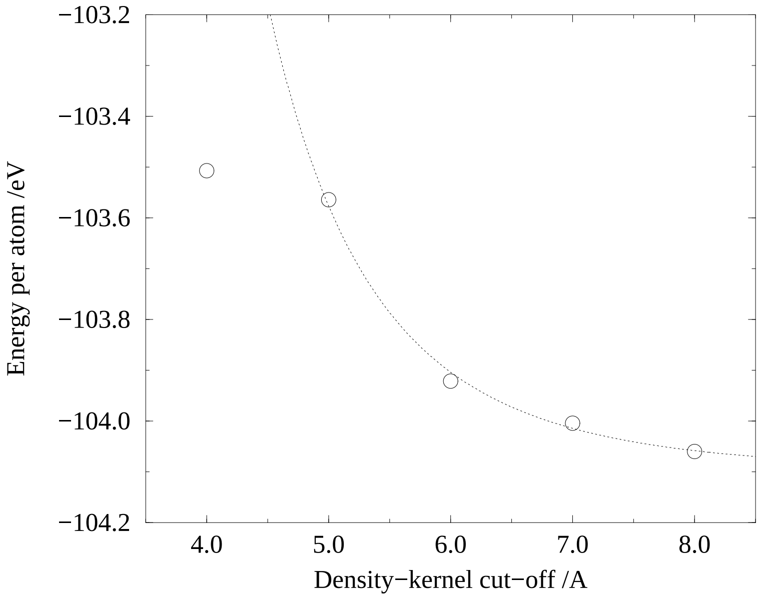

Figure 9.2: Convergence of total energy with respect to density-kernel cut-off.

energy converges to its limiting value from above, as expected, since the total energy is variational with respect to the density-matrix cut-off.

These results agree roughly with the calculations of Hernández *et al.* [127]. In their case, they used atom-centred support regions and included as many unoccupied bands as occupied bands, so that the convergence with respect to density-matrix cut-off should be more rapid in their case. They also used a local pseudopotential, which reduces the range of the Hamiltonian. Our calculations suggest a combined density-matrix cut-off of the order of 7.0 Å to obtain the same accuracy as they obtained with a cut-off of about 6.0 Å. We note that the band gap of silicon is relatively small (particularly within the LDA) so that the density-matrix decay is therefore slow. This makes silicon a difficult test case, and we can be confident that if we obtain reasonable results in this system, we shall be successful in others.

9.1.2 Electronic density

Since the minimising density-matrix is only approximately idempotent, the electronic density derived from it is not the exact ground-state density. However, in figure 9.3 we plot the electronic density in the (110) plane (containing the atoms highlighted in silver in figure 9.4) obtained from the minimising density-matrix with $r_{\text{reg}} = 3.1$ Å and $r_K = 6.0$ Å, and observe that it is still *qualitatively* correct. Since electronic densities are used primarily for visualisation purposes, rather than for quantitative analysis, the information most commonly required can still be obtained from the minimising density-matrix.

In figure 9.5 we plot the electronic density obtained using the CASTEP plane-wave code using the same pseudopotential and energy cut-off, and equivalent Brillouin zone sampling (a $3 \times 3 \times 3$ Monkhorst-Pack mesh for an 8-atom unit cell). We observe that there is less density concentrated in the bonds for the CASTEP density compared with the linear-scaling density, and this is to be expected since in the linear-scaling calculation, the lowest energy (i.e. most bonding) orbital is over-occupied and the highest energy (i.e. least bonding) orbital is under-occupied. In figure 9.6 we plot the difference obtained by subtracting the CASTEP density from the linear-scaling density and confirm this observation.

9.1.3 Predictions of physical properties

The converged value of the total energy agrees with the CASTEP value (again with equivalent energy cut-off, Brillouin zone sampling and pseudopotential) only within 3%. However, if energy differences are caused by density-matrix variations which are short-ranged, then they will be much better converged than absolute energies. In figure 9.7 we plot the total energy against volume V. For a lattice parameter $a = 5.430$ Å, which was used for the

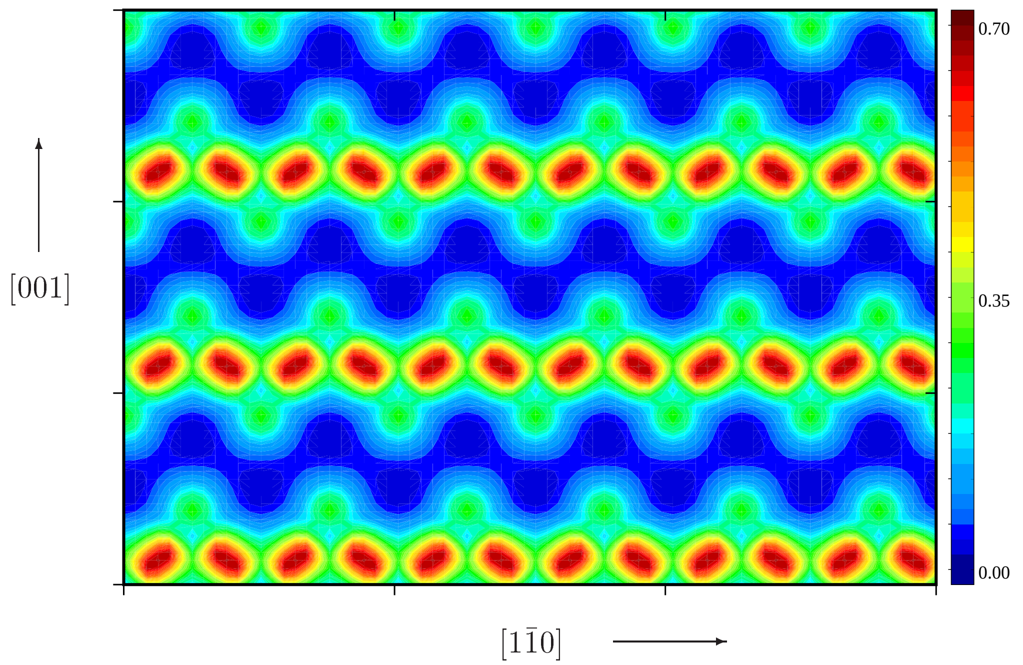

Figure 9.3: Electronic density of silicon in the (110) plane (units Å^{-3}).

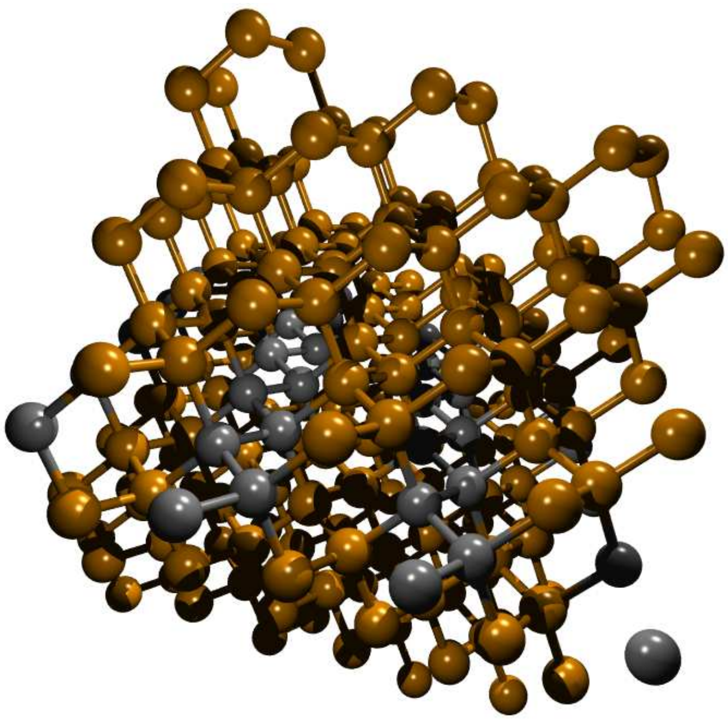

Figure 9.4: Diamond structure of silicon, highlighting a {110} plane.

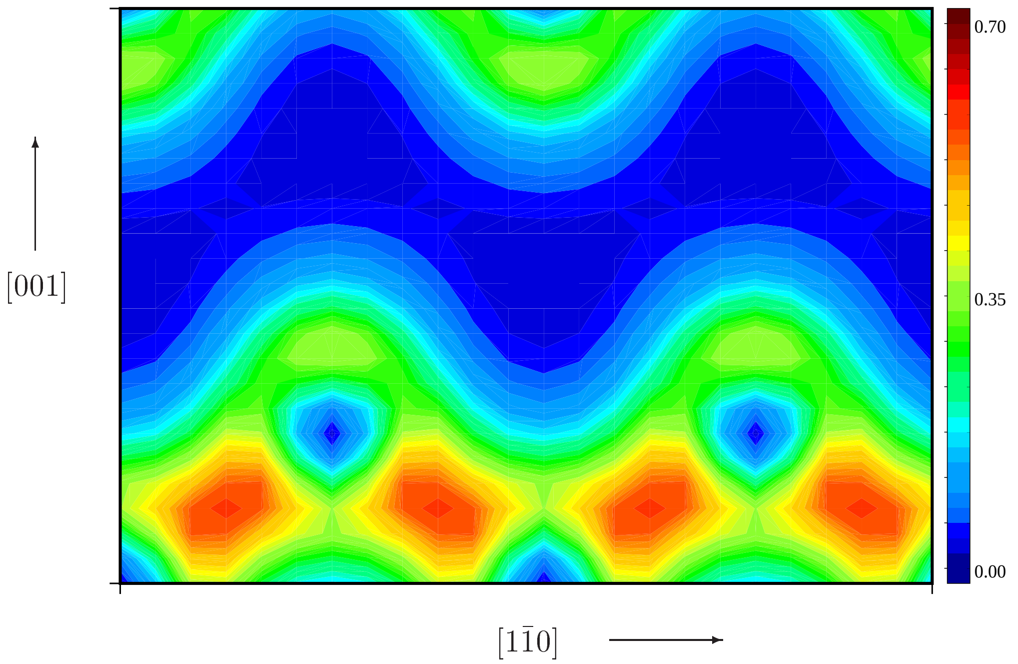

Figure 9.5: Electronic density of silicon in the (110) plane calculated by the CASTEP code (units Å^{-3}).

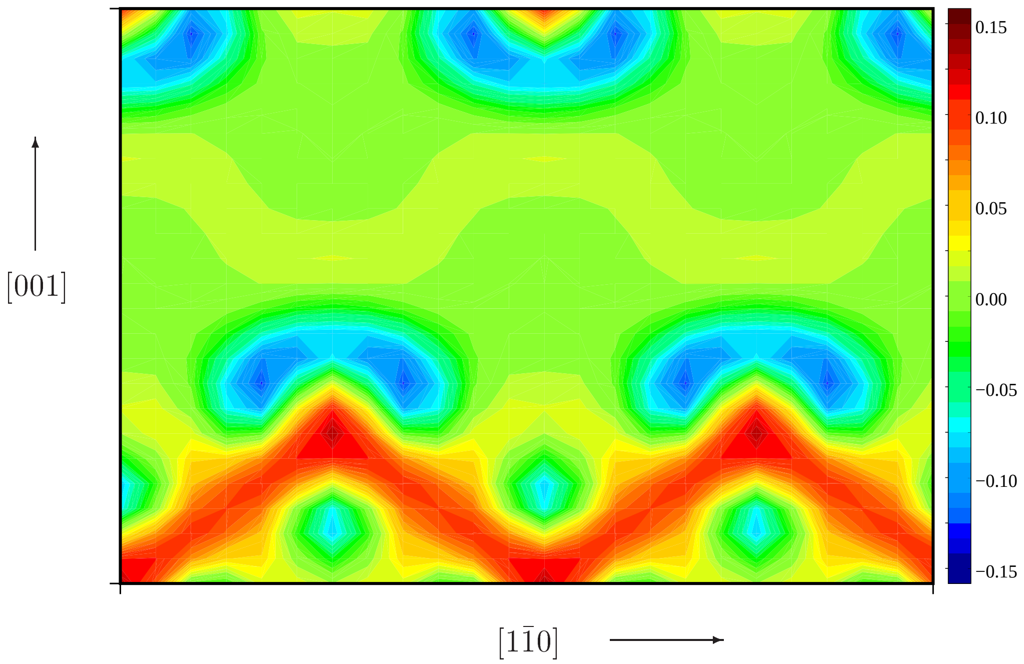

Figure 9.6: Difference between electronic densities of silicon calculated by the linear-scaling method and CASTEP (units Å^{-3}).

calculations in section 9.1.1, we used values of $r_{\rm reg} = 3.10$ Å, $r_K = 6.00$ Å and an energy cut-off of 200 eV. As the volume V was changed, the support region radius $r_{\rm reg}$, density-kernel cut-off r_K and energy cut-off $E_{\rm cut}$ were changed proportionally. The parameters used are listed in table 9.1.

a / Å	V / Å^3	$r_{\rm reg}$ / Å	r_K / Å	$E_{\rm cut}$ / eV
5.31	149.72	3.03	5.87	209
5.35	153.13	3.05	5.91	206
5.39	156.59	3.08	5.96	203
5.43	160.10	3.10	6.00	200
5.47	163.67	3.12	6.04	197
5.51	167.28	3.15	6.09	194

Table 9.1: Parameters used to calculate energy-volume curve.

Fitting the data to the Birch-Murnaghan equation of state allows values for the equilibrium volume V and bulk modulus B to be calculated, which are compared with the results obtained from a CASTEP calculation using the same pseudopotential and to experiment [174] in table 9.2. Generally we expect to obtain lattice parameters to within 2% and bulk moduli to within 10%. The bulk modulus is very sensitive to the data, so that whereas the prediction of the lattice parameter is in excellent agreement with both the CASTEP and experimental values, the value of the bulk modulus predicted by the linear-scaling method is about 8% too large. These results indicate that the linear-scaling calculation is not quite fully converged with the set of parameters used, but are very encouraging overall.

Calculation	Linear-scaling	CASTEP	Experiment
a / Å	5.423	5.390	5.430
V / Å^3	159.47	156.56	160.10
B / GPa	108.8	101.7	100.0

Table 9.2: Comparison of calculated and experimental data for silicon.

9.2 Scaling

In this section we consider the scaling of the method, firstly with respect to the system-size, and secondly with respect to the localisation region radius $r_{\rm reg}$ and the density-kernel cut-off r_K.

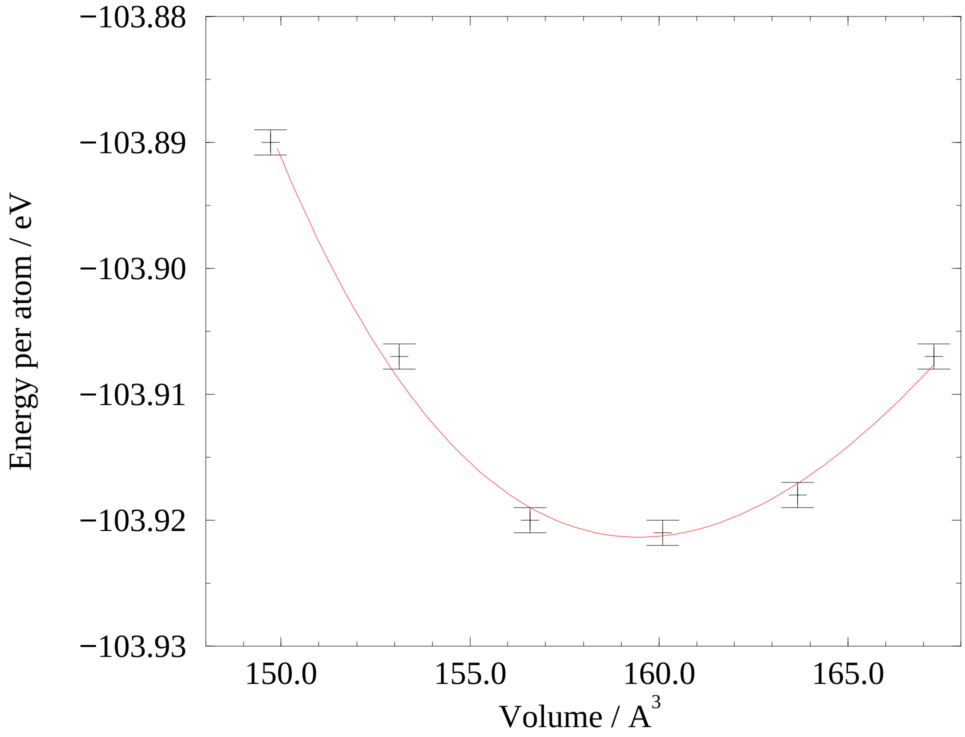

Figure 9.7: Energy-volume curve for silicon. The line is the best fit to the Birch-Murnaghan equation of state.

9.2.1 System-size scaling

As mentioned in chapter 7, there are several steps in the calculation which are not strictly $\mathcal{O}(N)$, such as the calculation of the structure factor, the calculation of the ion-ion interaction energy (by Ewald's method [175–178]) and possibly the calculation of the energy correction. All of these operations need only be performed once for each ionic configuration, and so do not contribute significantly to the total computational effort. However, there are a number of FFTs within the method which require an effort which scales as $\mathcal{O}(N \log_m N)$. To verify that these operations do not spoil the linear-scaling of the rest of the method, we plot the CPU time required per iteration in figure 9.8 and see that it is indeed linear with respect to system-size as required.

9.2.2 Scaling with density-matrix cut-off

We now consider the scaling with respect to the density-matrix cut-off r_{cut} which in practice is defined by two parameters; the support region radius r_{reg} and the density-kernel cut-off

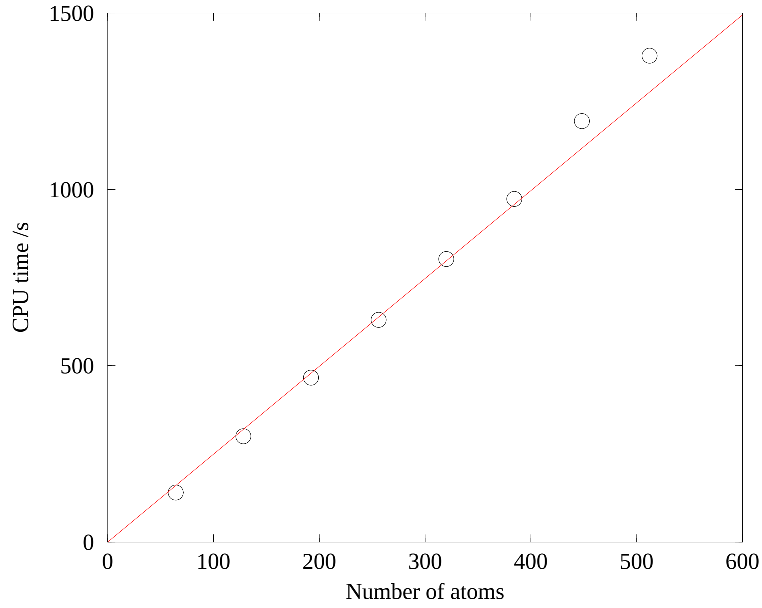

Figure 9.8: Variation of computational effort with system-size.

r_K. Two spherical support regions will overlap if the sum of their radii exceeds the distance between their centres. We assume that all support regions have the same radius r_{reg}, and thus the number of support regions which overlap a particular region equals the number of region centres lying within a sphere of radius $2r_{\mathrm{reg}}$. For bulk solids this number will be proportional to the volume of the sphere i.e. proportional to r_{reg}^3. Table 9.3 allows the precise number of overlaps to be determined for the case of atom-centred support regions in several common crystal structures. In the sparse overlap matrix, the number of non-zero elements in each row or column is therefore also proportional to r_{reg}^3. For sparse matrix multiplication, the computational effort scales quadratically with the number of non-zero elements per row (and linearly with the rank) so that we expect the method to scale with the sixth power of the support region radius i.e. $t_{\mathrm{comp}} \propto r_{\mathrm{reg}}^6$. This is often referred to as quadratic scaling with respect to the support region size (i.e. volume).

The argument follows in precisely the same manner for the density-kernel cut-off, replacing $2r_{\mathrm{reg}}$ by r_K. In general, as observed in section 9.1.1, $r_K \approx 2r_{\mathrm{reg}}$ when the energy is converged with respect to both parameters, so that the overlap matrix and density-kernel will generally share similar sparse structure. In bulk crystals, we thus expect the computational effort to scale with the sixth power of the density-matrix cut-off r_{cut} i.e. $t_{\mathrm{comp}} \propto r_{\mathrm{cut}}^6$.

In certain systems, however, this scaling may be different. For example, in long linear molecules e.g. hydrocarbon chains, which have an essentially one-dimensional structure, each support region will overlap a number of others which scales only linearly with the radius. In this case $t_{\mathrm{comp}} \propto r_{\mathrm{cut}}^2$, and this suggests that these linear-scaling methods may be more suited to studying molecular rather than crystalline systems.

Shell	# atoms	Radius $/a$	Diamond	FCC	BCC	Simple
1	4	0.43301	•			
2	12	0.70711	•	•		
3	8	0.86603			•	
4	12	0.82916	•			
5	6	1.00000	•	•	•	•
6	12	1.08972	•			
7	24	1.22474	•	•		
8	16	1.29904	•			
9	12	1.41421	•	•	•	•
10	24	1.47902	•			
11	24	1.58114	•	•		
12	12	1.63936	•			
13	24	1.65831			•	
14	8	1.73205	•	•	•	•
15	24	1.78536	•			
16	48	1.87083	•	•		
17	36	1.92029	•			
18	6	2.00000	•	•	•	•
19	12	2.04634	•			
20	36	2.12132	•	•		
21	28	2.16506	•			
22	24	2.17945			•	
23	24	2.23607	•	•	•	•
24	36	2.27761	•			
25	24	2.34521	•	•		
26	24	2.38485	•			
27	24	2.44949	•	•	•	•
28	36	2.48747	•			
29	72	2.54951	•	•		
30	36	2.58602	•			
31	32	2.59808			•	
32	24	2.68095	•	•		
33	48	2.73861	•			
34	24	2.77263	•	•		

Table 9.3: Table showing the number of atoms lying within support regions of varying radii centred on atoms for some common cubic crystal structures.

Chapter 10

Conclusions

10.1 Summary

In this dissertation I have attempted to explain the motivation for performing computational quantum-mechanical simulations and to describe the major difficulties encountered when one attempts to do so. The progress made so far by the introduction of density-functional theory, incorporating a local density approximation for exchange and correlation and the use of pseudopotentials already allows these calculations to be performed on systems which are of interest to scientists working in a variety of fields today. However, the scope of these calculations is limited by the unfavourable scaling of computational effort and resources required. Methods which exhibit optimal scaling, that is scale in the same way as the complexity of the problem to be solved, offer the prospect of extending the range of accessible scales much further, and will also take full advantage of future improvements in computer technology.

The work in this dissertation is based upon the density-matrix formulation of density-functional theory, which avoids the necessity of dealing directly with the extended wave-functions (which resulted in the unfavourable cubic scaling) and leads naturally to a linear-scaling method.

The spherical-wave basis-set proposed in chapter 5 provides a solution to the problem of representing the density-matrix in real-space while maintaining the accuracy of the kinetic energy (which is naturally calculated in reciprocal-space) and also efficiently calculating the action of the non-local pseudopotential. The analytic results derived have been implemented within the scheme described in chapters 6 and 7.

Secondly, methods to impose the non-linear idempotency constraint by the use of penalty functionals have been described. The failure of the original proposals by Kohn in computational implementations are shown to be due to the functional form of the penalty functional which must be chosen to obtain a variational principle. An original scheme has been proposed in which penalty functionals are chosen to be compatible with efficient minimisation algorithms and to approximately impose the idempotency constraint. The resulting errors in the total energy are corrected by considering the functional form of the penalty functional, so that accurate estimates of the true ground-state energy can be made.

Thirdly the relationship between traditional plane-wave methods based upon the Kohn-Sham wave-functions and density-matrix based schemes are discussed. We show how it is possible to interchange information about the electronic structure of the system between these two methods, and in particular apply this to the problem of obtaining initial density-matrices for use in linear-scaling calculations.

The results in chapters 5 and 6 have all been implemented in a total energy code, which has been tested on bulk crystalline silicon. The convergence of the energy with respect to support region radius and density-kernel cut-off has been examined. Predictions of some physical properties of bulk silicon are then compared with experimental values and results from the $\mathcal{O}(N^3)$ CASTEP plane-wave code. Finally, the scaling of the method with system-size is confirmed to be linear, and the scaling with respect to support region radius and density-kernel cut-off discussed.

10.2 Further work

Starting from the underlying quantum-mechanical theory, in this dissertation an original scheme to perform linear-scaling total energy calculations based upon the density-matrix and using a new basis-set has been outlined and its computational implementation discussed. The results obtained are very promising, but there is still much work to be done in developing and optimising the scheme e.g. the occupation number preconditioning outlined in section 7.5. One of the most computationally expensive steps is currently the evaluation of the electronic density on the real-space grid. By choosing to minimise the non-interacting Kohn-Sham energy non-self-consistently rather than the interacting energy self-consistently the number of times this evaluation has to be performed can be greatly reduced. Self-consistency can then be obtained by density mixing [179,180] . The problem of "charge-sloshing" which can arise in this case in traditional methods appears not to be present when localised functions are used, and can anyway be eliminated [83, 181].

Once an efficient electronic minimisation scheme is in place, the next step is to calculate ionic forces in order to perform ionic relaxation or even molecular dynamics. First it is worth noting that there are of $\mathcal{O}(N)$ ions in the system, and the computational effort to calculate the force on each (from the local pseudopotential) is also of $\mathcal{O}(N)$ so that a computational effort of $\mathcal{O}(N^2)$ is necessary to calculate all the forces. Secondly, the typical time-scale of molecular dynamics required by a system of volume V is $\tau \propto V^{\frac{2}{3}}$ so that this introduces an extra factor of $\mathcal{O}(N^{\frac{2}{3}})$ in the computational effort. The Hellmann-Feynman forces [182, 183] resulting from the derivative of the Hamiltonian with respect to the ionic positions have a contribution from the local pseudopotential (which is calculated using the reciprocal-space grid) and the non-local pseudopotential (which is calculated by taking analytic derivatives of the results for the non-local pseudopotential matrix elements). These forces have in fact been calculated and tested using the spherical-wave basis-set. However, because the support regions move with the ions, other contributions known as Pulay forces [184] arise which must be calculated. Since the correction to the energy derived from the penalty functional can be expressed analytically, it should be possible to calculate accurate forces which are consistent with the corrected energy.

Given the expected improvement in efficiency of the method when applied to molecular rather than crystalline systems (section 9.2.2), serious consideration should be given to converting the code to perform calculations on clusters, rather than using the supercell approximation. This would have the added advantage of eliminating the $\mathcal{O}(N^2)$ step to calculate the structure factor and the calculation of the ion-ion interaction energy (although still an $\mathcal{O}(N^2)$ step) would also become much cheaper.

In the long term it is essential that advantage be taken of the natural way in which linear-scaling methods based in real-space can be separated into simultaneous calculation of interacting fragments. This property means that the problem lends itself to implementation on massively parallel computers [185]. Even with the serial code on a single workstation it has been possible to model 512 silicon atoms, and there exist parallel computers consisting of a few hundred nodes each with the same power, so that in principle calculations of 100000 atoms are feasible. The development of schemes which will exploit the advantages of parallel processing is therefore essential to reap the full benefit of linear-scaling methods.

Appendix A

Bessel function identities

In this appendix we list some standard results used in the analysis of chapter 5 [186].

$$j_{\ell+1}(x) = \frac{\ell}{x} j_\ell(x) - j'_\ell(x) \tag{A.1}$$

$$j_{\ell-1}(x) = \frac{\ell+1}{x} j_\ell(x) + j'_\ell(x) \tag{A.2}$$

$$\exp[\mathrm{i}\mathbf{k}\cdot\mathbf{r}] = 4\pi \sum_{\ell=0}^{\infty} \sum_{m=-\ell}^{\ell} \mathrm{i}^\ell \; j_\ell(kr) \; \bar{Y}_{\ell m}(\Omega_\mathbf{k}) \; \bar{Y}_{\ell m}(\Omega_\mathbf{r}) \tag{A.3}$$

$$\begin{aligned} &\int_a^b j_\ell(mx) j_\ell(nx) x^2 \mathrm{d}x \\ &\quad = \frac{1}{m^2 - n^2} \left[x^2 \left\{ n j_\ell(mx) j_{\ell-1}(nx) - m j_{\ell-1}(mx) j_\ell(nx) \right\} \right]_a^b \end{aligned} \tag{A.4}$$

$$\begin{aligned} &\int_a^b j_\ell^2(mx) x^2 \mathrm{d}x = \tfrac{1}{2} \Bigg[x^2 \Bigg\{ x j_\ell^2(mx) + x j_{\ell-1}^2(mx) \\ &\quad - \frac{2\ell+1}{m} j_{\ell-1}(mx) j_\ell(mx) \Bigg\} \Bigg]_a^b \end{aligned} \tag{A.5}$$

Appendix B

Conjugate gradients

In order to find the minimum of some function $f(\mathbf{x})$, it is of course necessary to solve the equation $\nabla f(\mathbf{x}) = 0$, but this is not possible in practice. Rather, $\nabla f(\mathbf{x})$ is used as a search direction in the multi-dimensional parameter-space of vectors $\mathbf{x}$ to minimise the function iteratively. One way to do this is to move along these directions of *steepest descent*, finding the minimum along each one and then calculating a new direction from that minimum until we find the ground-state. The minimum along a certain direction (the line minimum) is found when the direction along which we are searching becomes perpendicular to the gradient. Thus if we use this method of steepest descents, consecutive search directions are always perpendicular, and it is clear that this is inefficient since we are only using the current steepest descent direction and throwing away all previous knowledge which could be used to build up a more accurate picture of the functional we are trying to minimise. In fact, the steepest descents method is only efficient when the minimum is "spherical" i.e. when the eigenvalues of the Hessian are all of the same order. If this is not the case, then the method is very slow, and is not guaranteed to converge to the minimum in a finite number of steps. A particularly bad case is that of the "narrow valley" illustrated in figure B.1.

By contrast, the method of conjugate gradients [187] takes information from previous steps into account, but only requires that the previous search direction (rather than all previous search directions as might be expected) be stored. For a full description see [188]. We consider a general quadratic scalar function of a number of variables, written as a vector $\mathbf{x}$:

$$f(\mathbf{x}) = \tfrac{1}{2}\mathbf{x} \cdot \mathcal{G} \cdot \mathbf{x} - \mathbf{b} \cdot \mathbf{x} \tag{B.1}$$

in which $\mathcal{G}$ is a positive definite symmetric matrix (so that the function has a single global minimum) and $\mathbf{b}$ is some constant vector. We denote the line minima (i.e. the points at which the search direction changes) by the set of points $\{\mathbf{x}_r\}$ and the gradients at those

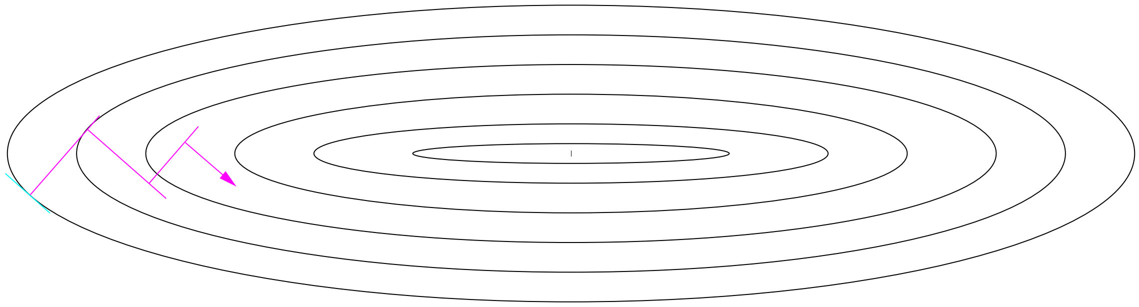

Figure B.1: Steepest descents method – a large number of steps is required to find the minimum.

points are $\{\mathbf{g}_r\}$

$$\mathbf{g}_r = \nabla f(\mathbf{x}_r) = \mathcal{G} \cdot \mathbf{x}_r - \mathbf{b}. \tag{B.2}$$

We label the search directions $\{\mathbf{p}_r\}$. In the steepest descents method, $\mathbf{p}_r = -\mathbf{g}_r$ and we move along this direction an amount described by the parameter α_r until at the end (at $\mathbf{x}_{r+1}$) the search direction is perpendicular to the gradient $\mathbf{g}_{r+1}$:

$$\mathbf{x}_{r+1} = \mathbf{x}_r + \alpha_r \mathbf{p}_r = \mathbf{x}_r - \alpha_r \mathbf{g}_r \tag{B.3}$$

$$\mathbf{g}_{r+1} \cdot \mathbf{p}_r = -\mathbf{g}_{r+1} \cdot \mathbf{g}_r = 0 \tag{B.4}$$

which proves that consecutive search directions are always mutually perpendicular in this method. Now, for $f(\mathbf{x})$ defined by equation B.1 we have

$$\mathbf{g}_r - \mathbf{g}_s = \mathcal{G} \cdot (\mathbf{x}_r - \mathbf{x}_s). \tag{B.5}$$

The minimum of $f(\mathbf{x})$ along the direction $\mathbf{p}_r$ is at $\mathbf{x}_{r+1} = \mathbf{x}_r + \alpha_r \mathbf{p}_r$ and is still given by condition (B.4), so that α_r is given by

$$\alpha_r = -\frac{\mathbf{p}_r \cdot \mathbf{g}_r}{\mathbf{p}_r \cdot \mathcal{G} \cdot \mathbf{p}_r} \tag{B.6}$$

and using (B.5) with $s = r + 1$ we obtain

$$\mathbf{g}_{r+1} = \mathbf{g}_r + \alpha_r \mathcal{G} \cdot \mathbf{p}_r. \tag{B.7}$$

A set of search directions $\{\mathbf{p}_r\}$ are said to be conjugate directions (with respect to $\mathcal{G}$)

if they satisfy the condition

$$\mathbf{p}_r \cdot \mathcal{G} \cdot \mathbf{p}_s = 0, \qquad r \neq s. \tag{B.8}$$

These directions are linearly independent which can be proved by *reductio ad absurdum*: assume the directions are linearly dependent i.e. there is a set of numbers $\{\lambda_i\}$, not all vanishing, for which $\sum_i \lambda_i \mathbf{p}_i = 0$. But operating on both sides by $\mathcal{G}$ and taking the scalar product with $\mathbf{p}_j$ implies $\lambda_j \mathbf{p}_j \cdot \mathcal{G} \cdot \mathbf{p}_j = 0$ for all j by (B.8), and $\mathbf{p}_j \cdot \mathcal{G} \cdot \mathbf{p}_j \neq 0$ since $\mathcal{G}$ is positive definite, and so we obtain the contradiction that $\lambda_j = 0$ for all j.

We can construct a set of these directions from a set of linearly dependent directions $\{\mathbf{u}_r\}$ using a procedure analogous to Gram-Schmidt orthogonalisation i.e.

$$\begin{aligned} \mathbf{p}_1 &= \mathbf{u}_1 \\ \mathbf{p}_{r+1} &= \mathbf{u}_{r+1} + \sum_{i=1}^{r} \beta_i^{(r)} \mathbf{p}_i \end{aligned} \tag{B.9}$$

where

$$\beta_i^{(r)} = -\frac{\mathbf{u}_{r+1} \cdot \mathcal{G} \cdot \mathbf{p}_i}{\mathbf{p}_i \cdot \mathcal{G} \cdot \mathbf{p}_i} \tag{B.10}$$

which we prove by induction. Assuming that we have r conjugate directions obeying (B.8) and construct $\mathbf{p}_{r+1}$ according to (B.9) then

$$\begin{aligned} \mathbf{p}_s \cdot \mathcal{G} \cdot \mathbf{p}_{r+1} &= \mathbf{p}_s \cdot \mathcal{G} \cdot \mathbf{u}_{r+1} - \sum_{i=1}^{r} \frac{\mathbf{u}_{r+1} \cdot \mathcal{G} \cdot \mathbf{p}_i}{\mathbf{p}_i \cdot \mathcal{G} \cdot \mathbf{p}_i} \mathbf{p}_s \cdot \mathcal{G} \cdot \mathbf{p}_i \\ &= \mathbf{p}_s \cdot \mathcal{G} \cdot \mathbf{u}_{r+1} - \frac{\mathbf{u}_{r+1} \cdot \mathcal{G} \cdot \mathbf{p}_s}{\mathbf{p}_s \cdot \mathcal{G} \cdot \mathbf{p}_s} \mathbf{p}_s \cdot \mathcal{G} \cdot \mathbf{p}_s = 0 \end{aligned} \tag{B.11}$$

for $s < r + 1$, since $\mathcal{G}$ is symmetric. Now $\mathbf{p}_1$ and $\mathbf{p}_2$ are trivially verified to be conjugate directions and so the proof is complete.

It follows that any other vector may be written as a combination of these conjugate directions, in particular the vector from the initial point $\mathbf{x}_1$ to the minimum $\mathbf{x}^*$ in an n-dimensional space is

$$\begin{aligned} \mathbf{x}^* - \mathbf{x}_1 &= \sum_{r=1}^{n} \alpha_r \mathbf{p}_r \\ \alpha_r &= \frac{\mathbf{p}_r \cdot \mathcal{G} \cdot (\mathbf{x}^* - \mathbf{x}_1)}{\mathbf{p}_r \cdot \mathcal{G} \cdot \mathbf{p}_r} \\ &= -\frac{\mathbf{p}_r \cdot \mathbf{g}_1}{\mathbf{p}_r \cdot \mathcal{G} \cdot \mathbf{p}_r} \end{aligned} \tag{B.12}$$

from equation B.2 and the fact that the gradient vanishes at the minimum i.e. $\mathbf{g}^* = \mathcal{G} \cdot \mathbf{x}^* - \mathbf{b} = 0$. We note therefore that $\mathbf{x}^*$ can be reached in $k \leq n$ steps from $\mathbf{x}_1$ where the

r-th step is given by

$$\mathbf{x}_{r+1} = \mathbf{x}_r + \alpha_r \mathbf{p}_r \tag{B.13}$$

with α_r given by (B.12). Applying (B.5) to

$$\mathbf{x}_r = \mathbf{x}_1 + \sum_{i=1}^{r-1} \alpha_i \mathbf{p}_i, \tag{B.14}$$

we obtain

$$\mathbf{g}_r = \mathbf{g}_1 + \sum_{i=1}^{r-1} \alpha_i \mathcal{G} \cdot \mathbf{p}_i. \tag{B.15}$$

When the scalar product with $\mathbf{p}_r$ is taken this gives $\mathbf{p}_r \cdot \mathbf{g}_1 = \mathbf{p}_r \cdot \mathbf{g}_r$. The expressions (B.6) and (B.12) are identical and so the steps from $\mathbf{x}_1$ to $\mathbf{x}^*$ proceed via points which are minima along each search direction. Taking the scalar product of (B.15) with $\mathbf{p}_s$ ($s < r$) instead we obtain

$$\mathbf{p}_s \cdot \mathbf{g}_r = \mathbf{p}_s \cdot \mathbf{g}_1 + \alpha_s \mathbf{p}_s \cdot \mathcal{G} \cdot \mathbf{p}_s = 0 \tag{B.16}$$

from equation B.12. Thus $\mathbf{g}_r$ is perpendicular to all previous search directions so that each point $\mathbf{x}_{r+1}$ is actually a minimum with respect to the whole subspace spanned by $\{\mathbf{p}_1, \mathbf{p}_2 \ldots \mathbf{p}_r\}$ i.e. we can consider each step as removing one dimension of the space from the problem, so that the minimum of a quadratic function must always be found in a number of steps less than or equal to the dimensionality of the space.

The method of conjugate gradients uses such a set of conjugate directions $\{\mathbf{p}_r\}$ based upon the steepest descent directions $\{-\mathbf{g}_r\}$ at successive points. For this to be valid, we must show that the gradients are linearly independent. They are in fact orthogonal, which can be proved by induction. Starting with $\mathbf{p}_1 = -\mathbf{g}_1$ then from the minimum condition (B.4) we have $\mathbf{g}_2 \cdot \mathbf{p}_1 = -\mathbf{g}_2 \cdot \mathbf{g}_1 = 0$ so that the first two gradients are orthogonal. Then assuming that we have a set of r orthogonal gradients, and conjugate directions obtained from them by (B.9). Using (B.16) we have $\mathbf{g}_{r+1} \cdot \mathbf{p}_s = 0$ for $s \leq r$. But $\mathbf{p}_s$ is given by (B.9) as

$$\mathbf{p}_s = -\mathbf{g}_s + \sum_{i=1}^{s-1} \beta_i^{(s-1)} \mathbf{p}_i \tag{B.17}$$

so that

$$\mathbf{g}_{r+1} \cdot \mathbf{g}_s = -\mathbf{g}_{r+1} \cdot \mathbf{p}_s + \sum_{i=1}^{s-1} \beta_i^{(s-1)} \mathbf{g}_{r+1} \cdot \mathbf{p}_i = 0 \tag{B.18}$$

and $\mathbf{g}_{r+1}$ is orthogonal to all the previous gradients and the proof is complete: the gradients are all mutually orthogonal and thus linearly independent so that they can be used to construct conjugate directions: the conjugate gradients.

In this case, equation B.9 becomes

$$\beta_i^{(r)} = \frac{\mathbf{g}_{r+1} \cdot \mathcal{G} \cdot \mathbf{p}_i}{\mathbf{p}_i \cdot \mathcal{G} \cdot \mathbf{p}_i} \tag{B.19}$$

which using (B.7) can be rewritten

$$(\mathbf{p}_i \cdot \mathcal{G} \cdot \mathbf{p}_i)\beta_i^{(r)} = \frac{1}{\alpha_i}\mathbf{g}_{r+1} \cdot (\mathbf{g}_{i+1} - \mathbf{g}_i) \tag{B.20}$$

so that by the orthogonality of the gradients, $\beta_i^{(r)} = 0$ for $i < r$ and the only non-vanishing coefficient is $\beta_r^{(r)}$:

$$\beta_r^{(r)} = -\frac{\mathbf{g}_{r+1} \cdot \mathbf{g}_{r+1}}{\mathbf{p}_r \cdot \mathbf{g}_r} \tag{B.21}$$

$$= \frac{\mathbf{g}_{r+1} \cdot \mathbf{g}_{r+1}}{\mathbf{g}_r \cdot \mathbf{g}_r} \tag{B.22}$$

by (B.16) and (B.9).

Thus the method involves starting by searching along the direction of steepest descent, finding the minimum point along each direction and then calculating a new search direction from the new gradient and previous search direction $\mathbf{p}_{r+1} = -\mathbf{g}_{r+1} + \beta_r \mathbf{p}_r$ where $\beta_r = \beta_r^{(r)}$ is calculated from either of the expressions in (B.21, B.22) (which *will* differ for a general function) or from

$$\beta_r = \frac{\mathbf{g}_{r+1} \cdot (\mathbf{g}_{r+1} - \mathbf{g}_r)}{\mathbf{p}_r \cdot (\mathbf{g}_{r+1} - \mathbf{g}_r)} \tag{B.23}$$

as suggested by Polak [189].

The minimum of the two-dimensional narrow valley, so problematic for the steepest descents method, is now found in just two steps by the conjugate gradients method (figure B.2).

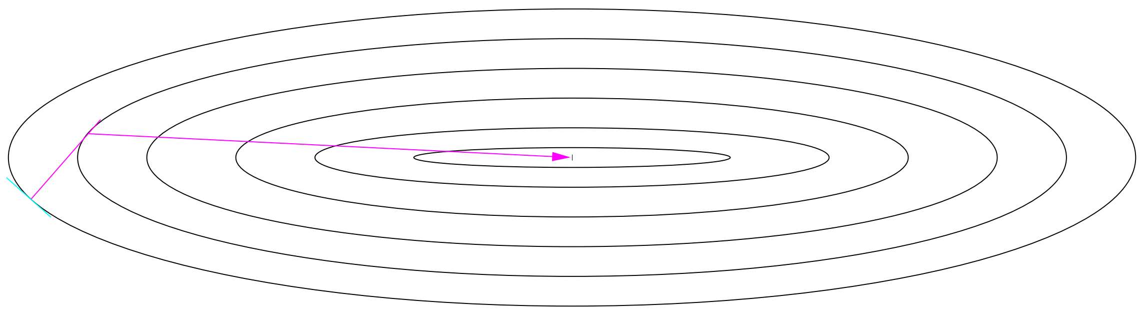

Figure B.2: Conjugate gradients method – only two steps are required to find the minimum.

Bibliography

[1] J. S. Bell. *Speakable and unspeakable in quantum mechanics* (Cambridge University Press, 1987).

[2] T. Kinoshita and W. B. Lindquist. Eighth-order anomalous magnetic moment of the electron. *Phys. Rev. Lett.* **47** (22), 1573 (November 1981).

[3] Robert S. Van Dyck Jr., Paul B. Schwinberg and Hans G. Dehmelt. New high-precision comparison of electron and positron g factors. *Phys. Rev. Lett.* **59** (1), 26 (July 1987).

[4] P. A. M. Dirac. *The Principles of Quantum Mechanics*, chap. I, p. 15ff. (Clarendon Press, Oxford, 1958), 4th edn.

[5] Alastair I. M. Rae. *Quantum Mechanics*, chap. 4, p. 63 (Adam Hilger, Bristol, 1986), 2nd edn.

[6] M. Born and R. Oppenheimer. Zur Quantentheorie der Molekeln. *Ann. Phys. (Leipzig)* **84** (20), 457 (1927).

[7] J. M. Ziman. *Principles of the Theory of Solids*, chap. 6, pp. 200–203 (Cambridge University Press, 1972), 2nd edn.

[8] Stephen Gasiorowicz. *Quantum Physics*, chap. 16, p. 255ff. (John Wiley & Sons, New York, 1974).

[9] M. P. Allen and D. J. Tildesley. *Computer Simulation of Liquids*, chap. 10, p. 270ff. (Oxford University Press, 1987).

[10] M. J. Gillan. The quantum simulation of hydrogen in metals. *Phil. Mag. A* **58** (1), 257 (1988).

[11] R. Car and M. Parrinello. Unified approach for molecular dynamics and density-functional theory. *Phys. Rev. Lett.* **55** (22), 2471 (November 1985).

[12] T. A. Arias, M. C. Payne and J. D. Joannopoulos. *Ab initio* molecular-dynamics techniques extended to large-length-scale systems. *Phys. Rev. B* **45** (4), 1538 (January 1992).

[13] M. V. Berry and J. M. Robbins. Indistinguishability for quantum particles: spin, statistics and the geometric phase. *Proc. R. Soc. Lond. A* **453**, 1771 (1997).

[14] L. D. Landau and E. M. Lifshitz. *Quantum Mechanics (Non-relativistic Theory)*, chap. IX, p. 241ff. (Pergamon Press, Oxford, 1973), 3rd edn.

[15] V. B. Berestetskii, E. M. Lifshitz and L. P. Pitaevskii. *Quantum Electrodynamics*, chap. II, III, pp. 33ff., 62ff. (Pergamon Press, Oxford, 1979), 2nd edn.

[16] P. Hohenberg and W. Kohn. Inhomogeneous electron gas. *Phys. Rev.* **136** (3B), 864 (November 1964).

[17] Mel Levy. Electron densities in search of Hamiltonians. *Phys. Rev. A* **26** (3), 1200 (September 1982).

[18] H. Englisch and R. Englisch. Exact density functionals for ground-state energies. *Phys. Stat. Sol. (b)* **123**, 711 (1984).

[19] H. Englisch and R. Englisch. Exact density functionals for ground-state energies. *Phys. Stat. Sol. (b)* **124**, 373 (1984).

[20] M. Levy. Universal variational functionals of electron densities, first-order density matrices, and natural spin-orbitals and solution of the v-representability problem. *Proc. Natl. Acad. Sci.* **76**, 6062 (1979).

[21] Mel Levy and John P. Perdew. The constrained search formulation of density functional theory. In *Density Functional Methods in Physics* (eds. Reiner M. Dreizler and Joao da Providencia), p. 11ff. (Plenum Publishing Corporation, New York, 1985).

[22] T. L. Gilbert. Hohenberg-Kohn theorem for nonlocal external potentials. *Phys. Rev. B* **12** (6), 2111 (September 1975).

[23] L. H. Thomas. The calculation of atomic fields. *Proc. Camb. Phil. Soc.* **23**, 542 (November 1927).

[24] E. Fermi. Un metodo statistico per la determinazione di alcune proprietà dell'atome. *Rend. Accad. Naz. Lincei* **6**, 602 (1927).

[25] E. Fermi. Eine statistische Methode zur Bestimmung einiger Eigenschaften des Atoms und ihre Anwendung auf die Theorie des periodischen Systems der Elemente. *Z. Phys.* **48**, 73 (1928).

[26] E. Teller. On the stability of molecules in the Thomas-Fermi theory. *Rev. Mod. Phys.* **34**, 627 (1962).

[27] Elliott H. Lieb. Thomas-Fermi and related theories of atoms and molecules. *Rev. Mod. Phys.* **53** (4), 603 (October 1981).

[28] Lin-Wang Wang and Michael P. Teter. Kinetic-energy functional of the electron density. *Phys. Rev. B* **45** (23), 13196 (June 1992).

[29] M. Pearson, E. Smargiassi and P. A. Madden. *Ab initio* molecular dynamics with an orbital-free density functional. *J. Phys.: Condens. Matter* **5**, 3221 (1993).

[30] F. Perrot. Hydrogen-hydrogen interaction in an electron gas. *J. Phys.: Condens. Matter* **6**, 431 (1994).

[31] Enrico Smargiassi and Paul A. Madden. Orbital-free kinetic-energy functionals for first-principles molecular dynamics. *Phys. Rev. B* **49** (8), 5220 (February 1994).

[32] Michael Foley and Paul A. Madden. Further orbital-free kinetic-energy functionals for *ab initio* molecular dynamics. *Phys. Rev. B* **53** (16), 10589 (April 1996).

[33] W. Kohn and L. J. Sham. Self-consistent equations including exchange and correlation effects. *Phys. Rev.* **140** (4A), 1133 (November 1965).

[34] John P. Perdew and Mel Levy. Extrema of the density functional for the energy: Excited states from the ground-state theory. *Phys. Rev. B* **31** (10), 6264 (May 1985).

[35] D. M. Ceperley and B. J. Alder. Ground state of the electron gas by a stochastic method. *Phys. Rev. Lett.* **45** (7), 566 (August 1980).

[36] J. P. Perdew and Alex Zunger. Self-interaction correction to density-functional approximations for many-electron systems. *Phys. Rev. B* **23** (10), 5048 (May 1981).

[37] R. O. Jones and O. Gunnarsson. The density functional formalism, its applications and prospects. *Rev. Mod. Phys.* **61** (3), 689 (July 1989).

[38] J. Harris and R. O. Jones. The surface energy of a bounded electron gas. *J. Phys. F* **4**, 1170 (August 1974).

[39] D. C. Langreth and J. P. Perdew. The exchange-correlation energy of a metallic surface. *Solid State Comm.* **17**, 1425 (1975).

[40] J. Harris. Adiabatic-connection approach to Kohn-Sham theory. *Phys. Rev. A* **29** (4), 1648 (April 1984).

[41] E. K. U. Gross, E. Runge and O. Heinonen. *Many-Particle Theory*, chap. 16, p. 179ff. (Adam Hilger, New York, 1991), English edn.

[42] O. Gunnarsson and B. I. Lundqvist. Exchange and correlation in atoms, molecules, and solids by the spin-density-functional formalism. *Phys. Rev. B* **13** (10), 4274 (May 1976).

[43] David C. Langreth and M. J. Mehl. Easily implementable nonlocal exchange-correlation energy functional. *Phys. Rev. Lett.* **47** (6), 446 (August 1981).

[44] David C. Langreth and M. J. Mehl. Beyond the local-density approximation in calculations of ground-state electronic properties. *Phys. Rev. B* **28** (4), 1809 (August 1983).

[45] Neil W. Ashcroft and N. David Mermin. *Solid State Physics*, chap. 8, p. 132ff. (Saunders College, Philadelphia, 1976), International edn.

[46] J. L. Lebowitz and Elliott H. Lieb. Existence of thermodynamics for real matter with Coulomb forces. *Phys. Rev. Lett.* **22** (13), 631 (March 1969).

[47] L. P. Bouckaert, R. Smoluchowski and E. Wigner. Theory of Brillouin zones and symmetry properties of wave functions in crystals. *Phys. Rev.* **50**, 58 (July 1936).

[48] A. Baldereschi. Mean-value point in the Brillouin zone. *Phys. Rev. B* **7** (12), 5212 (June 1973).

[49] D. J. Chadi and Marvin L. Cohen. Special points in the Brillouin zone. *Phys. Rev. B* **8** (12), 5747 (December 1973).

[50] Hendrik J. Monkhorst and James D. Pack. Special points for Brillouin-zone integrations. *Phys. Rev. B* **13** (12), 5188 (June 1976).

[51] D. J. Chadi. Special points for Brillouin-zone integrations. *Phys. Rev. B* **16** (4), 1746 (August 1977).

[52] R. A. Evarestov and V. P. Smirnov. Special points of the Brillouin zone and their use in the solid state theory. *Phys. Stat. Sol.* **119**, 9 (1983).

[53] Sverre Froyen. Brillouin-zone integration by Fourier quadrature: Special points for superlattice and supercell calculations. *Phys. Rev. B* **39** (5), 3168 (February 1989).

[54] I. J. Robertson and M. C. Payne. k-point sampling and the $k \cdot p$ method in pseudopotential total energy calculations. *J. Phys.: Condens. Matter* **2**, 9837 (1990).

[55] I. J. Robertson and M. C. Payne. The $k \cdot p$ method in pseudopotential total energy calculations: error reduction and absolute energies. *J. Phys.: Condens. Matter* **3**, 8841 (1991).

[56] James C. Phillips. Energy-band interpolation scheme based on a pseudopotential. *Phys. Rev.* **112** (3), 685 (November 1958).

[57] James C. Phillips and Leonard Kleinman. New method for calculating wave functions in crystals and molecules. *Phys. Rev.* **116** (2), 287 (October 1959).

[58] Volker Heine. *The Pseudopotential Concept*, vol. 24 of *Solid State Physics*, p. 1 (Academic Press, New York, 1970).

[59] J. Ihm. Total energy calculations in solid-state physics. *Rep. Prog. Phys.* **51** (1), 105 (1988).

[60] W. E. Pickett. Pseudopotential methods in condensed matter applications. *Comp. Phys. Rep.* **9** (3), 115 (1989).

[61] Conyers Herring. A new method for calculating wave functions in crystals. *Phys. Rev.* **57**, 1169 (June 1940).

[62] Leonard I. Schiff. *Quantum Mechanics*, chap. 5, p. 116ff. (McGraw-Hill, Singapore, 1968), 3rd edn.

[63] Michael Teter. Additional condition for transferability in pseudopotentials. *Phys. Rev. B* **48** (8), 5031 (August 1993).

[64] A. Filippetti, David Vanderbilt, W. Zhong, Yong Cai and G. B. Bachelet. Chemical hardness, linear response, and pseudopotential transferability. *Phys. Rev. B* **52** (16), 11793 (October 1995).

[65] Antonio Redondo, William A. Goddard III and T. C. McGill. *Ab initio* effective potentials for silicon. *Phys. Rev. B* **15** (10), 5038 (May 1977).

[66] D. R. Hamann, M. Schlüter and C. Chiang. Norm-conserving pseudopotentials. *Phys. Rev. Lett.* **43** (20), 1494 (November 1979).

[67] Alex Zunger and Marvin L. Cohen. First-principles nonlocal-pseudopotential approach in the density-functional formalism. II. Application to electronic and structural properties of solids. *Phys. Rev. B* **20** (10), 4082 (November 1979).

[68] G. P. Kerker. Non-singular atomic pseudopotentials for solid state applications. *J. Phys. C* **13** (9), L189 (March 1980).

[69] G. B. Bachelet, D. R. Hamann and M. Schlüter. Pseudopotentials that work: From H to Pu. *Phys. Rev. B* **26** (8), 4199 (October 1982).

[70] D. R. Hamann. Generalized norm-conserving pseudopotentials. *Phys. Rev. B* **40** (5), 2980 (August 1989).

[71] Andrew M. Rappe, Karin M. Rabe, Efthimios Kaxiras and J. D. Joannopoulos. Optimized pseudopotentials. *Phys. Rev. B* **41** (2), 1227 (January 1990).

[72] J. S. Lin, A. Qteish, M. C. Payne and V. Heine. Optimized and transferable nonlocal separable *ab initio* pseudopotentials. *Phys. Rev. B* **47** (8), 4174 (February 1993).

[73] Ming-Hsien Lee. *Advanced Pseudopotentials for Large Scale Electronic Structure Calculations*. Ph.D. thesis, University of Cambridge, Cavendish Laboratory (1994).

[74] N. Troullier and José Luís Martins. Efficient pseudopotentials for plane-wave calculations. *Phys. Rev. B* **43** (3), 1993 (January 1991).

[75] David Vanderbilt. Soft self-consistent pseudopotentials in a generalized eigenvalue formalism. *Phys. Rev. B* **41** (11), 7892 (April 1990).

[76] Eric L. Shirley, Douglas C. Allan, Richard M. Martin and J. D. Joannopoulos. Extended norm-conserving pseudopotentials. *Phys. Rev. B* **40** (6), 3652 (August 1989).

[77] Leonard Kleinman and D. M. Bylander. Efficacious form for model pseudopotentials. *Phys. Rev. Lett.* **48** (20), 1425 (May 1982).

[78] Peter E. Blöchl. Generalized separable potentials for electronic-structure calculations. *Phys. Rev. B* **41** (8), 5414 (March 1990).

[79] J. Ihm, Alex Zunger and Marvin L. Cohen. Momentum-space formalism for the total energy of solids. *J. Phys. C* **12**, 4409 (1979).

[80] P. J. H. Denteneer and W. van Haeringen. The pseudopotential-density-functional method in momentum space: details and test cases. *J. Phys. C* **18**, 4127 (1985).

[81] Michael P. Teter, Michael C. Payne and Douglas C. Allan. Solution of Schrödinger's equation for large systems. *Phys. Rev. B* **40** (18), 12255 (December 1989).

[82] M. C. Payne, M. P. Teter, D. C. Allan, T. A. Arias and J. D. Joannopoulos. Iterative minimization techniques for *ab initio* total-energy calculations: molecular dynamics and conjugate gradients. *Rev. Mod. Phys.* **64** (4), 1045 (October 1992).

[83] G. Kresse and J. Furthmuller. Efficient iterative schemes for *ab-initio* total-energy calculations using a plane-wave basis-set. *Phys. Rev. B* **54** (16), 11169 (1996).

[84] X.-P. Li, R. W. Nunes and David Vanderbilt. Density-matrix electronic-structure method with linear system-size scaling. *Phys. Rev. B* **47** (16), 10891 (April 1993).

[85] S.-Y. Qiu, C. Z. Wang, K. M. Ho and C. T. Chan. Tight-binding molecular dynamics with linear system-size scaling. *J. Phys.: Condens. Matter* **6**, 9153 (1994).

[86] A. Canning, G. Galli, F. Mauri, A. de Vita and R. Car. $O(N)$ tight-binding molecular dynamics on massively parallel computers: an orbital decomposition approach. *Comp. Phys. Comm.* **94**, 89 (1996).

[87] A. P. Horsfield, A. M. Bratkovsky, D. G. Pettifor and M. Aoki. Bond-order potential and cluster recursion for the description of chemical-bonds – efficient real-space methods for tight-binding molecular-dynamics. *Phys. Rev. B* **53** (3), 1656 (1996).

[88] D. R. Bowler, M. Aoki, C. M. Goringe, A. P. Horsfield and D. G. Pettifor. A comparison of linear scaling tight-binding methods. *Modelling Simul. Mater. Sci. Eng.* **5** (3), 199 (1997).

[89] Weitao Yang. Direct calculation of electron density in density-functional theory. *Phys. Rev. Lett.* **66** (11), 1438 (March 1991).

[90] Weitao Yang. A local projection method for the linear combination of atomic orbital implementation of density-functional theory. *J. Chem. Phys.* **94** (2), 1208 (January 1991).

[91] Qingsheng Zhao and Weitao Yang. Analytical energy gradients and geometry optimization in the divide-and-conquer method for large molecules. *J. Chem. Phys.* **102** (24), 9598 (June 1995).

[92] Weitao Yang and Tai-Sung Lee. A density-matrix divide-and-conquer approach for electronic structure calculations of large molecules. *J. Chem. Phys.* **103** (13), 5674 (October 1995).

[93] Jian Ping Lu and Weitao Yang. The shape of large single- and multiple-shell fullerenes. *Phys. Rev. B* **49** (16), 11421 (April 1994).

[94] Darrin M. York, Tai-Sung Lee and Weitao Yang. Quantum mechanical study of aqueous polarization effects on biological macromolecules. *J. Am. Chem. Soc.* **118**, 10940 (1996).

[95] R. Haydock, Volker Heine and M. J. Kelly. Electronic structure based on the local atomic environment for tight-binding bands. *J. Phys. C* **5**, 2845 (1972).

[96] Roger Haydock. *The Recursive Solution of the Schrödinger Equation*, vol. 35 of *Solid State Physics*, p. 215 (Academic Press, New York, 1980).

[97] S. Baroni and P. Giannozzi. Towards very large-scale electronic-structure calculations. *Europhys. Lett.* **17** (6), 547 (February 1992).

[98] David A. Drabold and Otto F. Sankey. Maximum entropy approach for linear scaling in the electronic structure problem. *Phys. Rev. Lett.* **70** (23), 3631 (June 1993).

[99] Lin-Wang Wang. Calculating the density of states and optical-absorption spectra of large quantum systems by the plane-wave moments method. *Phys. Rev. B* **49** (15), 10154 (April 1994).

[100] Otto F. Sankey, David A. Drabold and Andrew Gibson. Projected random vectors and the recursion method in the electronic-structure problem. *Phys. Rev. B* **50** (3), 1376 (July 1994).

[101] R. N. Silver and H. Röder. Calculation of the densities of states and spectral functions by Chebyshev recursion and maximum entropy. *Phys. Rev. E* **56** (4), 4822 (October 1997).

[102] Yang Wang, G. M. Stocks, W. A. Shelton, D. M. C. Nicholson, Z. Szotek and W. M. Temmerman. Order-N multiple scattering approach to electronic structure calculations. *Phys. Rev. Lett.* **75** (15), 2867 (October 1995).

[103] I. A. Abrikosov, A. M. N. Niklasson, S. I. Simak, B. Johansson, A. V. Ruban and H. L. Skriver. Order-N Green's function technique for local environment effects in alloys. *Phys. Rev. Lett.* **76** (22), 4203 (May 1996).

[104] I. A. Abrikosov, S. I. Simak, B. Johansson, A. V. Ruban and H. L. Skriver. Locally self-consistent Green's function approach to the electronic structure problem. *Phys. Rev. B* **56** (15), 9319 (October 1997).

[105] S. Goedecker and L. Colombo. Efficient linear scaling algorithm for tight-binding molecular dynamics. *Phys. Rev. Lett.* **73** (1), 122 (July 1994).

[106] S. Goedecker and M. Teter. Tight-binding electronic-structure calculations and tight-binding molecular dynamics with localized orbitals. *Phys. Rev. B* **51** (15), 9455 (April 1995).

[107] Roi Baer and Martin Head-Gordon. Chebyshev expansion methods for electronic structure calculations on large molecular systems. *J. Chem. Phys.* **107** (23), 10003 (December 1997).

[108] Uwe Stephan and David A. Drabold. Order-N projection method for first-principles computations of electronic quantities and Wannier functions. *Phys. Rev. B* **57** (11), 6391 (March 1998).

[109] S. Goedecker. Integral representation of the Fermi distribution and its applications in electronic-structure calculations. *Phys. Rev. B* **48** (23), 17573 (December 1993).

[110] D. M. C. Nicholson and X.-G. Zhang. Approximate occupation functions for density-functional calculations. *Phys. Rev. B* **56** (20), 12805 (November 1997).

[111] Florian Gagel. Finite-temperature evaluation of the Fermi density operator. *J. Comp. Phys.* **139**, 399 (1998).

[112] A. F. Voter, J. D. Kress and R. N. Silver. Linear-scaling tight binding from a truncated approach. *Phys. Rev. B* **53** (19), 12733 (May 1996).

[113] R. N. Silver, H. Roeder, A. F. Voter and J. D. Kress. Kernel polynomial approximations for densities of states and spectral functions. *J. Comp. Phys.* **124**, 115 (1996).

[114] Giulia Galli and Michele Parrinello. Large scale electronic structure calculations. *Phys. Rev. Lett.* **69** (24), 3547 (December 1992).

[115] Francesco Mauri, Giulia Galli and Roberto Car. Orbital formulation for electronic-structure calculations with linear system-size scaling. *Phys. Rev. B* **47** (15), 9973 (April 1993).

[116] Francesco Mauri and Giulia Galli. Electronic-structure calculations and molecular-dynamics simulations with linear system-size scaling. *Phys. Rev. B* **50** (7), 4316 (August 1994).

[117] Pablo Ordejón, David A. Drabold, Matthew P. Grumbach and Richard M. Martin. Unconstrained minimization approach for electronic computations that scales linearly with system size. *Phys. Rev. B* **48** (19), 14646 (November 1993).

[118] Pablo Ordejón, David A. Drabold, Richard M. Martin and Matthew P. Grumbach. Linear system-size scaling methods for electronic-structure calculations. *Phys. Rev. B* **51** (3), 1456 (January 1995).

[119] Jeongnim Kim, Francesco Mauri and Giulia Galli. Total-energy global optimizations using nonorthogonal localized orbitals. *Phys. Rev. B* **52** (3), 1640 (July 1995).

[120] K. C. Pandey, A. R. Williams and J. F. Janak. Localized orbital theory of electronic structure: A simple application. *Phys. Rev. B* **52** (20), 14415 (November 1995).

[121] Pablo Ordejón, Emilio Artacho and José M. Soler. Self-consistent order-N density-functional calculations for very large systems. *Phys. Rev. B* **53** (16), 10441 (April 1996).

[122] Jeongnim Kim, John W. Wilkins, Furrukh S. Khan and Andrew Canning. Extended Si {311} defects. *Phys. Rev. B* **55** (24), 16186 (June 1997).

[123] Giulia Galli. Linear scaling methods for electronic structure calculations and quantum molecular dynamics simulations. *Current Opinion in Solid State and Materials Science* **1** (6), 864 (1996).

[124] E. B. Stechel, A. R. Williams and Peter J. Feibelman. N-scaling algorithm for density-functional calculations of metals and insulators. *Phys. Rev. B* **49** (15), 10088 (April 1994).

[125] W. Hierse and E. B. Stechel. Order-N methods in self-consistent density-functional calculations. *Phys. Rev. B* **50** (24), 17811 (December 1994).

[126] E. Hernández and M. J. Gillan. Self-consistent first-principles technique with linear scaling. *Phys. Rev. B* **51** (15), 10157 (April 1995).

[127] E. Hernández, M. J. Gillan and C. M. Goringe. Linear-scaling density-functional-theory technique: The density-matrix approach. *Phys. Rev. B* **53** (11), 7147 (March 1996).

[128] John M. Millam and Gustavo E. Scuseria. Linear scaling conjugate gradient density matrix search as an alternative to diagonalization for first principles electronic structure calculations. *J. Chem. Phys.* **106** (13), 5569 (April 1997).

[129] Andrew D. Daniels, John M. Millam and Gustavo E. Scuseria. Semiempirical methods with conjugate gradient density-matrix search to replace diagonalization for molecular systems containing thousands of atoms. *J. Chem. Phys.* **107** (2), 425 (July 1997).

[130] Karl Blum. *Density Matrix Theory and Applications*, chap. 2, p. 37ff. (Plenum Press, New York, 1981).

[131] J. F. Janak. Proof that $\partial E/\partial n_i = \epsilon_i$ in density-functional theory. *Phys. Rev. B* **18** (12), 7165 (December 1978).

[132] M. Weinert and J. W. Davenport. Fractional occupations and density-functional energies and forces. *Phys. Rev. B* **45** (23), 13709 (June 1992).

[133] M. M. Valiev and G. W. Fernando. Occupation numbers in density-functional calculations. *Phys. Rev. B* **52** (15), 10697 (October 1995).

[134] R. McWeeny. Some recent advances in density matrix theory. *Rev. Mod. Phys.* **32** (2), 335 (April 1960).

[135] W. Kohn. Density functional and density matrix method scaling linearly with the number of atoms. *Phys. Rev. Lett.* **76** (17), 3168 (April 1996).

[136] W. Kohn. Analytic properties of Bloch waves and Wannier functions. *Phys. Rev.* **115** (4), 809 (August 1959).

[137] E. I. Blount. *Formalisms of Band Theory*, vol. 13 of *Solid State Physics*, p. 305 (Academic Press, New York, 1962).

[138] Jacques des Cloizeaux. Energy bands and projection operators in a crystal: Analytic and asymptotic properties. *Phys. Rev.* **135** (3A), 685 (August 1964).

[139] Jacques des Cloizeaux. Analytical properties of n-dimensional energy bands and Wannier functions. *Phys. Rev.* **135** (3A), 698 (August 1964).

[140] Roi Baer and Martin Head-Gordon. Sparsity of the density matrix in Kohn-Sham density functional theory and an assessment of linear system-size scaling methods. *Phys. Rev. Lett.* **79** (20), 3962 (November 1997).

[141] P. E. Maslen, C. Ochsenfeld, C. A. White, M. S. Lee and M. Head-Gordon. Locality and sparsity of ab initio one-particle density matrices and localized orbitals. *J. Phys. Chem.* **102**, 2215 (1998).

[142] Sohrab Ismail-Beigi and Tomás Arias. On the locality of physics in metals, semiconductors, and insulators. *Phys. Rev. Lett.* submitted.

[143] Gregory H. Wannier. The structure of electronic excitation levels in insulating crystals. *Phys. Rev.* **52**, 191 (August 1937).

[144] S. F. Boys. A general method of calculation for the stationary states of any molecular system. *Proc. R. Soc. Lond. A* **200**, 542 (1950).

[145] S. Obara and A. Saika. Efficient recursive computation of molecular integrals over Cartesian Gaussian functions. *J. Chem. Phys.* **84** (7), 3963 (April 1986).

[146] Otto F. Sankey and David J. Niklewski. *Ab initio* multicenter tight-binding model for molecular-dynamics simulations and other applications in covalent systems. *Phys. Rev. B* **40** (6), 3979 (August 1989).

[147] E. Hernández, M. J. Gillan and C. M. Goringe. Basis functions for linear-scaling first-principles calculations. *Phys. Rev. B* **55** (20), 13485 (May 1997).

[148] Ross A. Lippert, T. A. Arias and Alan Edelman. Multiscale computation with interpolating wavelets. *J. Comp. Phys.* **140**, 278 (1998).

[149] James R. Chelikowsky, N. Troullier and Y. Saad. Finite-difference-pseudopotential method: Electronic structure calculations without a basis. *Phys. Rev. Lett.* **72** (8), 1240 (February 1994).

[150] P. D. Haynes and M. C. Payne. Localised spherical-wave basis set for $O(N)$ total-energy pseudopotential calculations. *Comp. Phys. Comm.* **102** (1-3), 17 (June 1997).

[151] R. Courant and D. Hilbert. *Methods of Mathematical Physics*, vol. 1, p. 535ff. (Interscience Publishers, New York, 1953), 1st edn.

[152] R. D. King-Smith, M. C. Payne and J. S. Lin. Real-space implementation of nonlocal pseudopotentials for first-principles total-energy calculations. *Phys. Rev. B* **44** (23), 13063 (December 1991).

[153] S. Goedecker. Electronic structure methods exhibiting linear scaling of the computational effort with respect to the size of the system. *Rev. Mod. Phys.* submitted.

[154] Y. Saad. *Iterative methods for sparse linear systems* (PWS Publishing Co., Boston, 1996).

[155] D. R. Bowler and M. J. Gillan. Length-scale ill conditioning in linear-scaling dft. *Comp. Phys. Comm.* (1998). in press.

[156] Leslie Greengard. Fast algorithms for classical physics. *Science* **265**, 909 (August 1994).

[157] Christopher A. White, Benny G. Johnson, Peter M. W. Gill and Martin Head-Gordon. The continuous fast multipole method. *Chem. Phys. Lett.* **230**, 8 (November 1994).

[158] Matthew C. Strain, Gustavo E. Scuseria and Michael J. Frisch. Achieving linear scaling for the electronic quantum Coulomb problem. *Science* **271**, 51 (January 1996).

[159] Christopher A. White, Benny G. Johnson, Peter M. W. Gill and Martin Head-Gordon. Linear scaling density functional calculations via the continuous fast multipole method. *Chem. Phys. Lett.* **253**, 268 (May 1996).

[160] Ross D. Adamson, Jeremy P. Dombroski and Peter M. W. Gill. Chemistry without Coulomb tails. *Chem. Phys. Lett.* **254**, 329 (May 1996).

[161] José M. Pérez-Jordá and Weitao Yang. Fast evaluation of the Coulomb energy for electron densities. *J. Chem. Phys.* **107** (4), 1218 (July 1997).

[162] S. Goedecker and O. V. Ivanov. Linear scaling solution of the Coulomb problem using wavelets. *Solid State Comm.* **105** (11), 665 (1998).

[163] Christopher A. White, Paul Maslen, Michael S. Lee and Martin Head-Gordon. The tensor properties of energy gradients within a non-orthogonal basis. *Chem. Phys. Lett.* **276**, 133 (September 1997).

[164] Nicola Marzari. *Ab initio Molecular Dynamics for Metallic Systems*. Ph.D. thesis, University of Cambridge, Cavendish Laboratory (1996).

[165] Nicola Marzari, David Vanderbilt and M. C. Payne. Ensemble density-functional theory for *ab initio* molecular dynamics of metals and finite-temperature insulators. *Phys. Rev. Lett.* **79** (7), 1337 (August 1997).

[166] Daniel Sánchez-Portal, Emilio Artacho and José M. Soler. Projection of plane-wave calculations into atomic orbitals. *Solid State Comm.* **95** (10), 685 (1995).

[167] Daniel Sánchez-Portal, Emilio Artacho and José M. Soler. Analysis of atomic orbital basis sets from the projection of plane-wave results. *J. Phys.: Condens. Matter* **8**, 3859 (1996).

[168] M. D. Segall, C. J. Pickard, R. Shah and M. C. Payne. Population analysis in plane wave electronic structure calculations. *Mol. Phys.* **89** (2), 571 (1996).

[169] W. Hierse and E. B. Stechel. Robust localized-orbital transferability using the Harris functional. *Phys. Rev. B* **54** (23), 16515 (December 1996).

[170] Pablo Fernández, Andrea Dal Corso, Alfonso Baldereschi and Francesco Mauri. First-principles wannier functions of silicon and gallium arsenide. *Phys. Rev. B* **55** (4), 1909 (January 1997).

[171] Nicola Marzari and David Vanderbilt. Maximally localized generalized Wannier functions for composite energy bands. *Phys. Rev. B* **56** (20), 12847 (November 1997).

[172] Walter Kohn. Density functional/Wannier function theory for systems of very many atoms. *Chem. Phys. Lett.* **208** (3,4), 167 (June 1993).

[173] A. P. Sutton, M. W. Finnis, D. G. Pettifor and Y. Ohta. The tight-binding bond model. *J. Phys. C* **21**, 35 (1988).

[174] Jim Asher, Owen C. Jones, John G. Noyes and Geoffrey F. Phillips, eds. *Kaye & Laby's Tables of Physical and Chemical Constants*, pp. 45, 214 (Longman, Harlow, Essex, 1995), 16th edn.

[175] P. P. Ewald. Zur Begründung der Kristalloptik. *Ann. Phys. (Leipzig)* **54** (23), 519 (1917).

[176] P. P. Ewald. Zur Begründung der Kristalloptik. *Ann. Phys. (Leipzig)* **54** (24), 557 (1917).

[177] P. P. Ewald. Die Berechnung optischer und elektrostatischer Gitterpotentiale. *Ann. Phys. (Leipzig)* **64**, 253 (1921).

[178] J. M. Ziman. *Principles of the Theory of Solids*, chap. 2, pp. 37–42 (Cambridge University Press, Cambridge, 1972), 2nd edn.

[179] Kai-Ming Ho, J. Ihm and J. D. Joannopoulos. Dielectric matrix scheme for fast convergence in self-consistent electronic-structure calculations. *Phys. Rev. B* **25** (6), 4260 (March 1982).

[180] P. H. Dederichs and R. Zeller. Self-consistency iterations in electronic-structure calculations. *Phys. Rev. B* **28** (10), 5462 (November 1983).

[181] G. P. Kerker. Efficient iteration scheme for self-consistent pseudopotential calculations. *Phys. Rev. B* **23** (6), 3082 (March 1981).

[182] H. Hellmann. *Einfuhrung in die Quantumchemie* (Deuticke, Leipzig, 1937).

[183] R. P. Feynman. Forces in molecules. *Phys. Rev.* **56**, 340 (August 1939).

[184] P. Pulay. *Ab initio* calculation of force constants and equilibrium geometries in polyatomic molecules. i. theory. *Mol. Phys.* **17** (2), 197 (1969).

[185] C. M. Goringe, E. Hernández, M. J. Gillan and I. J. Bush. Linear-scaling DFT-pseudopotential calculations on parallel computers. *Comp. Phys. Comm.* **102** (1-3), 1 (1997).

[186] M. Abramowitz and I. Stegun. *Handbook of Mathematical Functions*, chap. 10, p. 435 (Dover, New York, 1965).

[187] R. Fletcher and C. M. Reeves. Function minimisation by conjugate gradients. *Comp. J.* **7**, 149 (1964).

[188] D. M. Greig. *Optimisation*, chap. 2, p. 41ff. (Longman, London, 1980).

[189] E. Polak. *Computational Methods in Optimisation* (Academic Press, 1971).